

Developing Clean Fuels: Novel Techniques for Desulfurization

James P. Nehlsen

**A Dissertation Presented to the Faculty of Princeton University in
Candidacy for the Degree of Doctor of Philosophy**

**Recommended for Acceptance by the Department of Chemical
Engineering**

November 2005

©Copyright by James Patrick Nehlsen, 2005. All rights reserved.

Abstract

The removal of sulfur compounds from petroleum is crucial to producing clean burning fuels. Sulfur compounds poison emission control catalysts and are the source of acid rain. New federal regulations require the removal of sulfur in both gasoline and diesel to very low levels, forcing existing technologies to be pushed into inefficient operating regimes. New technology is required to efficiently produce low sulfur fuels.

Two processes for the removal of sulfur compounds from petroleum have been developed: the removal of alkanethiols by heterogeneous reaction with metal oxides; and oxidative desulfurization of sulfides and thiophene by reaction with sulfuric acid. Alkanethiols, common in hydrotreated gasoline, can be selectively removed and recovered from a hydrocarbon stream by heterogeneous reaction with oxides of Pb, Hg(II), and Ba. The choice of reactive metal oxides may be predicted from simple thermodynamic considerations. The reaction is found to be autocatalytic, first order in water, and zero order in thiol in the presence of excess oxide. The thiols are recovered by reactive extraction with dilute oxidizing acid.

The potential for using polymer membrane hydrogenation reactors (PEMHRs) to perform hydrogenation reactions such as hydrodesulfurization is explored by hydrogenating ketones and olefins over Pt and Au group metals. The dependence of reaction rate on current density suggests that the first hydrogen addition to the olefin is the rate limiting step, rather than the adsorption of hydrogen, for all of the metals tested. PEMHRs proved unsuccessful in hydrogenating sulfur compounds to perform HDS.

For the removal of sulfides, a two-phase reactor is used in which concentrated sulfuric acid oxidizes aromatic and aliphatic sulfides present in a hydrocarbon solvent, generating sulfoxides and sulfones. The polar oxidized species are extracted into the acid phase, effectively desulfurizing the hydrocarbon. A reaction scheme is proposed for this system and is justified with a thermodynamic analysis and an experimental determination of the reaction rate law.

Table of Contents

Abstract	iii
List of Tables and Figures	vi
List of Publications	ix
1. Introduction.....	10
2. Background	14
2.1. Petroleum Refining.....	14
2.2. Hydrogenation Reactors	22
3. Reaction Mechanisms in Polymer Electrolyte Membrane Hydrogenation Reactors ...	31
3.1. A Comparison of Catalytic Hydrogenation Mechanisms in Polymer Membrane Hydrogenation Reactors	31
3.2. Electrochemical Reactions in a Polymer Membrane Reactor	55
3.3. Desulfurization in a Polymer Membrane Hydrogenation Reactor	61
4. Removal and Recovery of Alkanethiols	65
4.1. Chemistry and Reactions	65
4.2. Process Demonstration	86
5. Oxidation of Aliphatic and Aromatic Sulfides Using Sulfuric Acid	108
5.1. Introduction to Oxidative Desulfurization.....	108
5.2. The Use of Sulfuric Acid in ODS	114
5.3. Experimental.....	114
5.4. Results.....	116
5.5. Discussion.....	124
5.6. Conclusions	128
6. Conclusions	129
7. References	134
Acknowledgements.....	144

List of Tables and Figures

Tables

Table 2.1: Petroleum distillate fractions and their boiling points.	16
Table 2.2: Aromatic sulfur species found in petroleum.	17
Table 3.1: Relative rates of hydrogenation of olefin and ketone species in a PEMHR. ...	42
Table 3.2: Fitting parameters for all mechanisms. Current density, i , has units mA cm^{-2} except in the power laws in which the units are $\text{nmol sec}^{-1} \text{cm}^{-2}$	48
Table 4.1: Predicted heats of reaction of metal oxides with observed reactivity.	83
Table 4.2: Thiol content of several light streams used in gasoline production.	88
Table 5.1: Partition coefficients for the sulfides studied.	127

Figures

Figure 1.1: Forest in Poland destroyed by sulfur emissions from a coal-fired power plant without sulfur emission controls. Courtesy of the US Geological Survey.	11
Figure 2.1: Example recombination reaction producing an alkanethiol in an HDS reactor.	18
Figure 2.2: A conventional slurry hydrogenation reactor and associated processes. Adapted from ⁴¹	25
Figure 3.1: Photographs of sample MEAs created by the airbrushing technique. On left, an MEA after pressing showing good dispersion of Ag powder over the initially black carbon cloth. On right, spraying of Cu powder onto carbon cloth using the airbrush. The carbon cloth is pinned at one edge between glass slides during spraying.	35
Figure 3.2: Photographs of the membrane reactor. Clockwise from top left are 1) the two reactor plates with gaskets; 2) detail of one reactor plate showing flow channels and o-ring groove; 3) previous version of reactor in operation with galvanostat and cartridge heaters attached; 4) previous version of reactor showing flow channels and gaskets; and 5) assembled reactor showing aluminum backing plates and Teflon tubing adapters.	37
Figure 3.3: Experimental apparatus schematic.	38

Figure 3.4: Rate of hydrogenation of 1-decene over various catalysts. Lines are fits to $kt^{0.5}$. The values of k are listed in Table 3.2.	40
Figure 3.5: Rate of hydrogenation of 1-decene over ineffective catalysts. Data enlarged from Figure 3.4, note the change in scale. Uncertainty in the data is considerable, shown by sample error bars for Cu. Line is an example fit to $t^{0.5}$	41
Figure 3.6: Rate of hydrogenation of acetone over Pt and Cu catalysts. Lines are fits to the Tafel / Langmuir-Hinshelwood mechanism and the power law, $kt^{0.75}$. The fit parameters are listed in Table 3.2.	43
Figure 3.7: Comparison of two common hydrogenation mechanisms. Rate equations are simplified by assuming constant surface coverage of organic. F is Faraday's constant, U is the unsaturated organic species, and S is the saturated organic species.	46
Figure 3.8: Rate of hydrogenation of 1-decene over Pt and Pd catalysts (from Figure 3.4) compared to Langmuir-Hinshelwood and Eley-Rideal style mechanisms. The fit of the power law $kt^{0.5}$ is also shown.	49
Figure 3.9: Reaction mechanism for the dehydrogenation of isopropanol and electrolysis of water. The removal of the first electron is rate limiting in each mechanism.	56
Figure 3.10: Rate of dehydrogenation of isopropanol over Pt and C anodes. Lines are fits to EQ. Fitting parameters for Pt are $k_w/k_{iso} = 0.0135$, $\alpha_w - \alpha_{iso} = 0$. Parameters for C are $k_w/k_{iso} = 0.0102$, $\alpha_w - \alpha_{iso} = 0.026$	59
Figure 3.11: Cyclic voltammogram of an Ag electrode in a tetrahydrothiophene solution. The anodic (oxidation) current increases with sulfur concentration, indicating the production of more Ag_2S . The smaller cathodic wave near 0 V is the reduction of some of the Ag_2S	64
Figure 4.1: TGA results showing decomposition of $Pb(SC_8H_{17})_2$	72
Figure 4.2: WAXD pattern of recrystallized $Pb(SC_8H_{17})_2$. Calculated average d-spacing is 26.2 Å.	73
Figure 4.3: Sketch of likely structure of a $Pb(SC_8H_{17})_2$ crystal.	74
Figure 4.4: Graphical representation of predicted heats of formation of metal thiolates from the oxide.	81
Figure 4.5: Graphical representation of observed metal oxide activity.	82
Figure 4.6: The Exomer process, designed by ExxonMobil and Merichem, Inc. to remove high molecular weight recombinant mercaptans. Adapted from ⁹⁷	89

Figure 4.7: Diagram of the thiol removal process using lead oxides, showing the key operations including reaction, separation, and extraction.	92
Figure 4.8: The yield of thiolates, indicating the degree to which PbO was converted into Pb(SR) ₂ in excess thiol.	96
Figure 4.9: Reaction rate of PbO and octanethiol with water added and water removed from the reactor.	104
Figure 4.10: Batch reaction rate of PbO and octanethiol. Solid line is fit of the rate law shown to the data using a two parameter fit, with parameter values given in the figure.	105
Figure 5.1: ASR-2 oxidative desulfurization process developed by UniPure. Adapted from ³⁷	112
Figure 5.2: Photographs of the Tyndall sunset effect in a solution of toluene, tetrahydrothiophene, and thiophene.	118
Figure 5.3: GC/MS spectra for the reaction products of tetrahydrothiophene and sulfuric acid. The mass spectrum for product B matches that of tetrahydrothiophene 1-oxide. The spectrum of product A suggests a species with two oxygen atoms, such as the sulfone or ketosulfoxide. Mass spectrum C could be the adduct of sulfuric acid and tetrahydrothiophene.	120
Figure 5.4: Reaction rate of 2000 ppm solutions of thiophene, tetrahydrothiophene, and dibutyl sulfide with 16M H ₂ SO ₄ . Data are fit by a rate law that is first order in sulfide concentration, shown above. For the given rate constants, sulfide concentration is given in units of ppm S.	121
Figure 5.5: Consumption of tetrahydrothiophene from a 2000 ppm S solution after 1 hour reaction with various concentrations of sulfuric acid. Data is fit by a rate law first order in acid concentration shown. [H ₂ SO ₄ [*]] is acid concentration above the threshold value shown by the intercept (2.4 M).	122
Figure 5.6: Reaction rate of tetrahydrothiophene from a 2000 ppm S solution reacting with 9M H ₂ SO ₄ . Rate is constant at 0.0055 min ⁻¹	123

List of Publications

Desulfurization Technologies:

1. Nehlsen, J. P.; Benziger, J. B.; Kevrekidis, I. G., Removal of alkanethiols from a hydrocarbon mixture by a heterogeneous reaction with metal oxides. *Industrial & Engineering Chemistry Research* **2003**, 42, (26), 6919-6923.
2. Nehlsen, J. P.; Benziger, J. B.; Kevrekidis, I. G., A process for the removal of thiols from a hydrocarbon stream by a heterogeneous reaction with lead oxide. *Energy & Fuels* **2004**, 18, (3), 721-726.
3. Nehlsen, J. P.; Benziger, J. B.; Kevrekidis, I. G., Oxidation of Aliphatic and Aromatic Sulfides Using Sulfuric Acid. Submitted to *Industrial & Engineering Chemistry Research*, July 2005.

Fuel Cell Design and Control:

5. Benziger, J.B., Nehlsen, J.P., Blackwell, D., Brennan, T., and Itescu, J., Water Flow in the Gas Diffusion Layer of Fuel Cells. In press, *Journal of Membrane Science*, Mar 2005.
6. Benziger, J.B., Satterfield, M.B., Hogarth, W.H.J., Nehlsen, J.P., and Kevrekidis, I.G., The Power Performance Curve for Engineering Analysis of Fuel Cells. In press, *Journal of Power Sources*, May, 2005.
7. Hogarth W.H.J., Nehlsen, J.P., and Benziger, J.B., Fuel Cell Design: The Impact of PEM Fuel Cell Dynamics on Control and Systems Design. Submitted to *AIChE Journal*, May 2005.
8. Benziger, J.B., Hogarth, W.H.J., and Nehlsen, J.P., Fuel Cell Power and Efficiency: Universal Constraints. Submitted to *IEEE Transactions on Power Conversion*, July 2005.

1. Introduction

Energy production is one of the most pressing issues of modern times. Economic activity and energy usage are intimately linked. The production of useful goods and services requires energy, and more global economic output requires more energy usage. World energy usage increased by an average of 1.7% annually from 1980-2001, to a total of 404 quadrillion BTUs.¹ Although the percentage of energy obtained from fossil fuels declined over the same period, the share of world energy from fossil fuels is still over 82%, half of which comes from petroleum.¹

Unfortunately, the predominant modern technique for producing energy, the burning of fossil fuels, has a severe impact on the global environment. Some of this impact is the result of impure fuels. Naturally occurring sulfur compounds left in fuels lead to the emission of sulfur oxide gases. These gases react with water in the atmosphere to form sulfates and acid rain which damages buildings, destroys automotive paint finishes, and acidifies soil, ultimately leading to loss of forests and other ecosystems.² Figure 1.1 illustrates the devastating effects unchecked sulfur emissions can have on the local environment. Sulfur emissions also cause respiratory illnesses, aggravate heart disease, trigger asthma, and contribute to formation of atmospheric particulates.³

Federal programs designed to reduce sulfur emissions from electric utilities and other industrial sources have been successful. A cap-and trade program instituted by the EPA in 1990 has led to decreased acidification of lakes and streams and an estimated human health benefit of \$70 billion. The cost of this program is estimated between \$1-2 billion.²



Figure 1.1: Forest in Poland destroyed by sulfur emissions from a coal-fired power plant without sulfur emission controls. Courtesy of the US Geological Survey.

Utilities are not the only source for atmospheric sulfur. Automobiles are also adversely affected by sulfur compounds. Sulfur levels in automotive fuels have a profound effect on the efficacy of catalytic converters. Sulfur affects these emission control devices by strongly adsorbing to the precious metal catalysts, preventing the adsorption and reaction of hydrocarbons, nitrogen oxides, and carbon monoxide. The EPA estimates⁴ that reducing sulfur levels from 400 ppm to 50 ppm reduces emissions of hydrocarbons by 45.9%, NO_x by 7.01%, and CO by 31.12% (based on Tier 1 running specification) by reducing the poisoning effect of sulfur. Obviously, emissions of SO_x are also reduced by an amount equivalent to the sulfur reduction. The US national average sulfur level in automotive fuel in 1997 was 339 ppm.⁴

Producing energy in a clean and responsible manner can be accomplished in a number of ways. The use of non-fossil fuel energy sources such as solar, wind, and nuclear power will eventually replace fossil fuels. However, many of these technologies will require many years before they are able to provide the amounts of energy needed. In the immediate future, fossil fuel-based energy production will continue, and new technologies need to be developed in order to produce clean fuels to power our societies.

The present work focuses on new ways to remove sulfur compounds from petroleum. Sulfur compounds represent one of the most prevalent impurities found in crude oil. As the world market for crude oil tightens with increasing demand, lower quality oils containing higher levels of sulfur are used. Developing techniques to remove the sulfur

from these lower quality feedstocks efficiently will ensure that energy is available at a reasonable cost.

The development of the new desulfurization techniques in this Thesis begins with a study of polymer membrane reactors. These reactors offer a new way to perform hydrogenation reactions including, possibly, hydrodesulfurization. The fundamental reaction mechanisms in such reactors are studied to provide a basis for the development of desulfurization techniques. Although polymer membrane reactors ultimately proved unsuccessful for desulfurization, two new techniques for desulfurization are demonstrated and evaluated.

First, the removal of alkanethiols by heterogeneous reaction with metal oxides is presented. This method reduces the level of one category of sulfur compound to <20 ppm by weight sulfur by selectively reacting the thiols with certain metal oxides, forming metal thiolates. The metal thiolates are insoluble in hydrocarbons and water at sufficiently low temperatures, permitting their removal by filtration. The metal oxide can also be recovered by decomposing the thiolate with an oxidizing acid.

The second technique is the removal of sulfides and thiophene by oxidation using sulfuric acid. Sulfuric acid is shown to be a fast and effective oxidizer of aromatic and aliphatic sulfides, yielding sulfoxides and sulfones, which can then be extracted into a polar phase. Both of these techniques, plus the study of polymer membrane reaction mechanisms, are described in detail in this volume.

2. Background

2.1. *Petroleum Refining*

Refining crude oil is a complicated series of chemical processes designed to separate petroleum into a variety of useful products, each meeting certain compositional criteria. Refining begins by fractionating (distilling) crude oil into a series of streams with defined boiling ranges. Table 2.1 shows some of the fractions and their boiling ranges.

Fuels, including gasoline, diesel, and kerosene (jet fuel), are the most valuable products from petroleum. To enhance the quantity of these fuels produced from a single barrel of crude, heavier streams are cracked, or broken down into smaller molecules. Fluid catalytic cracking (FCC) typically utilizes a solid acid zeolite catalyst, often promoted with rare earth metals⁵ in a fluidized bed. Large molecules are broken down to create additional material in the naphtha range in order to produce more gasoline, a valuable product. The “cracked naphtha” stream often contains larger amounts of sulfur than virgin naphtha, since much of the sulfur in crude is in the form of heavy polynuclear aromatic molecules present in the FCC feed stream.

Two additional processes are used to improve the quality of the resulting fuels, particularly gasoline. Reforming uses Pt based catalysts to isomerize linear paraffins, such as *n*-hexane, to higher octane number branched paraffins like 2,3-dimethylbutane. Pt supported on chlorided alumina, sulfated zirconia, and zeolites are all used.⁶ The support alters the activity of the catalyst, with alumina being most active and zeolites being least

active. However, high activity catalysts are more susceptible to poisoning by sulfur and water.⁶ Removal of sulfur compounds before reforming gasoline streams is therefore required.

The second process used to improve the quality of gasoline is alkylation. Alkylation reacts *n*-butene with isobutane to create 2,2,4-trimethylpentane, also called isooctane, and other branched paraffins.⁷ Alkylation also uses an acid catalyst, but due to excessive coking, only liquid acid catalysts are currently used. Alkylation reactors blend either sulfuric or hydrofluoric acid with the butane/isobutene stream to create alkylate, a high quality gasoline that is blended into other gasoline streams.

The last major process used in oil refining is hydrotreating, or hydrodesulfurization (HDS). Crude petroleum typically contains from 0.1 wt% to 3.0 wt% sulfur, depending on the source. Crude from Norway and the North Sea typically have the lowest sulfur concentration, while that from the Arabian Peninsula contains the most.⁸ Table 2.2 shows the distribution of some aromatic sulfur species found in petroleum by boiling point. The most common light species, denoted “gasoline-range sulfur” in the table, are methane-, ethane-, and *t*-butanethiol, dimethyl sulfide, carbonyl sulfide (COS), and tetrahydrothiophene.⁹

Table 2.1: Petroleum distillate fractions and their boiling points. Adapted from Pafko.¹⁰

Distillate Fraction	Boiling Point (°C)	Carbon Number
Gases / LPG	<30	1-4
Straight-run gasoline	30-210	5-12
Naphtha	100-200	8-12
Kerosene	150-250	11-13
Diesel & fuel oil	160-400	13-17
Atmospheric gas oil	220-345	17-20
Heavy fuel oil	315-540	20-45
Atmospheric residue	>450	30+
Vacuum residue	>615	60+

Table 2.2: Aromatic sulfur species found in petroleum. Data from ¹¹.

Sulfur Species	Boiling Range (°F)
Gasoline-range sulfur	< 425
Benzothiophene	429
C ₁ -benzothiophenes	430-500
C ₂ -benzothiophenes	500-535
C ₃ -benzothiophenes	535-584
C ₄₊ -benzothiophenes	584-630
Dibenzothiophene	633
C ₁ -dibenzothiophenes	635-685
C ₂ -dibenzothiophenes	685-720
4,6-dimethyldibenzothiophene	691
C ₃₊ -dibenzothiophenes	720

HDS reduces these sulfur-containing compounds in a stream using hydrogen and a catalyst. HDS can be performed either before FCC or after, depending on the refinery design. HDS must be performed before reforming, however, due to the poisoning effect of sulfur on Pt. In the HDS reactor, sulfur is reduced, liberating H₂S, which is then removed from the flue gas by amine scrubbing. HDS is the primary desulfurization technology used today,¹² although caustic washing to remove low molecular weight thiols is also performed.¹³ Most HDS operations also remove nitrogen compounds and some metal impurities.

Typical operating conditions for the HDS reactor are 300-450°C and 35-270 bar.¹⁴ However, under these harsh conditions, olefins are also hydrogenated, leading to a loss of octane rating and excess hydrogen consumption. Under mild HDS conditions, H₂S can react with olefins in the reactor to create recombinant mercaptans which are linear or branched thiols of typically 5-12 carbons. An example of this reaction is shown in Figure 2.1. The reaction is completely analogous to the formation of alcohols by hydration of olefins. The formation of recombinant mercaptans causes sulfur to be retained in the product, limiting the effectiveness of the HDS process. The balance between degree of sulfur removal and degradation of fuel quality provides the impetus for continued research into HDS catalysts and process designs.^{12,15}



Figure 2.1: Example recombination reaction producing an alkanethiol in an HDS reactor.

By far, the most common catalysts used in HDS are cobalt or nickel promoted molybdenum sulfide.^{12,14} The development of improved catalysts for HDS is the focus of virtually all research in HDS. The leader in the field of HDS catalyst development is Haldor-Topsøe, with much of the original characterization of cobalt promoted molybdenum catalysts attributed to Henrik Topsøe and coworkers.^{16,17} Development of nickel promoted molybdenum sulfide catalysts for HDS of diesel fuel, which contains more substituted polynuclear aromatic sulfur compounds than gasoline, is ongoing.¹²

2.1.1.1.1. New Developments in Desulfurization

Most research in the field of desulfurization is focused into three categories: oxidative desulfurization, metabolism of sulfur compounds using microbes, and selective adsorbents. Of these three, only oxidative desulfurization is being widely developed for commercial use.

Oxidative desulfurization (ODS) is based on the removal of heavy sulfides, usually in the form of polynuclear aromatics where one ring is a thiophene structure. In ODS, these compounds are oxidized by adding one or two oxygen atoms to the sulfur without breaking any carbon-sulfur bonds, yielding the sulfoxide and sulfone, respectively. These oxidized compounds can then be effectively extracted or adsorbed from the petroleum stream. A detailed explanation of ODS, including the commercial processes, is given in section 5.1.

Removal of sulfur by metabolism using microbes is a new concept to improve the refining process using biotechnology. Several species of bacteria have the ability to metabolize organosulfur compounds in one of three ways: reductive C-S bond cleavage, oxidative C-S bond cleavage, or oxidative C-C bond cleavage. For example, *desulfovibrio desulfuricans* can metabolize dibenzothiophene, releasing the sulfur as H₂S in the presence of a reducing agent.¹⁸ The genes responsible for the “4S” metabolic pathway (oxidative C-S cleavage), in which organosulfur is oxidized to sulfite or sulfate, have been transferred to several bacterial species¹⁹ after its initial discovery in *Rhodococcus erythropolis* strain IGTS8.²⁰ SO₂ in flue gas has also been removed by reaction with water to sulfite followed by metabolism to sulfate.²¹

Biological removal of sulfur has several limitations that prevent it from being applied today.²² The metabolism of sulfur compounds is typically slow compared to chemical reactions. Sulfur-metabolizing bacteria have been shown to reduce the sulfur content of diesel fuel from 535 ppm to 75 ppm in 24 hours.²³ The rate of metabolism is rate limiting in the process, though mass transfer resistance from the oil/water interface to the microbe is also slow compared to the rate of transfer of the sulfur compound to the oil-water interface.²⁴ Large amounts of biomass are needed (typically 2.5 g biomass per g sulfur), and biological systems must be kept alive to function, which can be difficult under the variable input conditions found in refineries. The rate of desulfurization depends strongly on pH, temperature, and dissolved oxygen concentration.²⁵ Separation of the cells from the oil can also be difficult²⁶, and immobilized cells often have lower activity and limited lifetimes.^{19,22}

Adsorbents for sulfur compounds are also commonly studied. Removal of H₂S, dibenzothiophene, and other sulfur compounds is performed over zeolites^{27,28}, aluminosilicates²⁹, carbon aerogels³⁰, activated carbon, alumina²⁸, and zinc oxide³¹, for example. Adsorbents have been shown to be highly selective for sulfur compounds, including difficult to hydrotreat molecules such as 4,6-dimethyldibenzothiophene.³² While highly effective, these adsorbents are difficult to regenerate, often requiring calcination^{28,31} or solvent washing.

The adsorption capacity of many adsorbents is low. The capacity of an unspecified transition metal on silica adsorbent was measured at 0.123 mol S per mol metal.³³ Economical clay materials displayed capacities of 1-4 mg S compound per g clay³⁴, thus requiring huge amounts of adsorbent. Pressure swing adsorption is not effective due to the strong interaction of sulfur with the adsorbent. Large adsorbent beds are therefore required to minimize the number of turnovers, and multiple beds are needed to keep a refinery on-stream. Repeated calcinations can also lead to a loss of surface area due to sintering, reducing the amount of sulfur a bed can remove. Most research efforts therefore focus on creating less expensive³⁵ and higher surface area materials³⁶.

Most commercial desulfurization processes, such as ExxonMobil's SCANfining process¹⁵ and UniPure's ASR-2³⁷ involve combinations of several desulfurization technologies. These combinations remove sulfur to low levels by focusing on the strengths of each technology. SCANfining, for example, can involve mild HDS,

mercaptan extraction, and amine scrubbing to remove H₂S. ASR-2, which is an ODS process, includes two extraction and several adsorption steps.

Despite these research areas, the primary method for sulfur removal is still HDS, which is a conventional, heterogeneous hydrogenation reaction. The extensive use of catalytic hydrogenation for sulfur removal suggests that better techniques for desulfurization may be found in atypical hydrogenation reactors. Before they can be applied to desulfurization, however, the operation of different types of hydrogenation reactors must be understood.

2.2. Hydrogenation Reactors

Hydrogenation reactions are critically important in the modern chemical industries. The petrochemical industry uses vast amounts of hydrogen to reform petroleum during catalytic cracking and hydrotreating. Edible oils are hydrogenated to convert unsaturated vegetable oils into semisolids used in margarine.^{38,39} Hydrogenations are used to convert phenol to ϵ -caprolactam, a precursor of nylon.⁴⁰ Alcohols are formed from esters or fatty acids, as are amines from nitriles, through hydrogenation reactions.⁴¹ Hydrogenation reactions are a common and integral part of modern chemical processes.

Virtually all commercial hydrogenations are performed using packed bed reactor technology that has been refined for many years. While this technology has proven useful and efficient, it has begun to reach its limitations in some areas. High temperatures and pressures, usually ranging from 120-400°C and 1-1000 atmospheres, limit hydrogenation

to stable molecules.⁴² Alternate types of hydrogenation reactors do exist, however. Three types of hydrogenation reactors are discussed below.

2.2.1. Conventional Reactors

By far, most hydrogenation reactions in commercial applications today are performed in conventional packed bed or slurry reactors. Since the addition of hydrogen to most functional groups or double bonds is exothermic and thermodynamically favorable, mixing the reactant, hydrogen, and catalyst together is sufficient to perform the reaction. In conventional reactors, the bed or solid fraction of the slurry is made up of catalyst in the form of a metal or metal oxide on an inorganic support of alumina, silica, or carbon. The supports provide a high specific surface area to reduce the required volume of catalyst and improve catalyst utilization. The active metal lowers the activation energy of the reaction sufficiently to allow a reasonable reaction velocity.

The catalysts of choice are noble metals such as platinum, palladium, rhodium, and ruthenium, with nickel as a lower-cost alternative that requires harsher conditions. Osmium and iridium are occasionally used as well. Copper chromite serves to convert esters to alcohols, while cobalt and iron hydrogenate nitriles.⁴³ The catalysts are tailored to the specific reaction to ensure high yield with minimal side reactions. The catalyst loading, surface area, and resistance to poisoning are all important factors in catalyst choice.⁴³

Conventional reactors can be operated with either a gas phase or a liquid phase unsaturated molecule. Gas phase hydrogenation is used for low molecular weight species and does not suffer from the hydrogen mass transfer limitations experienced in liquid phase reactors. Consequently, gas phase hydrogenation reactions can be performed at much lower pressures. Some examples of gas phase hydrogenations are the production of cyclohexane from benzene (both gas and liquid phase reactions are used industrially), production of oxo-alcohols from aldehydes, production of allyl alcohols, ammonia synthesis, and methanol synthesis.⁴⁴

Conventional liquid phase reactors attempt to dissolve gaseous hydrogen into the liquid reactant, where it is then transported to the catalytic surface, dissociates, and reacts. The dissolution of the hydrogen is achieved by bubbling hydrogen through the packed bed, or by intense mixing in a slurry reactor at high pressures. Despite the use of pressures ranging from 1-1000 atmospheres, the solubility of hydrogen remains low. As a result, most conventional reactors are limited by the rate of hydrogen transport to the catalyst surface.⁴³ An exception is the hydrogenation of edible oils, which is usually limited by the rate of heat removal. Bubbling the gas through a packed bed also requires large compressors, both to pressurize the hydrogen initially and to recycle the gas that does not dissolve.⁴² Figure 2.2 gives an example of this type of reactor.

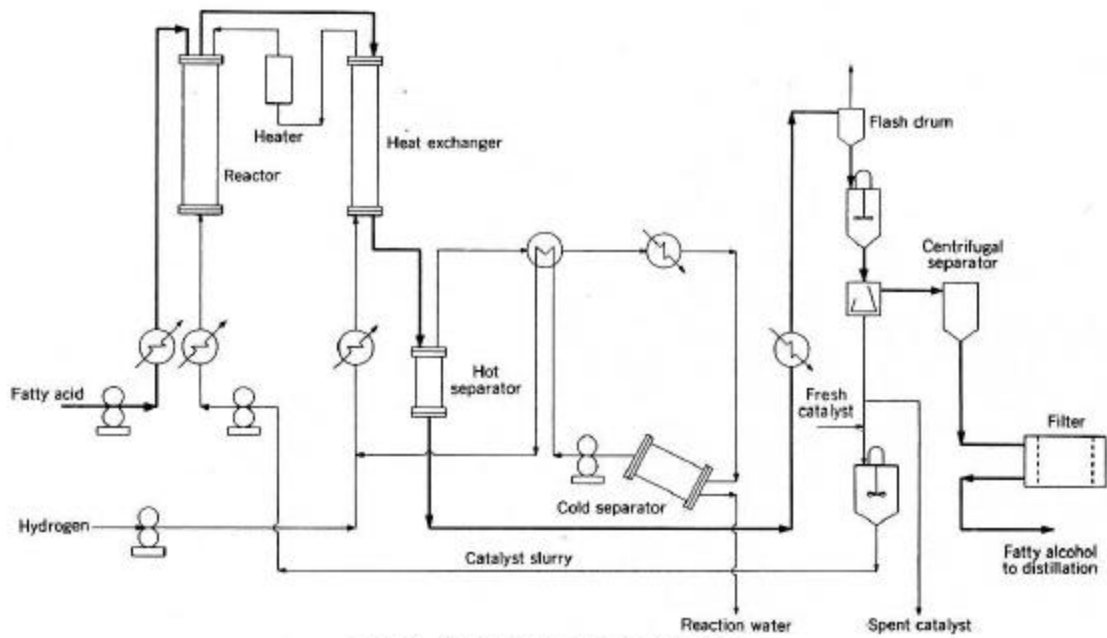


Figure 2.2: A conventional slurry hydrogenation reactor and associated processes. Adapted from ⁴¹.

The temperature of the reaction must be carefully controlled. Typical temperatures for hydrogenations range from 120-400°C. Higher temperatures increase the reaction rate, but usually reduce the selectivity of the reaction, allowing more side reactions to occur. Elevated temperatures also reduce catalyst life due to coking and similar blockages.⁴²

An engineer designing a conventional hydrogenation reactor has a number of variables with which to optimize the performance. Increases in temperature, pressure, agitation rate, and catalyst loading all increase the reaction rate, but with varying effects on selectivity. The rate of hydrogen supplied to the reactor and the catalyst choice also affect the selectivity, as can the presence of solvent.⁴² Many years of refinement in this area has led to the efficient operation of these reactors, although safety remains an important issue.

2.2.2. Palladium Membrane Reactors

A second type of hydrogenation reactor uses a thin membrane of palladium metal. Palladium has a uniquely high permeability to hydrogen, and it is also an active catalyst for many types of hydrogenation. Membranes are created by depositing a thin layer of palladium metal onto a porous support, such as porous stainless steel, porous ceramics, or Vycor glass by one of several different deposition methods.⁴⁵

The most widely studied reaction in palladium membrane reactors is the dehydrogenation of saturated hydrocarbons. Typically, these reactions are performed in conventional reactors over platinum-group metal catalysts. The reactions are equilibrium

limited, but can be pushed towards the product via elevated temperatures, usually 700-800°C.

Studies have concluded that countercurrent palladium membrane reactors, where gas phase cyclohexane is reacted near a palladium membrane with a low pressure sweep gas on the other side, can produce nearly 100% conversion to benzene.⁴⁶ In these reactors, the membrane acts to remove hydrogen from the reactant stream, allowing the reaction to proceed to completion. Membranes made from alloys, such as Pd-Au-Ag, which are more permeable to hydrogen than pure Pd, show faster overall reaction rates. The membrane, however, is also shown to play little part in the catalysis of the reaction. Instead, conventional catalyst packed on the reactant side of the membrane is responsible for the reaction.⁴⁶ Such reactors have shown similar results for the steam reforming of methane and methanol.⁴⁵

Palladium membrane reactors provide a way to simultaneously react and separate a given mixture, similar to reactive distillation. Such a reactor reduces the number of unit operations required for a given process. Temperatures around 500°C are still required for the reaction. By comparison, the reactors studied in the present work are capable of dehydrogenation reactions at room temperature and can remove generated protons by using an applied voltage as the driving force.

2.2.3. Polymer Electrolyte Membrane Hydrogenation Reactors

Polymer electrolyte membrane hydrogenation reactors (PEMHRs) are electrochemical systems using a polymer membrane to separate the anode and the cathode. The membrane used in the current work is Nafion[®] (DuPont), which is a sulfonated fluoropolymer. The sulfonic acid groups form clusters, or ionic domains, within a fluorocarbon matrix. In an aqueous environment, these clusters swell with water, hydrating the sulfonic acid groups and creating a cation-conducting electrolyte within the clusters.⁴⁷

In a polymer electrolyte membrane hydrogenation reactor, the membrane separates two compartments, each with an electrode. For hydrogenation reactions, water is circulated through the anode compartment, while the liquid to be hydrogenated is placed in the cathode compartment. When a voltage is applied to the electrodes, the water undergoes electrolysis, splitting into oxygen atoms, protons, and electrons. The electrons are carried out through the anode, while the protons, under the influence of a concentration gradient and the electric field, migrate through the membrane via the swollen ionic domains. Two oxygen atoms combine to form molecular oxygen on the anode and leave the system in the form of gas bubbles.

Hydrogenation occurs once the protons reach the cathode. At the cathode, the protons are reduced to atomic hydrogen, which then react to hydrogenate unsaturated compounds in the catholyte. It is also possible for two hydrogen atoms to react and leave the system as hydrogen gas.

PEMHRs have several advantages over conventional hydrogenation reactors. When the protons reach the cathode, they are converted into adsorbed hydrogen atoms directly. Elevated pressure to dissolve molecular hydrogen in the liquid is not required. By controlling the current density, the rate of hydrogen supplied to the surface can be easily controlled. The use of water as the hydrogen source limits PEMHRs to operation below 100°C unless pressurized. The lower temperatures allow thermally unstable molecules to be hydrogenated while using the galvanostatically controlled current density to increase the transport rate of hydrogen to the surface, compensating for the decreased reaction rate constant.

PEMHRs are also relatively easy to set up at the laboratory scale, and they are much safer than conventional reactors. A conventional reactor mixes hydrogen, a catalyst, and flammable hydrocarbon together at high temperature and pressure. Introducing a small amount of oxygen to the system, perhaps from a leak, is enough to cause a catastrophic explosion. PEMHRs do not use compressed hydrogen, operate at lower pressures and temperatures, and half of the liquid in the reactor at any given time is water, making them considerably safer.

Research on PEMHRs has been limited to only a few groups. Most of the early work was performed by Ogumi.⁴⁸⁻⁵² His group studied hydrogenation of olefins, but most of their remaining work was in oxidation of organic molecules or reduction of other functions such as nitro groups in a PEMR. Sarrazin developed a water electrolyzer based

on the PEMHR principle.⁵³ More recently, Pintauro et al. studied the hydrogenation of edible oils in a PEMHR.^{38,39,54} Other recent work^{55,56} has focused on other unique applications of PEMHR-style reactors, such as electroreduction of CO₂, albeit with limited success.

The PEMHR was chosen for study due its unique control parameters, such as the ability to directly control the rate of formation of surface adsorbed hydrogen by altering the current. Before a PEMHR can be applied to desulfurization, however, several fundamental aspects of its operation need to be determined.

3. Reaction Mechanisms in Polymer Electrolyte Membrane Hydrogenation Reactors

3.1. A Comparison of Catalytic Hydrogenation Mechanisms in Polymer Membrane Hydrogenation Reactors

3.1.1. Introduction

Hydrogenation reactions are an integral part of the manufacture of many chemicals, from pharmaceuticals to petrochemicals. Most hydrogenations are performed in two- or three-phase reactors in which the gas or liquid to be hydrogenated is mixed with hydrogen over a catalyst, typically Pt-group metals or alloys. The rate of reaction can be controlled in several ways including altering the partial pressure of hydrogen in order to increase the concentration of hydrogen on the surface of the catalyst.

The polymer electrolyte membrane hydrogenation reactor (PEMHR) performs hydrogenations using hydrogen produced from electrolysis of water.⁴⁸ A polymer electrolyte membrane separates the water from the organic phase. A porous catalyst on an electrically conductive support (e.g. carbon) is pressed against the polymer membrane at the organic side of the membrane; this forms the essential three phase interface between the polymer electrolyte membrane (PEM), the catalyst, and the organic phase.

A second electrode is placed in the aqueous phase; it does not need to be in direct contact with the polymer membrane. When a voltage is applied between the electrode in the aqueous phase (the anode) and the electrode at the membrane-organic phase interface (the cathode), water is oxidized at the anode, generating molecular oxygen and protons. The protons move through the membrane driven by an electrical potential gradient. The membrane is permeable only to cations, so only protons move through the membrane. An electron current passes through an external circuit from the anode to the cathode to balance the ion current. The protons and electrons recombine at the cathode, directly forming surface adsorbed hydrogen. The cathode may then act as a catalyst to promote the hydrogenation of an unsaturated compound. At steady state, the adsorbed hydrogen formed at the cathode either hydrogenates the organic or combines with another adsorbed hydrogen atom and desorbs as H_2 ; the current is equal to the sum of the rates of these two reactions multiplied by two. The reaction selectivity is the rate of the hydrogenation reaction divided by half the current.

The route of formation of the surface adsorbed hydrogen differentiates the PEMHR from conventional three phase hydrogenation reactors. A conventional hydrogenation reactor relies on the dissociative adsorption of di-hydrogen molecules. In the PEMHR, adsorbed hydrogen is formed directly during reduction of the protons. Both sources of hydrogen form adsorbed hydrogen on the catalyst surface.⁵⁷ The advantage of the PEMHR is that adsorbed hydrogen can be supplied to the catalyst surface in a liquid phase without the need for high pressure.

In a conventional hydrogenation reactor using molecular hydrogen, the partial pressure of hydrogen dictates the rate of hydrogen adsorption onto the catalyst surface. In a PEMHR, the applied current is a direct measurement of the rate of arrival of protons to the catalyst surface, where they become adsorbed hydrogen. Increasing the current is analogous to increasing the partial pressure of hydrogen in a conventional three phase reactor, as both increase the rate of arrival of hydrogen at the catalyst surface.

Since adsorbed hydrogen can be formed directly on any cathode surface, metals that do not readily dissociate hydrogen might be activated for hydrogenations in a PEMHR. To examine this possibility and to confirm the analogy between current density and partial pressure, a PEMHR was used to evaluate the hydrogenation of olefin and ketone groups on the Pt group metals, known for their catalytic activity, and Au group metals, which are typically inactive.

3.1.2. Experimental

Catalytic cathodes were made using Pt, Pd, Ni, Au, Ag, and Cu by suspending 50 mg of the powdered metal in about 20 mL of isopropanol. The nominal metal particle size was 0.3-2.5 μm . 125 mg of 5 wt% Nafion solution (Ion Power, Inc., Liquion 1100) was added to the suspension. The suspension was sprayed onto carbon cloth (E-tek, Inc., Type B-1) using an artist's airbrush. The metal loadings were circa 8 mg/cm^2 and the Nafion load was 1 mg/cm^2 . The resulting layers of metal powder on the electrodes were evenly dispersed. The electrodes were dried at 60°C for 1 hour and then 140°C for 20 minutes. The electrodes were pressed onto Nafion 115 membranes (Ion Power, Inc.) for 3 minutes

at 140°C at 1.7 MPa. A Pt mesh anode was suspended in close proximity to the plain Nafion side of the membrane-electrode-assembly. This process is shown in Figure 3.1.

The reactor consists of two graphite plates with a serpentine flow channel, as shown in Figure 3.2. The graphite plates were backed with aluminum blocks with a Teflon spacer between. The Pt mesh anode and the pressed membrane/electrode were sandwiched between the graphite plates and the whole assembly was bolted together. A Viton gasket sealed the membrane-graphite interface. The total active area of the cell is 5 cm².

A solution of 40 mL 1-decene (Fluka, 95%) and 400 mL cyclohexane (Aldrich, 99%) was prepared for the olefin studies. A solution of 29 mL 4heptanone (Alfa Aesar, 98%) and 400 mL cyclohexane was prepared for the carbonyl hydrogenation studies. A 1:10 by volume solution of acetone (Fisher, 99.5%) in deionized water was also prepared for the carbonyl hydrogenation studies.

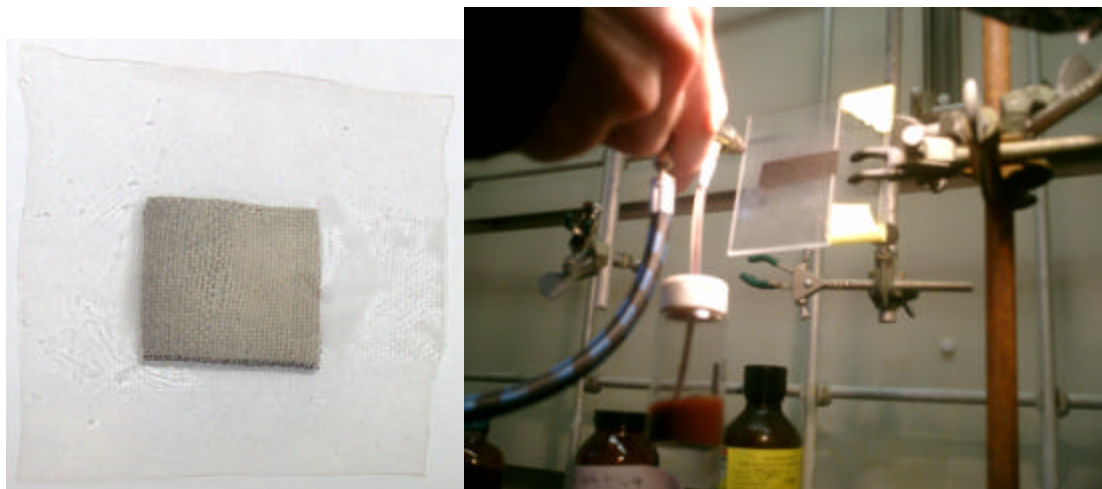


Figure 3.1: Photographs of sample MEAs created by the airbrushing technique. On left, an MEA after pressing showing good dispersion of Ag powder over the initially black carbon cloth. On right, spraying of Cu powder onto carbon cloth using the airbrush. The carbon cloth is pinned at one edge between glass slides during spraying.

The reactor was run in batch mode using the design shown in Figure 3.3. Ten mL of each solution were circulated through the reactor for one hour, permitting sufficient conversion to effectively measure the products with gas chromatography. The anode was fed with 20 mL of 0.1 M H_2SO_4 . The sulfuric acid permitted the anode to be separated from the membrane to promote uniform proton current distribution with negligible voltage drop. The proton current from the anode to the cathode was controlled by a galvanostat (Arbin Instruments MSTAT4+). In the studies reported here the current was limited to 0-30 mA cm^{-2} (typically the applied voltage was $\sim 2\text{V}$). All reactions were performed at 50°C . After the reaction, each organic solution was analyzed by gas chromatography for the reactant and saturated product. Small amounts of octane (or ethanol for the acetone solution) were added to the stock solutions for use as an internal standard. Calibration of peak area was performed using solutions of known product concentration.

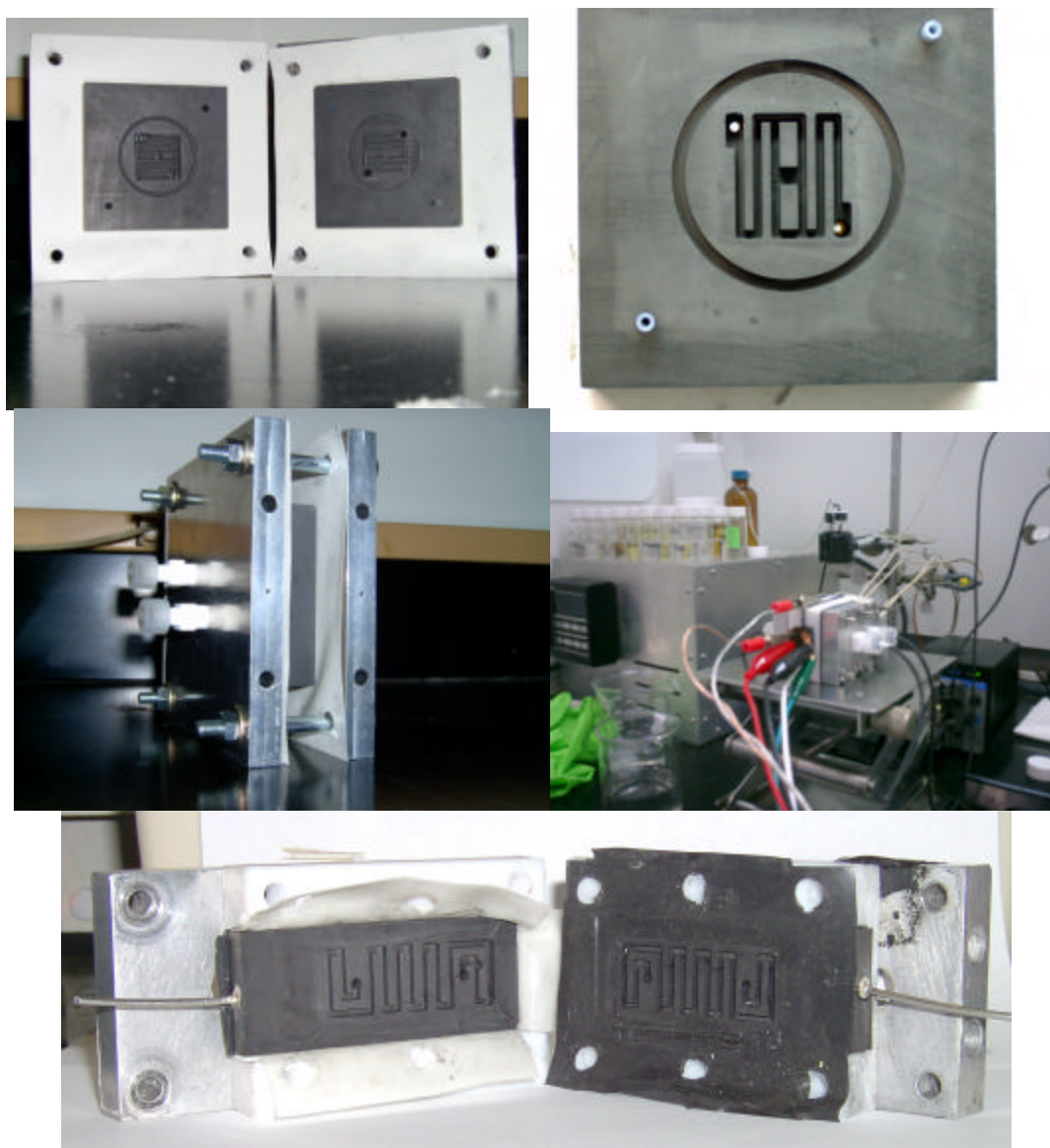


Figure 3.2: Photographs of the membrane reactor. Clockwise from top left are 1) the two reactor plates with gaskets; 2) detail of one reactor plate showing flow channels and o-ring groove; 3) previous version of reactor in operation with galvanostat and cartridge heaters attached; 4) previous version of reactor showing flow channels and gaskets; and 5) assembled reactor showing aluminum backing plates and Teflon tubing adapters.

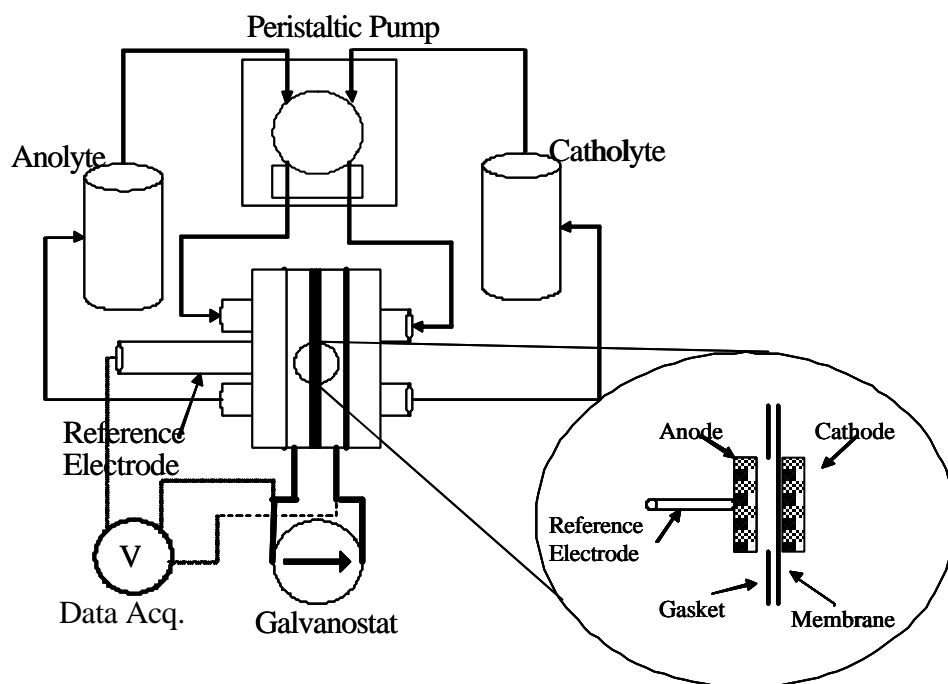


Figure 3.3: Experimental apparatus schematic.

3.1.3. Results

3.1.3.1. Olefins

Only Pt and Pd showed significant activity for the hydrogenation of 1-decene to decane under the experimental conditions. Figure 3.4 and Figure 3.5 show the variation in rate of hydrogenation with current density, i . Pd was slightly more active than Pt, consistent with observations in conventional hydrogenation reactors and in previous studies of this type of reactor.⁵⁴ The reaction rate for olefin hydrogenation over Pd and Pt increased with the square root of the current. Decene hydrogenation was 100 times slower on Ni and Cu, Ag and Au catalysts as shown in Figure 3.5. Proton current to electrodes with these metals primarily evolved hydrogen gas. There was no systematic variation of rate of olefin hydrogenation with current for the low activity metals; the rates of hydrogenation on Ni and the group IB metals all seem to be independent of the current.

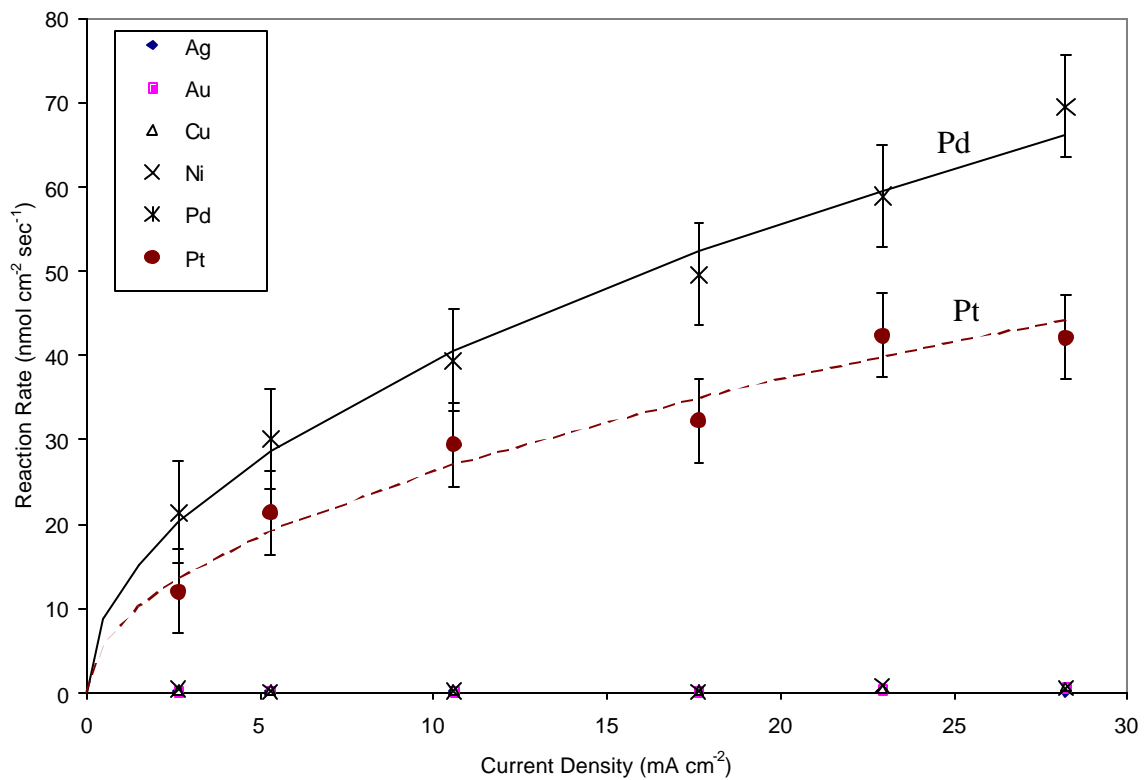


Figure 3.4: Rate of hydrogenation of 1-decene over various catalysts. Lines are fits to $ki^{0.5}$. The values of k are listed in Table 3.2.

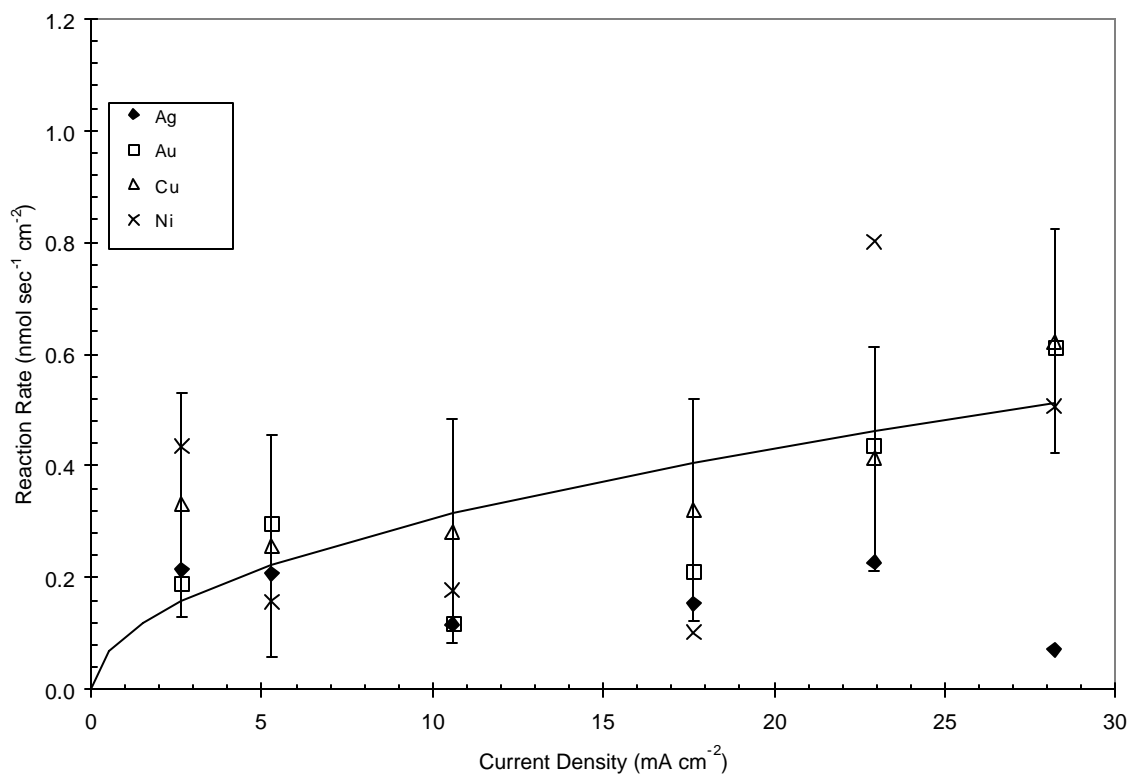


Figure 3.5: Rate of hydrogenation of 1-decene over ineffective catalysts. Data enlarged from Figure 3.4, note the change in scale. Uncertainty in the data is considerable, shown by sample error bars for Cu. Line is an example fit to $i^{0.5}$.

3.1.3.2. Ketones

Under the experimental conditions, none of the metals showed activity for hydrogenation of 4-heptanone. Similar results have been previously reported.⁵⁸ One possible explanation of this result is that the butyl chains sterically block access to the adsorbed carbonyl. Acetone hydrogenation over Pt and Cu was examined, and the results are summarized in Figure 3.6. The rate of acetone hydrogenation over Pt was one order of magnitude less than for decene on Pt. The rate of hydrogenation of acetone over Cu was approximately one order of magnitude less than that over Pt, but it was comparable to the rate of decene hydrogenation over Cu. The extremely low reactivity of 4-heptanone compared to acetone suggests that there is a steric effect caused by the alkyl chains, with longer chains blocking access to the carbonyl. The relative reaction rates are summarized in Table 3.1.

Table 3.1: Relative rates of hydrogenation of olefin and ketone species in a PEMHR.

Cathode	Relative hydrogenation reaction rate
Pt	1-decene > acetone >> 4-heptanone
Cu	1-decene ~ acetone >> 4-heptanone

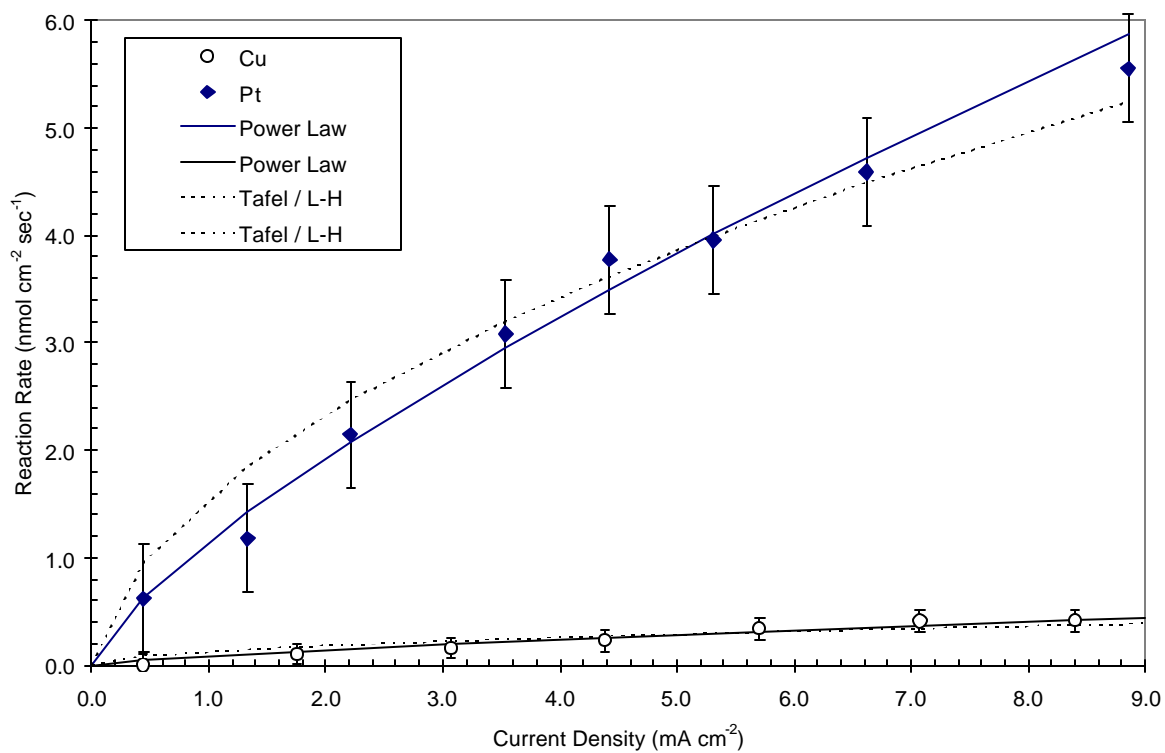


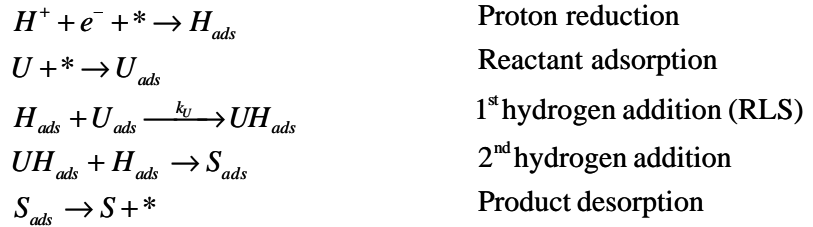
Figure 3.6: Rate of hydrogenation of acetone over Pt and Cu catalysts. Lines are fits to the Tafel / Langmuir-Hinshelwood mechanism and the power law, $k_i^{0.75}$. The fit parameters are listed in Table 3.2.

3.1.4. Discussion

The results of the olefin and carbonyl hydrogenation study, shown in Figure 3.4 through Figure 3.6, reveal important mechanistic information about hydrogenations in PEMHRs. Catalytic hydrogenations are generally accepted to follow the Horiuti-Polanyi mechanism in which the addition of the first hydrogen atom to the adsorbed organic molecule is rate limiting.^{59,60} Different rate laws and reaction selectivity can be derived from this starting point, each yielding different reaction orders depending on the reaction steps involved with molecular hydrogen formation. Due to the complexities associated with most hydrogenation reactions, rate laws are often determined empirically in the form $rate = kP_{H_2}^x P_{unsat}^y$, where P_n is the partial pressure of reactant n and x and y are between 0-1.⁶⁰

Figure 3.7 summarizes the steps for hydrogenation by the Horiuti-Polyani mechanism. The rate of adsorbed hydrogen formation is equal to the current. Adsorbed hydrogen atoms add sequentially to an adsorbed unsaturated hydrocarbon molecule. The rate-limiting step is normally hypothesized to be the addition of the first hydrogen. Adsorbed hydrogen can also recombine and desorb from the catalyst surface. Two common mechanisms for hydrogen recombination found in the literature are the Langmuir-Hinshelwood desorption mechanism where associative desorption occurs between two neutral hydrogen atoms from the surface, and an Eley-Rideal mechanism in which a neutral hydrogen atom on the surface reacts with an incoming proton in a combination reduction-desorption step.⁶¹ In the electrochemical literature these are called the Tafel reaction and the Heyrovski reaction respectively. These two mechanisms result in

different functional relationships between current and hydrogenation rate. Figure 3.7 shows the steps in these mechanisms and the resulting rate laws. The rate laws are simplified by assuming a constant coverage of organic species, equivalent to assuming non-competitive adsorption which has been suggested to occur.⁶² The two rate laws each have a single adjustable fitting parameter. The parameter to fit the Eley-Rideal mechanism is the group $k_U \Theta_U / k_{HH}$, where Θ_U is the surface coverage of unsaturated hydrocarbon, k_U is the rate constant for the first hydrogen addition and k_{HH} is the rate constant of molecular hydrogen formation by the Heyrovski reaction. The fit parameter for the Langmuir-Hinshelwood mechanism is $(k_U \Theta_U)^2 / 2k_{HT}$, where k_{HT} is the rate constant for molecular hydrogen formation by the Tafel reaction.



Heyrovski / Eley-Rideal	Tafel / Langmuir-Hinshelwood
$H_{ads} + H^+ + e^- \xrightarrow{k_{HH}} H_2 + *$	$2H_{ads} \xrightarrow{k_{HT}} H_2 + 2*$ Hydrogen Desorption
	Rate Law
$\frac{i}{2F} = k_{HH} \Theta_H \frac{i}{F} + k_U \Theta_U \Theta_H$ $\Theta_H = \frac{\frac{i}{2F}}{k_{HH} \frac{i}{F} + k_U \Theta_U}$ $r = k_U \Theta_H \Theta_U = \frac{\frac{i}{2F}}{\left(\frac{k_{HH}}{k_U \Theta_U}\right) \frac{i}{F} + 1}$	$\frac{i}{2F} = k_{HT} \Theta_H^2 + k_U \Theta_U \Theta_H$ $\Theta_H = \left(\frac{i}{2F k_{HT}} + \left(\frac{k_U \Theta_U}{2k_{HT}} \right)^2 \right)^{1/2} - \frac{k_U \Theta_U}{2k_{HT}}$ $r = k_U \Theta_H \Theta_U = \left(\frac{i}{F} \frac{(k_U \Theta_U)^2}{2k_{HT}} + \left(\frac{(k_U \Theta_U)^2}{2k_{HT}} \right)^2 \right)^{1/2} - \frac{(k_U \Theta_U)^2}{2k_{HT}}$

Figure 3.7: Comparison of two common hydrogenation mechanisms. Rate equations are simplified by assuming constant surface coverage of organic. F is Faraday's constant, U is the unsaturated organic species, and S is the saturated organic species.

Figure 3.8 provides a comparison between the fit of these two mechanisms to the experimental data for hydrogenation of 1-decene. The power law fit of $k^{0.5}$ is also shown. All three laws match the experimental data well; the data does not discriminate between the models. All of the fitting parameters are given in Table 2.

The two mechanisms shown in Figure 3.7 both predict reaction rates lower than the experimental values at low current density. The reaction rates at low current, particularly on Pd, may be higher than expected due to palladium's ability to absorb hydrogen into the bulk in large quantities⁶³, an effect enhanced by the negative potential applied to the cathode. Absorption into the bulk may lower the rate of desorption of hydrogen, though this hydrogen is still active for hydrogenations.⁵⁸ An alternative explanation is that the predicted rates should be higher at the low currents and the model over-estimates the reaction rates at high current density. This could be the case if hydrogen adsorption and recombination on the carbon support became significant when the hydrogen coverage on the metal catalyst surface became saturated.

The analogy between current and hydrogen pressure becomes clear upon closer inspection of the rate laws derived in Figure 3.7. The Eley-Rideal mechanism with the simplifying assumption of constant organic surface coverage becomes a monomolecular adsorption (of H^+) followed by a surface reaction first order in hydrogen coverage. If such a reaction occurred from the gas phase, the resulting rate law would be

$$r = \frac{k_1 P_H}{1 + k_2 P_H} \quad (3.1)$$

where P_H is the pressure of the "monomolecular" hydrogen gas. This familiar rate law is the same form obtained in Figure 3.7, but with pressure replacing current.

The relationship between current and pressure also arises in the Langmuir-Hinshelwood mechanism from Figure 3.7. In deriving kinetic expressions of this type, the steady state surface coverage of a species is found by equating the rates of adsorption and desorption. Following Langmuir⁶⁴, the rate of adsorption of hydrogen from the gas is $kP_H(1-\Theta_H)^2$. In a PEMHR, the rate of adsorption is i/F . The current term in any of the expressions in the Langmuir-Hinshelwood mechanism shown in Figure 3.7 can be replaced by $kP_H(1-\Theta_H)^2$ to yield the same result as if the derivation were performed for a gas phase reaction.

In addition to the mechanisms presented in Figure 3.7, the data is also well fit by $k_i^{0.5}$. Dependencies of $(P_{H_2})^{0.5}$ are found in traditional catalytic hydrogenation studies⁶⁵ and result from one hydrogen atom being involved in the rate limiting step. The Tafel / Langmuir-Hinshelwood mechanism in Figure 3.7 shows a very similar dependence.

Table 3.2: Fitting parameters for all mechanisms. Current density, i , has units mA cm^{-2} except in the power laws in which the units are $\text{nmol sec}^{-1} \text{cm}^{-2}$.

Rate Law	Parameter	1-Decene			Acetone	
		Pt	Pd	Cu	Pt	Cu
Tafel / Langmuir-Hinshelwood	$(k_U\Theta_U)^2/2k_{HT}$	10.5	31.6	---	0.338	0.0016
Heyrovski / Eley-Rideal	$k_U\Theta_U/k_{HH}$	58.5	121.8	---	---	---
Rate = $k_i^{0.5}$	k	3.66	5.47	0.042	---	---
Rate = $k_i^{0.75}$	k	---	---	---	0.333	0.0248

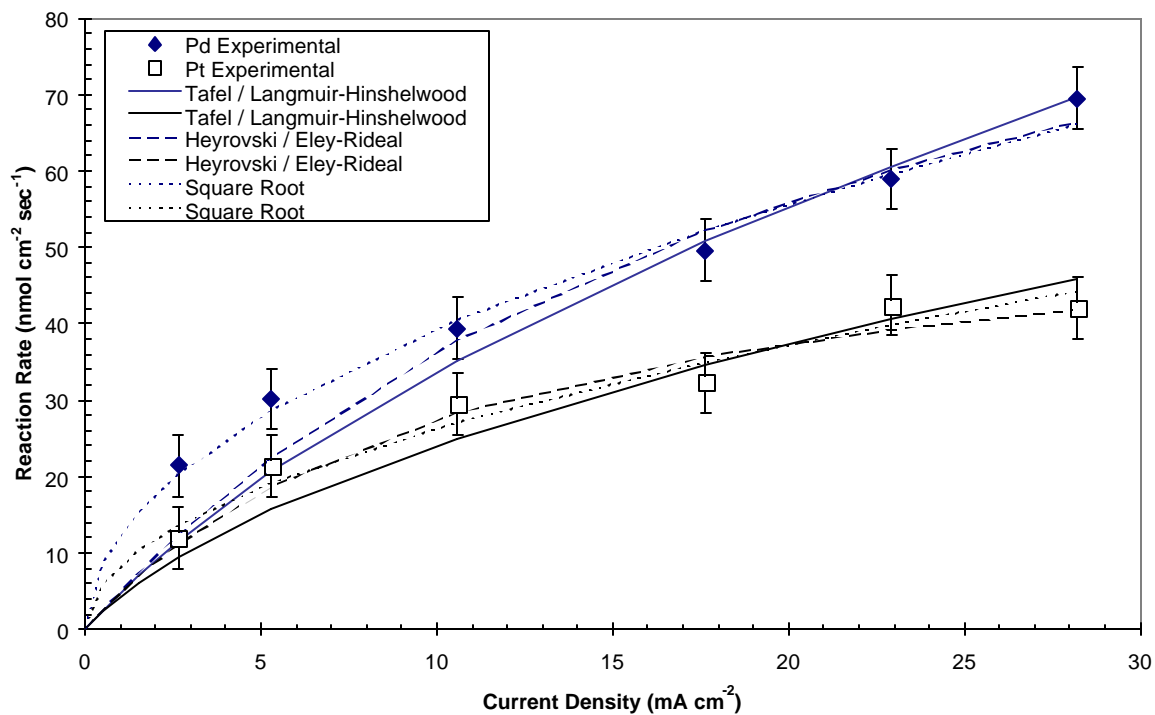


Figure 3.8: Rate of hydrogenation of 1-decene over Pt and Pd catalysts (from Figure 3.4) compared to Langmuir-Hinshelwood and Eley-Rideal style mechanisms. The fit of the power law $k^{0.5}$ is also shown.

The acetone hydrogenation results, shown in Figure 3.6, are not fit particularly well by either of these rate laws. Instead, a better fit was obtained with a power law with exponent 0.75 for both Pt and Cu. The exponent in this fit is perhaps a result of the averaging of two competing mechanisms or multiple rate limiting steps, one with the 0.5 power seen with the olefin, and the other with a linear dependence on current. Such a situation might arise from non-uniform distribution of protons arriving at the catalyst, leading to some areas where hydrogenation is rate limiting (0.5 power) and others where hydrogen supply is limiting (1.0 power).

It can be concluded from these results that the rate of hydrogen formation on the surface of the catalyst is not the rate limiting step for current densities above 3 mA cm^{-2} , as suggested previously.⁵⁸ If proton reduction were rate limiting, the plots in Figures 2-4 would be linear with current. All the data show that the rate increases less than linearly with current, especially at high current density. This conclusion is further supported by the absence of reaction on the ineffective catalyst metals. If hydrogen adsorption were rate limiting, reaction would occur on all of the metals when current is applied.

The current density (or pressure for gas phase reactions) necessary to shift the reaction from mass transport limited to reaction limited depends on the relative rates of mass transport and surface reaction. A fast surface reaction will require large currents or pressures to become reaction limited. In this study, the rates of hydrogenation on Pt and Pd are accelerated by increasing the current density, suggesting that the reaction rate is of a similar order of magnitude as the rate of mass transfer. On the ineffective catalysts,

however, the rate of reaction is independent of current, suggesting a much slower reaction rate. When the rate of surface reaction is slow the adsorbed hydrogen primarily reacts by recombination and desorption as H₂. In the rate laws listed in Figure 5 this corresponds to the first term on the right hand side of the rate laws being dominant. The rate of mass transport is controlled by the current and is therefore the same on both the active and inactive catalysts, but the reaction selectivity depends on the catalytic activity. In a PEMHR the rate determining step and reaction selectivity changes with the current.

In catalytic reactions using gas phase hydrogen, the rate limiting step changes with pressure; the overall reaction is limited by mass transfer of hydrogen to the surface (adsorption) at low pressure and then shifts to surface reaction limited at higher pressures. Increasing agitation speed in a slurry reactor can have the same effect of reducing mass transfer limitations, causing a shift in rate limiting step.^{66,67} Pressure or mixing is employed to alter the reaction rate in conventional hydrogenation reactors.

For example, the Langmuir-Hinshelwood rate law for a generic surface reaction A + B → C is

$$\frac{dn_A}{dt} = -k \frac{b_A P_A b_b P_B}{(1 + b_A P_A + b_b P_B + b_C P_C)^2} \quad (3.2)$$

where P_x is the partial pressure of species x and b_x are constants. This type of rate equation is representative of hydrogenation reactions where A is the olefin, B is hydrogen and C is the paraffin product. At low pressures of B, the rate appears first order in B. The rate then passes through a maximum at moderate pressures of B. At higher pressures of B, species B displaces A on the surface and the reaction rate decreases.

Analogously, the rate-limiting step in PEM hydrogenation reactors may change from being linear in current at low current density (relative to the rate of the surface reaction) to less than linear at higher current density. At very high current density, the hydrogen gas generation may displace the organic at the electrode surface, causing a decrease in reaction rate. A maximum in the rate of hydrogenation was not observed here because the rate of H₂ generation became disruptive to the measurements before that point could be reached.

Hydrogen surface coverage is the true controlling variable for catalytic hydrogenation. In gas phase reactions the hydrogen pressure is manipulated to control hydrogen coverage. In the PEMHR the current is manipulated to control the hydrogen coverage. Ideally the rate should be related to the current supplied to the active catalyst surface. Some of the proton current can also be reduced on the carbon electrode support, where hydrogen diffusion and/or recombination can occur. Ideally the current density should be based on the active catalyst area, as reaction rates are normalized to the active catalyst area for supported metals. In a PEMHR, active catalyst must be accessible to both the organic and the proton current to ensure that the two reactants mix on the surface. Catalytic electrodes with extremely high surface areas, such as those consisting of supported metal particles, may have a lower hydrogen surface coverage at a given current than one of the same size with a smooth surface. High electrode surface area-to-current ratios are equivalent to very low hydrogen partial pressures, since the true current density (defined per unit surface area of the metal) is very low. Because of the complex structure

of the cathode/polymer electrolyte/hydrocarbon interface, good analytic tools to identify the active catalyst surface are not available. We have followed tradition and reported current density based the geometric area of the electrode.

3.1.5. Conclusions

Hydrogenation with a PEM hydrogenation reactor is similar to traditional catalytic hydrogenation, with the added benefit of generating high surface coverages of hydrogen at ambient pressure. Current density in a PEMHR is analogous to hydrogen partial pressure in a conventional catalytic hydrogenation reactor. The rate of hydrogenation of 1-decene in a PEMHR is limited by the addition of one atom of hydrogen to the adsorbed olefin rather than the rate of hydrogen adsorption onto the catalyst for all of the Pt and Au group metals. The rate is well fit by a rate law in the form $k_i^{0.5}$, analogous to rates found in conventional hydrogenation reactors. Aliphatic ketones hydrogenate much more slowly than olefins at the experimental conditions. Acetone hydrogenated one order of magnitude slower than 1-decene on Pt, and 4-heptanone did not react, suggesting a steric effect blocking access to the central carbonyl. Acetone hydrogenation over Pt and Cu was fit by $k_i^{0.75}$, suggesting a more complex mechanism for this reaction. Since the hydrogenation mechanisms in PEMHRs are catalytic, the true hydrogen surface coverage controls the rate of reaction rather than current density, which is often not defined in terms of the surface area of catalyst but rather in terms of the geometric area of the electrode.

3.1.6. Acknowledgements

The author would like to thank Professor Weiyong Ying of the Department of Chemical Engineering, East China University of Science and Technology, Shanghai, China, who contributed to the experimental work described in this section.

3.2. Electrochemical Reactions in a Polymer Membrane Reactor

3.2.1. Introduction and Theory

In the preceding sections, hydrogenation reactions occurring in a PEMHR were shown to be catalytic. These reactions are exothermic and are thermodynamically favorable, but rely on the interaction between the reacting molecules and the catalytic surface. Another type of reaction is also possible in PEMHRs: electrochemical reactions. Electrochemical reactions are driven by the potential at one of the two electrodes and can be thermodynamically unfavorable (positive ΔG_{rxn}).

The dehydrogenation of isopropanol is used to demonstrate the differences between catalytic and electrochemical reactions. This reaction is the reverse of the hydrogenation of acetone reaction discussed earlier. Like most dehydrogenation reactions, it has a positive $\Delta G_{\text{rxn}} = 27.6$ kJ/mol and is driven by the positive potential at the anode. In the current study, water electrolysis competes with isopropanol dehydrogenation. The charge is balanced for both reactions by the reduction of protons at the cathode to form H_2 . The mechanism for these reactions is given as Figure 3.9.

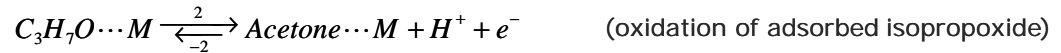
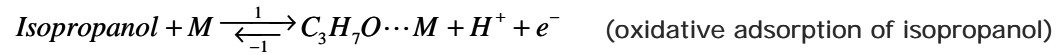
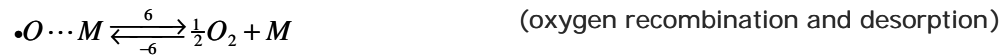
Dehydrogenation of isopropanol*Electrolysis of water*

Figure 3.9: Reaction mechanism for the dehydrogenation of isopropanol and electrolysis of water.

The removal of the first electron is rate limiting in each mechanism.

Assuming the removal of the first electron and proton from isopropanol and water is the rate limiting step, the mechanisms shown in Figure 3.9 suggest the rate law shown in equation (3.6). The expression derived states that the rate of dehydrogenation of isopropanol is the total current times the selectivity for the isopropanol reaction over the water reaction.

$$r_{iso} = k_{iso}[Isopropanol]M_T q_M \exp(\alpha_{iso} F \epsilon(i)/(RT)) \quad (3.3)$$

$$r_w = k_w[Water]M_T q_M \exp(\alpha_w F \epsilon(i)/(RT)) \quad (3.4)$$

$$r_{iso} = (i/(2F))(r_{iso}/(r_{iso} + r_{water})) \quad (3.5)$$

$$r_{iso} = \frac{\left(\frac{i}{2F}\right)}{1 + \left(\frac{k_{water}}{k_{iso}}\right) \left(\frac{[H_2O]}{[Isopropanol]}\right) \exp\left(\frac{(\alpha_{water} - \alpha_{iso}) F \epsilon(i)}{RT}\right)} \quad (3.6)$$

where F is Faraday's constant, ϵ is the potential of the anode, i is the current density, and α is the asymmetry factor which accounts for differences between the forward and reverse reaction mechanisms.

Equation (3.6) suggests that the rate of dehydrogenation should be a linear function of current if the two asymmetry factors are the same. The asymmetry factor for any reaction is 0.5 if the reaction has the same forward and reverse reaction mechanism. Also, if the reaction is electrochemical, the anode material should not affect the reaction rate, in strong contrast to a catalytic reaction.

3.2.2. Experimental

The dehydrogenation reaction was performed in the PEMHR using 10 vol% isopropanol in DI water, with 0.1 M H₂SO₄ as the supporting electrolyte. The same

solution was used on both sides of the reactor due to the high permeability of isopropanol through Nafion. The reaction was performed over Pt mesh and carbon cloth anodes using a Pt mesh cathode. The reaction temperature was 50°C and reaction time was 1 hour. The same experimental setup and protocols were used as for the acetone hydrogenation described previously. Product analysis was performed by gas chromatography.

3.2.3. Results and Discussion

Figure 3.10 confirms the electrochemical nature of this reaction. On the Pt anode, the rate of dehydrogenation of isopropanol is linear with current, as predicted by equation (3.6). On the C anode, the rate is linear at low current but reaches a maximum at higher current. The reaction rate over C is also predicted by equation (3.6) by assuming that $\alpha_{\text{iso}} \approx \alpha_{\text{w}}$. The difference in the asymmetry factors over C likely arises from a surface interaction of the isopropanol or an intermediate with the carbon causing the mechanism of the dehydrogenation to change slightly. Figure 3.10 also demonstrates how the electrode material has little effect on the rate of the reaction. Until the asymmetry difference becomes dominant at high current, the rate of dehydrogenation over Pt and C are equal.

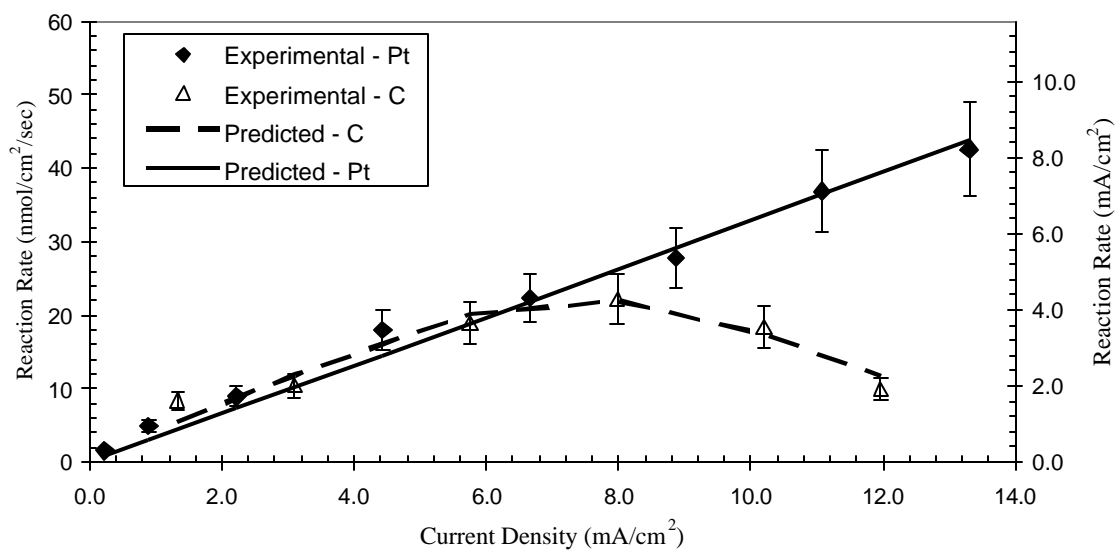


Figure 3.10: Rate of dehydrogenation of isopropanol over Pt and C anodes. Lines are fits to EQ.

Fitting parameters for Pt are $k_w/k_{iso} = 0.0135$, $a_w - a_{iso} = 0$. Parameters for C are $k_w/k_{iso} = 0.0102$, $a_w - a_{iso} = 0.026$.

The dehydrogenation of isopropanol clearly demonstrates the difference between a catalytic and an electrochemical reaction. Electrochemical reactions are less sensitive to electrode material and surface area and the rate limiting step involves a charge transfer. Because charge transfer is rate limiting, more applied current yields a higher reaction rate, unless asymmetries exist between competing reactions, as observed with the carbon anode.

3.3. Desulfurization in a Polymer Membrane Hydrogenation Reactor

Numerous attempts were made to achieve desulfurization reactions in a polymer membrane reactor. The most reactive species, alkanethiol, was tested in a PEMHR using Pt, Pd, Cu, Al, Pb, Fe, C, Co-Mo (deposited on C from the salts), and Ag electrodes. Solutions of 10 vol% dodecanethiol in cyclohexane were reacted at current densities from 1-15 mA cm⁻², and also under cyclic voltage and current programs.

Adsorption of thiol was evident on high surface area carbon electrodes, and a trace amount of the desulfurization product, dodecane, was detected. The production of dodecane from activated carbon electrodes probably results from surface adsorption and reaction. No application of current or voltage was able to regenerate the surface to allow the reaction to continue once the initial trace amounts of thiol had adsorbed and reacted. This result is consistent with the difficulty of regenerating high surface area adsorbents for desulfurization, which typically require calcination.⁶⁸

Pb electrodes, which are capable of high energy electroreductions⁶⁹, also were unable to reduce thiols. The only product observed was lead thiolate, described in the following chapter. Cu electrodes produced a small amount of a waxy polymeric material, but no dodecane was produced. The other metals were completely ineffective in reducing thiols under any conditions.

Cyclic voltammetry was performed for Cu, Ni, Pb, Ag, Pd, and Pt electrodes to determine if any reactions involving an electron transfer, such as a direct electroreduction

of thiol, were occurring. Electrodes of each metal were submersed in solutions of approximately 60 vol% ethanol and 36 vol% deionized water. The balance of the solution is sulfuric acid (supporting electrolyte) and the sulfur compound of interest. The counter electrode was a Pt wire. Potential was controlled with an Arbin MSTAT4+ battery testing station. The potential was referenced against a Pt wire in the same electrolyte solution. The potential window was experimentally determined for each compound by scanning until the current exceeded about 10 mA.

No irreversible reduction of thiol was observed for any of the studied electrodes, although Ag would react with some sulfur compounds to form a non-adherent layer of Ag_2S . Unfortunately, the metal was not able to be completely regenerated by electrochemical means, leading to the disintegration of the electrode. Figure 3.11 shows the cyclic voltammogram of an Ag electrode in an electrolyte solution containing tetrahydrothiophene. The difference in size of the anodic (downward) and cathodic (upwards) peaks is the amount of metal that cannot be regenerated. The use of a Ag electrode in the PEMHR was unsuccessful in producing any desulfurization products.

While sulfur compounds were observed to interact with several of the metals in a potential-dependent manner, the lack of a reduction reaction occurring at the surface, either catalytic or electrochemical, suggests that PEMHRs are not suited to desulfurization reactions. The high temperatures and specific catalysts required for HDS are not possible in a PEMHR. Additionally, economics requires that any desulfurization

reaction occur quickly to minimize the necessary reactor area. Other techniques for desulfurization are therefore required.

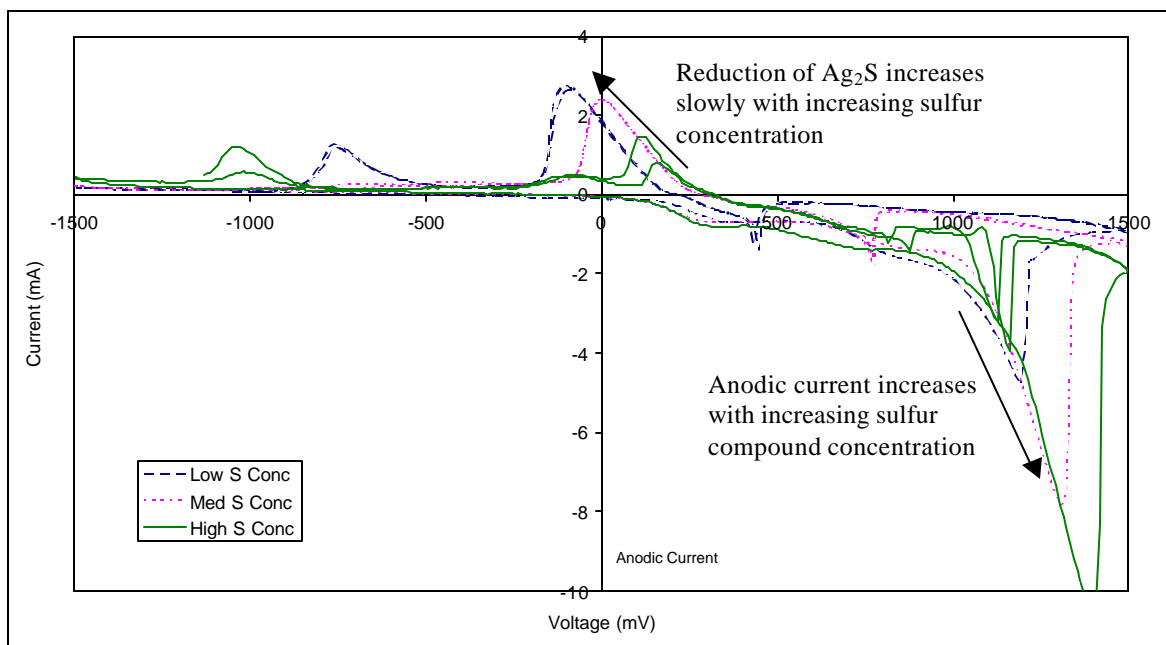


Figure 3.11: Cyclic voltammogram of an Ag electrode in a tetrahydrothiophene solution. The anodic (oxidation) current increases with sulfur concentration, indicating the production of more Ag₂S. The smaller cathodic wave near 0 V is the reduction of some of the Ag₂S.

4. Removal and Recovery of Alkanethiols

Thiols are present in petroleum from many parts of the world. The “sweet” designation of crude refers to low thiol content, while “sour” petroleum has high concentrations of thiols. Alkanethiols are also produced in HDS reactors by the reaction of olefins with H_2S present in the reactor. Here we present a new process for the removal and recovery of alkanethiols from petroleum.

4.1. Chemistry and Reactions

4.1.1. Introduction

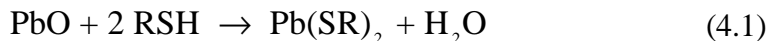
The removal of thiols from hydrocarbon streams, such as petroleum, has been a concern since the earliest days of refining. Thiols have a strong and unpleasant odor and also can be acidic. The removal of thiols from petroleum is commonly called sweetening. Most crude oils contain some thiol species, and a few contain significant quantities of thiols.⁷⁰

Over the past fifty years, the removal of sulfur from petroleum products has become an essential part of the refining process. Sulfur poisoning of Pt reforming catalysts led to the widespread use of hydrodesulfurization (HDS).^{14,71} HDS reacts organosulfur compounds with hydrogen over a catalyst at elevated temperature ($T = 300-450\text{ }^\circ\text{C}$) and pressure ($P = 35-270\text{ bar}$) to produce a hydrocarbon and H_2S .¹⁴ The feedstocks treated by HDS are

primarily those used for catalytic reforming to make gasoline. Desulfurization of diesel fuel is now required to meet new environmental emissions standards.⁷²

The reaction described here provides the basis for a simple, low temperature method for the removal of thiols from a hydrocarbon stream. In this reaction, thiols are converted directly to insoluble metal thiolates by heterogeneous reaction with certain metal oxides or hydroxides. The thiolates can then be mechanically filtered from the hydrocarbon stream. The metal and the original thiols can then be recovered in a reactive liquid-liquid extraction step. This reaction could form a process to complement conventional HDS by reducing the sulfur load on an HDS reactor while recovering the thiols for other uses.⁷³⁻⁷⁵

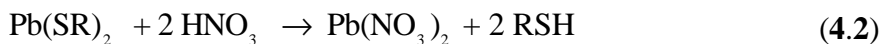
The reaction is based on thiolate chemistry in which thiols react with metal ions to form metal thiolates.^{76,77} Most work in this area focuses on the reaction of thiols with aqueous solutions of heavy metal salts⁷⁷⁻⁷⁹ or with surface reactions on metals⁸⁰⁻⁸⁴ and metal oxides.⁸⁵⁻⁸⁷ The reaction system applied here is distinct from these works because the reaction removes ions from the surface of the oxide, allowing a dense oxide particle to be completely consumed. While the heterogeneous reaction was almost certainly observed previously, the reaction is absent from much of the literature.^{88,89} Sources indicating that such a reaction occurs do not specify the reaction.⁷⁶ We demonstrate here some preliminary results of the heterogeneous reaction between a liquid thiol and a solid metal oxide to form a solid thiolate and water, and apply this obscure reaction to the modern day problem of removing and recovering thiols from a hydrocarbon mixture. An example reaction with PbO is



The reaction works with any combination of thiols and metal oxides that form stable, insoluble thiolates. We have found numerous oxides and hydroxides of Pb, Hg(II), and Ba to react with alkanethiols.

The reaction of thiols with these metal oxides or hydroxides occurs quickly and completely at room temperature and atmospheric pressure. Under these conditions, the thiolates are solid and insoluble in either aqueous or hydrocarbon liquids, consistent with older studies of Pb thiolates.⁷⁸

After separation of the thiolates from the hydrocarbon solution, the recovery of the metals is achieved by reactive extraction with a dilute oxidizing acid. The choice of acid depends on the metal salt desired. An example reaction is



This simple process uses inexpensive materials and very little energy compared to conventional desulfurization techniques.

Potentially reactive oxides are identified through simple thermodynamic considerations. The reaction of a thiol with a metal oxide involves the breaking of an S-H and an M-O bond and the formation of an M-S and an O-H bond per reacting thiol molecule. An estimate of ΔH_{rxn} can be obtained by comparing the heats of formation of

the metal oxide and the metal sulfide. This technique identifies which reactions are favorable but does not quantitatively predict the kinetics of the reaction.

4.1.2. Experimental

Powdered PbO (massicot form, Aldrich) of mass between 0.02 and 0.2 g was added to a glass vial. An *n*-alkanethiol, either 1-hexanethiol, 1-octanethiol, or 1-dodecanethiol (Aldrich), was added to the vial. An inert hydrocarbon, usually cyclohexane or toluene, was sometimes added to prevent the reaction product from becoming a paste. The solid product could be suspended in the hydrocarbon by stirring to facilitate filtration. Some samples were stirred using a magnetic stir bar, and some were heated to about 70°C on a hotplate and cooled before filtering.

The solid reaction product, a yellow powder, was gravity filtered (Whatman #50 hardened circles), then rinsed several times with water, acetone, cyclohexane, and then pentane and dried at room temperature.

The Pb was extracted from the thiolates by liquid-liquid extraction with dilute (0.2-0.3 M) nitric acid. The solid thiolates were added to cyclohexane and the mixture was heated to the melting point of the thiolate, approximately 60-80 °C. This mixture was added to the nitric acid and agitated by rapid stirring. The hydrocarbon layer was then analyzed for thiol content by gas chromatography (Hewlett Packard HP-1 column). The aqueous layer was evaporated and the Pb was recovered as Pb(NO₃)₂ crystals.

Other metal oxides and hydroxides were tested by adding 1-octanethiol to a small amount (approx. 0.15-0.5 g) of the oxide or hydroxide in a glass vial. The formation of thiolates was evidenced by a dramatic increase in apparent solid volume and in some cases, a color change. Reacted mixtures were filtered and dried as above, then weighed to determine conversion. The compounds tested were BaO, Bi₂O₃, CaO, CdO, CoO, Cr₂O₃, CuO, HgO, MgO, MoO₃, metallic Pb wire, PbO, Pb₃O₄, PbO₂, Pb(OH)₂, Pb(NO₃)₂, PbS, SbO, SnO, and Sr(OH)₂.

4.1.3. Results

4.1.3.1. Reactions

All of the tested oxides of Pb (Aldrich), Pb(OH)₂ (made from oxide), metallic Pb wire (Alfa-Aesar), HgO (Fisher), Ba(OH)₂, and BaO (Barium and Chemicals, Inc.) formed stable, insoluble thiolates of several alkanethiols. Based on these results, we assume that Hg(OH)₂ would also form a stable thiolate. These oxides did not react with butyl disulfide (97%, Aldrich), butyl sulfide (96%, Aldrich), tetrahydrothiophene (99%, Aldrich), or thiophene (99+%, Aldrich).

Although dynamic scanning calorimetry was not performed, a melting point analysis was conducted. The thiolates of the tested alkanethiols were solid at room temperature, but melted at temperatures above about 50°C when mixed with a hydrocarbon solvent. The melting point was lower for lower molecular weight thiolates. In the presence of cyclohexane, a miscible solution of the dioctylthiolate, Pb(SC₈H₁₇)₂, was formed at 54-55°C. The melting temperature of the dried dialkylthiolates increased with molecular

weight and was 70-80°C for the dioctylthiolate. The observed melting point was lower than reported elsewhere⁷⁷, probably due to impurities or incomplete removal of the hydrocarbon solvent. The melting range was also wide, further suggesting the presence of unremoved solvent. Vacuum drying may be necessary to completely dry the thiolates. The thiolates were insoluble in cyclohexane, toluene, acetone, and water at room temperature. The thiolate melts were miscible with cyclohexane and toluene, but immiscible with water. The thiolates recrystallize when a melt, either diluted with solvent or not, was cooled to room temperature.

Lead dioctylthiolate, made from the reaction of PbO and octanethiol, is stable to about 100°C. Thermogravimetric analysis (TGA) revealed that this material, when dried, decomposes slowly between 100-140°C, followed by a rapid decomposition between 140-220°C. After decomposition, the mass of the remaining material corresponds reasonably well to PbS, a known decomposition product. The difference probably results from some formation of PbO at the higher temperatures. The TGA data is given as Figure 4.1. The temperature ramp rate was 1°C/min from 32-100°C and 2°C/min afterwards.

Figure 4.2 shows the WAXD pattern of a sample of $\text{Pb}(n\text{-C}_8\text{H}_{17}\text{S})_2$ prepared from solid PbO by this reaction. The thiolate was recrystallized once from hot toluene. The WAXD pattern shows two similar crystal morphologies, as indicated by the double peaks. The average d-spacing, calculated from Bragg's Law, is 26.2 Å, in close agreement with the reported value of 25.8 Å.⁷⁷ The high order peaks result from dense layers of Pb atoms separated at regular spacing by a bilayer of hydrocarbon chains. The measured d-spacing

represents the distance between two layers of Pb atoms and increases with increasing alkyl chain length.⁷⁷ A sketch of this structure is given as Figure 4.3. This crystal structure is most likely responsible for two physical properties of these materials. The strong adhesion of the PbS cores prevents dissolution at low temperatures and the lamellar structure with loosely bound sheets provides the greasy smearing behavior of the compound when not completely free of organic solvents.

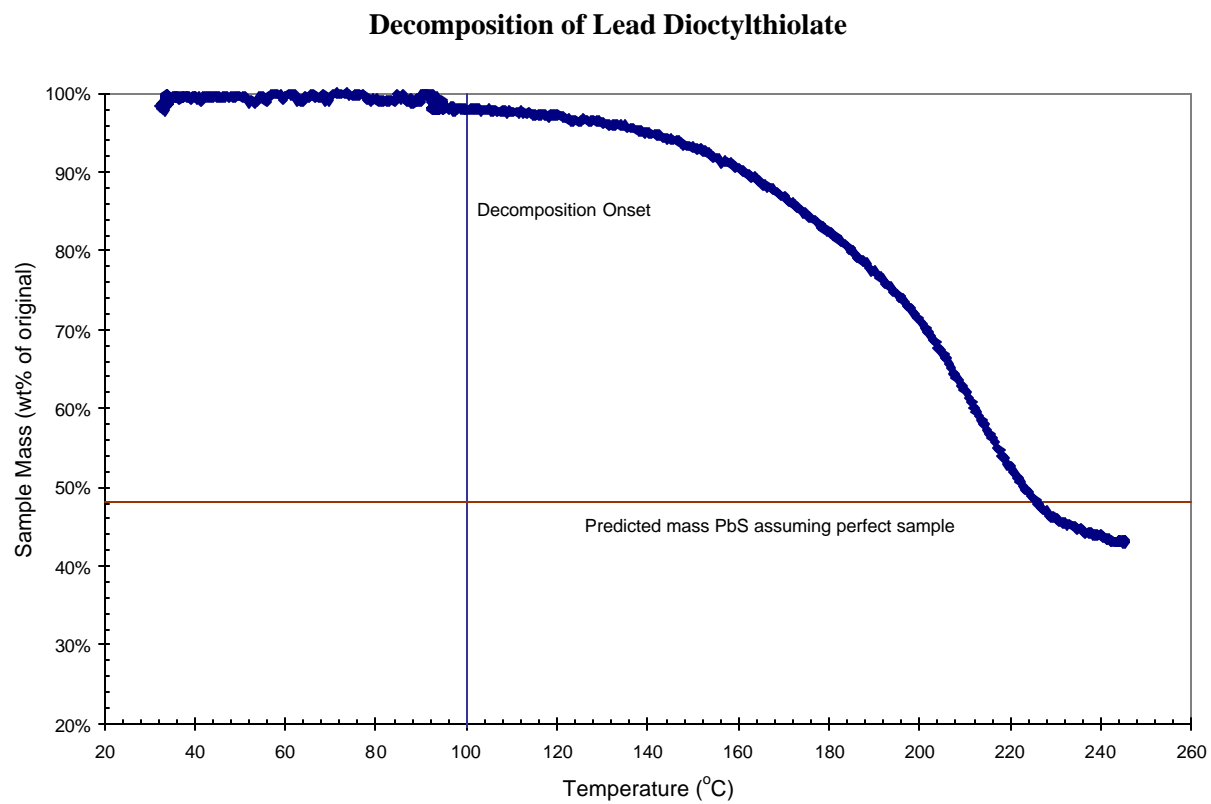


Figure 4.1: TGA results showing decomposition of $\text{Pb}(\text{SC}_8\text{H}_{17})_2$.

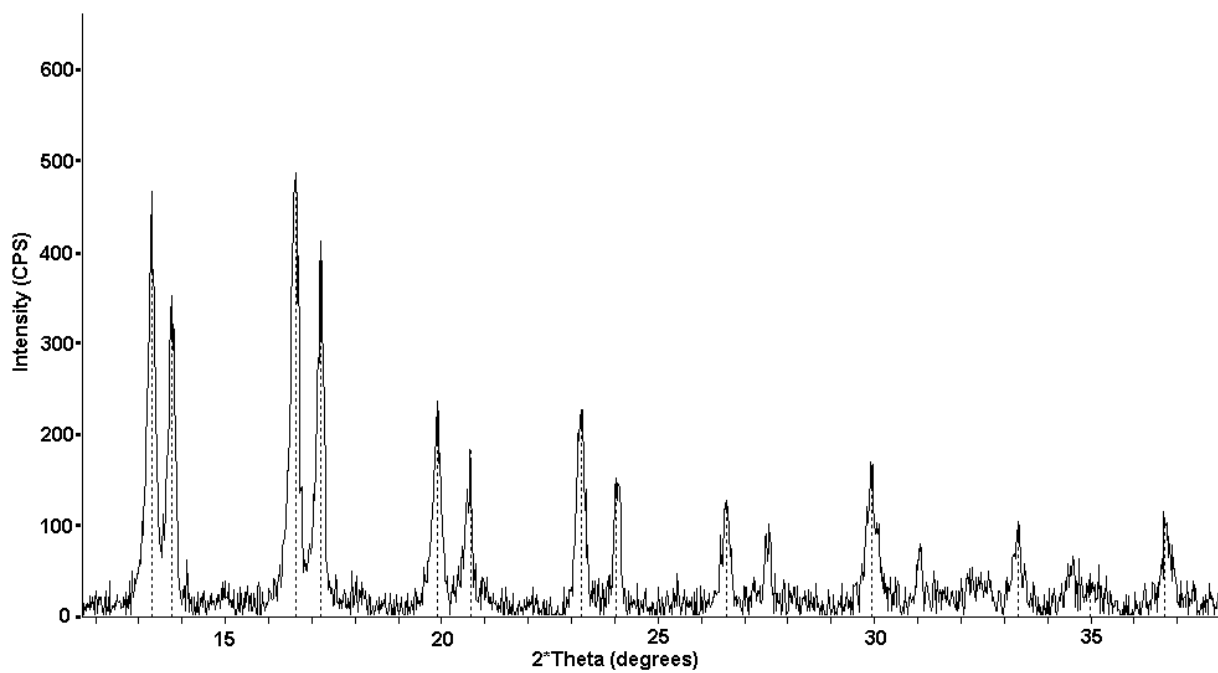


Figure 4.2: WAXD pattern of recrystallized $\text{Pb}(\text{SC}_8\text{H}_{17})_2$. Calculated average d-spacing is 26.2 Å.

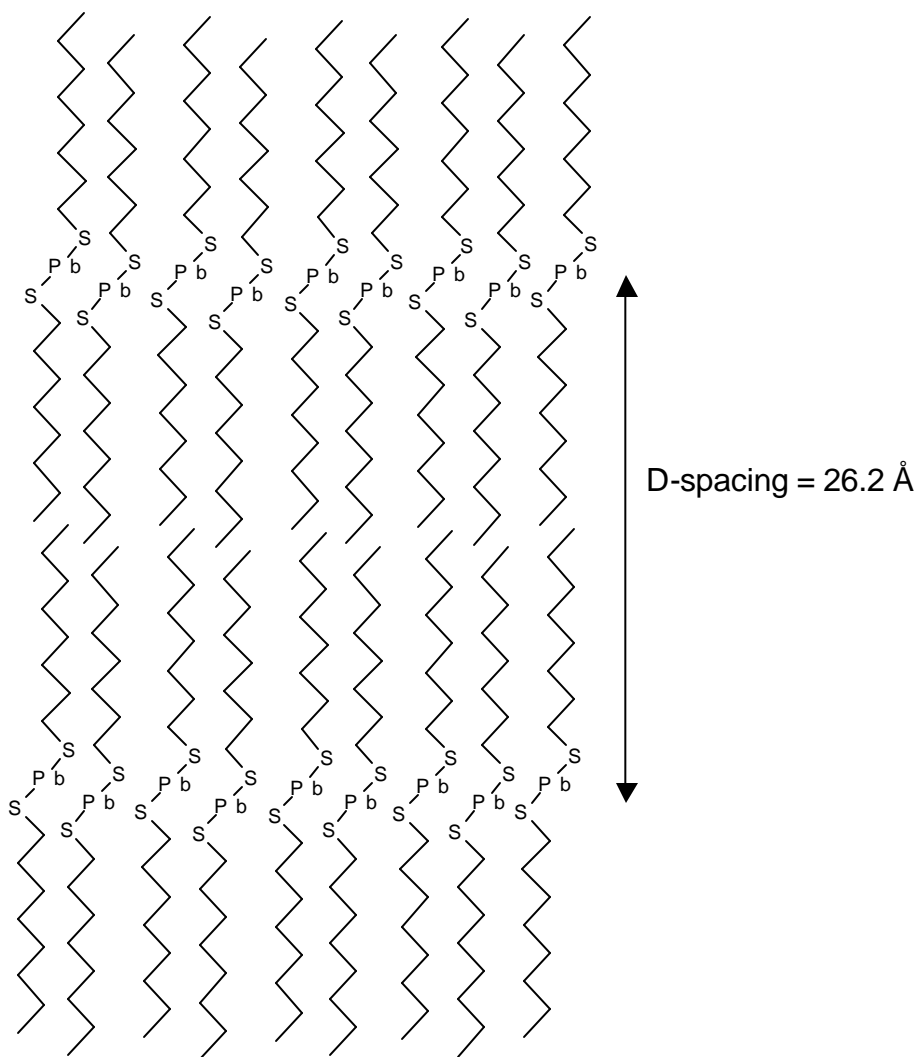


Figure 4.3: Sketch of likely structure of a $\text{Pb}(\text{SC}_8\text{H}_{17})_2$ crystal.

PbO, Pb₃O₄, Pb(OH)₂, and PbO₂ reacted quickly yielding an insoluble, yellow thiolate. No other reaction products were detected. Reactions were typically complete in about 1 hour without agitation or heat. The thiolate does not appear to foul the surface of the oxide, allowing the reaction to go to completion without agitation. Yields of Pb(SC₈H₁₇)₂ were typically 80-90%, including transfer losses. Heating the product above the melting temperature of the thiolate revealed no remaining solid oxide, indicating that some amounts of sub-thiolate, such as Pb(SC₈H₁₇)(OH), may have been formed, reducing the yield. Pb⁴⁺ compounds only reacted with two thiols per Pb, probably resulting in the formation of PbO(SC₈H₁₇)₂ or Pb(OH)₂(SC₈H₁₇)₂.

In the presence of a 48% stoichiometric excess of PbO, a final thiol concentration of 13 μmol/mL, or 527 ppm S by weight, was achieved. This reaction was performed without optimization of reaction conditions and was carried out in a glass vial with mild agitation.

Metallic Pb wire was also active in forming thiolates. The thiol reacted with the Pb, or more likely the natural coating of oxides present on a Pb surface when exposed to air, to form an insoluble yellow thiolate. The extent of reaction on a Pb wire was very low when carried out in an inert nitrogen atmosphere. The reaction occurred at the surface of the wire, forming plates of thiolate that were pushed outwards as new thiolate was formed. Mechanical agitation to remove the thiolate layer is usually sufficient to maintain an active surface if oxygen is available.

Hg(II)O reacted exothermically to generate a white, insoluble thiolate. The reaction occurred faster with HgO than for PbO or BaO. Experimenters should be aware that adding undiluted thiol to HgO directly releases sufficient heat to vaporize some of the generated thiolate on contact. Diluting the thiol with an inert solvent is sufficient to prevent a potentially dangerous heat release. The yield of $\text{Hg}(\text{SC}_8\text{H}_{17})_2$ was 99%.

The initial reaction proceeded more quickly with HgO than PbO, but the thiolate formed hindered the reaction of the underlying oxide more than in the Pb reaction. The higher degree of fouling may be the result of the thiolate recrystallizing around the oxide after melting in the initial heat release. Again, diluting the thiol should alleviate this problem. The reaction went to completion with mild agitation.

BaO and $\text{Ba}(\text{OH})_2$ also reacted with alkanethiols to generate an insoluble, white thiolate. The reaction was fast and occurred without agitation, but the yield of 54% was lower than for PbO or HgO. The lower yield is again most likely due to the formation of sub-thiolate, $\text{Ba}(\text{SC}_8\text{H}_{17})(\text{OH})$. This reaction is interesting, however, because of the lower environmental and health risks associated with Ba as opposed to Hg and Pb.

Bi_2O_3 reacted more slowly to yield an orange-yellow thiolate that was soluble in cyclohexane. The thiolate was recoverable by evaporating the cyclohexane. Since we are interested in using these reactions to remove thiols from hydrocarbon streams, a soluble thiolate will not work in this process and Bi was not studied further.

CuO and a mixture of MoO₃ and CoO both reacted very slowly to generate grey-white thiolates. The reactions were incomplete, leaving some unreacted metal oxide even after several weeks. Other metals were excluded from the study. Some transition metals such as Pt, Au, Ru, Rh, Os, and Ir and the lanthanide series are too expensive to be practical in desulfurization reactions. Tl and Po were excluded due to their very high toxicity.

4.1.3.2. Metal Recovery

Filtration of the solid thiolates from the hydrocarbon affects the separation of the thiols from the original mixture. The separation requires that the thiolates be solid and must be performed at a temperature below the miscibility point of the thiolates, approximately 55°C for the compounds in this study. Once the thiolates have been filtered from the original hydrocarbon stream, the metal can be recovered by extraction with dilute oxidizing acid. An example reaction was given previously as equation (4.2).

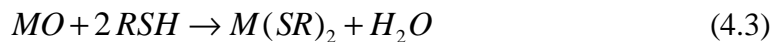
Reactive liquid-liquid extraction can be performed by heating the thiolates to melting, either with or without the addition of a hydrocarbon solvent. Agitating the thiolates with a dilute solution (0.1-0.3 M typically) of an oxidizing acid, such as nitric, allows the reaction to reach completion in about 2 hours. Improved contacting between the liquid phases and using more concentrated acids can reduce the time required. The result is an aqueous phase containing the metal salt and a hydrocarbon phase containing the original thiols and any added solvent.

The choice of acid depends on the desired metal salt. If the resulting salt is soluble in the acid phase, as in the above example, the metal can be recovered by evaporation of the water. An insoluble metal salt can be filtered. A mixture of nitric and sulfuric acid will decompose Pb thiolates and precipitate the metal as PbSO₄. A reusable oxide can be obtained by roasting most metal salts in air.

Using this technique, thiolates made from reaction with PbO were extracted with 0.21 M HNO₃. The yellow diluted melt of Pb(SC₈H₁₇)₂ changed to colorless as the reaction proceeded. The recovery of Pb as Pb(NO₃)₂ was 102%, or essentially all of the lead, within experimental error. A second trial with thiolates made from PbO₂ and 0.31 M HNO₃ yielded a 95% Pb recovery. Thiol recoveries in the hydrocarbon phase, as measured by GC, for these two runs were 78% and 90%, respectively.

4.1.3.3. Thermodynamic Predictions

The reaction of the thiols to make metal thiolates is thermodynamically driven by the concurrent production of water. For example,



Equation (4.3) is more favorable than equation (4.4) for any metal that forms an oxide reducible by hydrogen, as shown in equation (4.5).

$$\Delta H_{Rxn\ 3} - \Delta H_{Rxn\ 4} = \Delta H_f(H_2O) - \Delta H_f(MO) \quad (4.5)$$

Metals in the 2^+ oxidation state have the simplest stoichiometry, requiring interaction between two thiol molecules and only one metal atom per water molecule formed. Metals in other oxidation states require the coupling of the reduction reaction at two metal atoms to generate the stable products. This coupling will likely slow down the reaction. PbO_2 reacted with only two thiols per Pb atom rather than forming $\text{Pb}(\text{SC}_8\text{H}_{17})_4$. This reaction retains the simple stoichiometry observed with Pb^{2+} compounds.

The search for reactive oxides can be narrowed by calculating the heat of formation of the thiolates from the metal oxides. Reactions with small negative or positive values for ΔG_{rxn} are not thermodynamically favorable and will not react spontaneously, as desired in this process. Only those oxides with large negative values of ΔG_{rxn} need be studied.

Unfortunately, very little information regarding the enthalpy and entropy of formation of specific metal thiolates is available. Most available information pertains to thiol adsorption on gold surfaces.⁹⁰ Calculations of metal-sulfur bond energies from studies of dialkyldithiocarbamates⁹¹⁻⁹³ were not successful. A method for estimating ΔG_{rxn} from readily available data is required.

The free energy of reaction for each metal oxide can be estimated from the heat of formation of the metal oxide and sulfide. For a bivalent metal, the ΔH_f of the metal oxide, MO, is assumed to equal twice the M-O bond energy. Similarly, ΔH_f of the sulfide, MS, is assumed equal to twice the M-S bond energy. Water and H_2S are used in the same

manner to estimate the O-H and S-H bond energies. The complete equation for a bivalent metal is

$$\Delta H_{\text{rxn}} = \Delta H_f(\text{MS}) + \Delta H_f(\text{H}_2\text{O}) - \Delta H_f(\text{MO}) - \Delta H_f(\text{H}_2\text{S}) . \quad (4.6)$$

Equation (4.6) can be corrected for stoichiometry for use with metals of other oxidation states. The entropic effects are neglected since ΔS_f data is not available, but the entropic contribution should be small when the products and reactants each consist of one solid and one liquid phase.

The data required for this estimate are widely available for many metals.^{94,95} The heats of reaction calculated by this method range from -378 kJ/mol for Ru(IV) to +159 kJ/mol for B(III). A graphical representation of the results is shown in Figure 4.4.

The most active metals are those with small exothermic heats of formation, surrounding the noble metal Au, whose oxide is unstable. The heavier group 1 and 2 metals are also highly favorable. Figure 4.5 shows the experimental results. All four of the highly reactive metal oxides, (Ba, Hg, Pb, Bi) are predicted to be highly favorable. The estimated values of ΔH_{rxn} are shown in Table 4.1.

	1	2	3	4	5	6	7	8	9	10	11	12	13	14	15	16	17	18
1	H																	He
2	Li	Be											B	C	N	O	F	Ne
3	Na	Mg											Al	Si	P	S	Cl	Ar
4	K	Ca	Sc	Ti	V	Cr	Mn	Fe	Co	Ni	Cu	Zn	Ga	Ge	As	Se	Br	Kr
5	Rb	Sr	Y	Zr	Nb	Mo	Tc	Ru	Rh	Pd	Ag	Cd	In	Sn	Sb	Te	I	Xe
6	Cs	Ba	La-Lu	Hf	Ta	W	Re	Os	Ir	Pt	Au	Hg	Tl	Pb	Bi	Po	At	Rn
7	Fr	Ra	Ac-Lr	Rf	Db	Sg	Bh	Hs	Mt	Uun	Uuu	Uub						

Lanthanides	La	Ce	Pr	Nd	Pm	Sm	Eu	Gd	Tb	Dy	Ho	Er	Tm	Yb	Lu
Actinides	Ac	Th	Pa	U	Np	Pu	Am	Cm	Bk	Cf	Es	Fm	Md	No	Lr

Legend:	
Pb	$\Delta H_{rxn} < -100$ kJ/mol
Fe	$\Delta H_{rxn} < -60$ kJ/mol
Al	$\Delta H_{rxn} > -60$ kJ/mol

Figure 4.4: Graphical representation of predicted heats of formation of metal thiolates from the oxide.

	1	2	3	4	5	6	7	8	9	10	11	12	13	14	15	16	17	18
1	H																	He
2	Li	Be											B	C	N	O	F	Ne
3	Na	Mg											Al	Si	P	Se	Cl	Ar
4	K	Ca	Sc	Ti	V	Cr	Mn	Fe	Co	Ni	Cu	Zn	Ga	Ge	As	Se	Br	Kr
5	Rb	Sr	Y	Zr	Nb	Mo	Tc	Ru	Rh	Pd	Ag	Cd	In	Sn	Sb	Te	I	Xe
6	Cs	Ba	La-Lu	Hf	Ta	W	Re	Os	Ir	Pt	Au	Hg	Tl	Pb	Bi	Po	At	Rn
7	Fr	Ra	Ac-Lr	Rf	Db	Sg	Bh	Hs	Mt	Uun	Uuu	Uub						

Lanthanides	La	Ce	Pr	Nd	Pm	Sm	Eu	Gd	Tb	Dy	Ho	Er	Tm	Yb	Lu
Actinoids	Ac	Th	Pa	U	Np	Pu	Am	Cm	Bk	Cf	Es	Fm	Md	No	Lr

Legend:	
Pb	Fast Reaction Observed
Cu	Slow Reaction Observed
Sr	No Reaction Observed

Figure 4.5: Graphical representation of observed metal oxide activity.

Metal	ΔH_{rxn}	Observed
	[kJ/mol]	
Hg	-205.7	Fast Rxn
Ba	-150.3	Rxn
Bi	-142.1	Rxn
Cu	-134.1	Slow Rxn
Mo	-123.9	Slow Rxn
Pb	-121.4	Rxn
Co	-83.2	Slow Rxn

Table 4.1: Predicted heats of reaction of metal oxides with observed reactivity.

Thermodynamics only indicates whether a reaction can proceed without an energy input, but are of limited value in predicting reaction rates. Large activation energy barriers slow the kinetics of a reaction, preventing it from happening on a useful time scale. For example, Cu has a larger predicted value of ΔH_{rxn} than Pb, but the reaction proceeds much more slowly. Metals such as Cd and Sr do not react, despite having favorable values of ΔH_{rxn} . As expected, however, none of the metals with small or positive value of ΔH_{rxn} were observed to be reactive.

If we require both favorable thermodynamics and an M^{2+} oxide or hydroxide for favorable stoichiometry, the resulting prediction of metals is an excellent match to the group of metals for which the reaction to form thiolates is favorable.

4.1.4. Conclusions

Thiols can be removed from hydrocarbon streams by heterogeneous reaction with oxides and hydroxides of Pb, Hg(II), and Ba. The thiolates formed are insoluble in both aqueous and hydrocarbon solvents, allowing them to be filtered from the remaining stream. Once the thiolates are separated from the original feed stream, the metal and the thiols can be separated again using liquid-liquid extraction with a dilute acid. The metal is recovered as a salt from the aqueous phase and the thiol remains in the hydrocarbon phase. This process uses inexpensive materials and requires very little energy. Reactive metal oxides can be easily predicted from the heats of formation of the metal oxide and sulfide after accounting for the favorable M^{2+} oxidation state.

The process is limited to thiols, since sulfides and disulfides lack the hydrogen required to make water by equation (4.1). The formation of water as a byproduct of the reaction makes the reaction thermodynamically favorable.

Considerable work to measure properties such as solubility and the effects of other reactive compounds found in petroleum is still required for any process optimization. However, some applications of this process are readily apparent. Replaceable filter cartridges filled with one of the active oxides for sweetening could be added to delivery lines or storage tanks. The thiolates formed would be retained in the cartridge, which could be returned to the manufacturer for reprocessing by the extraction technique when full. The system would require no additional energy inputs aside from existing pumps. The process also recovers thiols which are a valuable feedstock to the food and fragrance industries as well as the pharmaceutical industry.⁷³⁻⁷⁵

4.2. Process Demonstration

4.2.1. Introduction

Hydrodesulfurization (HDS) is effective for removing sulfur from certain petroleum feedstocks by converting organo-sulfur compounds into hydrocarbons and H_2S ¹⁴. The removal of sulfur from gasoline fractions is necessary to prevent the poisoning of Pt reforming catalysts⁷¹ as well as reducing the emission of SO_2 with the combustion products from engines.

Thiols constitute a considerable amount of the sulfur found in light streams. Table 4.2 indicates the prevalence of thiols in various streams used for gasoline production. Thiols can also be created by selectively hydrotreating other sulfur containing species. HDS reactors operate most efficiently under mild reaction conditions. At higher temperature and pressures, olefins are also hydrogenated, leading to a loss of octane and unnecessary consumption of hydrogen. Under mild conditions, however, H_2S in the reactor reacts with olefins to form recombinant mercaptans, high molecular weight straight and branched chain thiols that are not caustic extractable.⁹⁶

ExxonMobil Research and Engineering Co. and Merichem Chemicals and Refinery Services LLC have recently introduced a process called the Exomer process to remove thiol species formed during selective hydrotreating by caustic extraction with a proprietary liquid extractant.^{96,97} The Exomer process, shown in Figure 4.6 is more

complicated than the process presented here, and the ability to recover the thiols is not reported.

Many new desulfurization processes focus on adsorption of sulfur-containing species onto metal oxides and zeolites.^{68,98-100} Unfortunately, regeneration of the adsorbent is usually difficult. The adsorbed sulfur compounds decompose, forming metal sulfides at elevated temperatures.^{85,101} Calcining these adsorbents in air requires additional process steps to remove SO₂ generated during the oxidation.

A simple, low cost process that reduces the mercaptan sulfur content of petroleum distillates, especially recombinant mercaptans, could provide the environmental benefits of desulfurization without significantly increasing the cost of the fuels. The economics of such a process would be improved if the sulfur compounds removed could be recovered rather than converted to H₂S, since many of these compounds have commercial value.^{73,75}

The heterogeneous reaction of thiols with metal oxides enables a process that meets these criteria. Section 4.1 demonstrated that liquid alkanethiols can be removed from hydrocarbon mixtures by heterogeneous reaction with certain metal oxides at room temperature. Here we present an entire process by which this reaction can be used to achieve the separation of thiols from hydrocarbons using lead oxide. The process is selective for thiols. No reaction is observed between PbO and disulfide, sulfide, or thiophenic species.¹⁰²

Gasoline Feedstock	End Point (°F)	Mercaptan Sulfur (wt% of total S)
Amylene	N/A	92%
Light Coker Naphtha	212	75%
Light FCC	340	48%
FCC	400	45%

Table 4.2: Thiol content of several light streams used in gasoline production. Data from ¹⁰³.

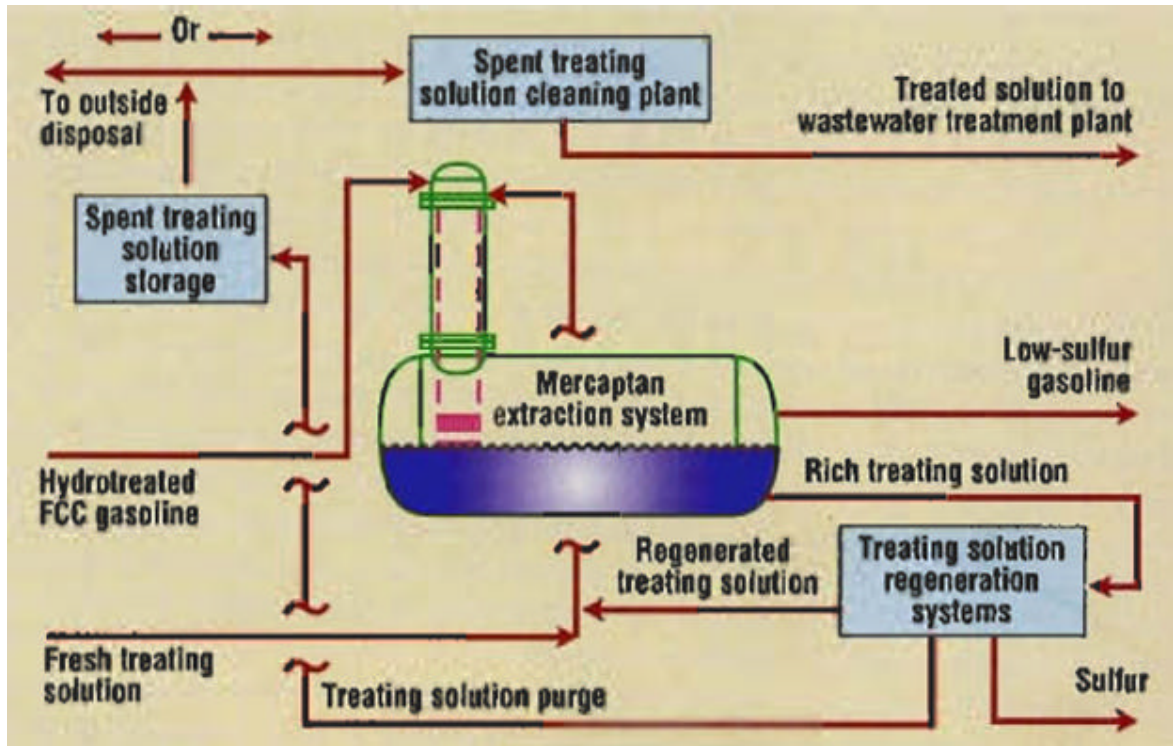
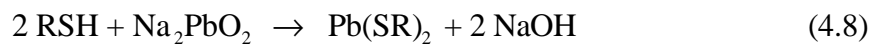


Figure 4.6: The Exomer process, designed by ExxonMobil and Merichem, Inc. to remove high molecular weight recombinant mercaptans. Adapted from ⁹⁷

The Doctor Sweetening process is a technique developed in the 1860's that also uses PbO to eliminate thiols from petroleum.¹⁰⁴ The Doctor process combines PbO with NaOH to form an aqueous solution of lead plumbites, as given in equation (4.7). The plumbites react with thiols in a petroleum stream to form lead thiolates (also called mercaptides) according to equation (4.8). At the standard operating temperature of this reaction (circa 100-150°C), the thiolates were miscible with the petroleum and were converted to organic disulfides by the addition of powdered sulfur, as shown in equation (4.9).



The proposed process is distinct from the Doctor process in several ways. First, the proposed process removes the thiols from the petroleum stream rather than converting them to disulfides. Second, the process uses powdered PbO rather than aqueous solutions of Pb salts, eliminating an extraction operation. Third, no addition of sulfur is required. Fourth, the thiols can be recovered.

4.2.2. Process Description

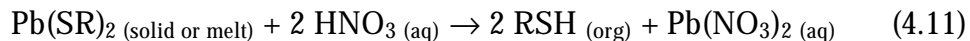
The complete process for the separation of thiols from hydrocarbons with PbO and the recovery of both the PbO and the thiols is diagrammed in Figure 4.7. The hydrocarbon stream is contacted with powdered PbO or any other metal oxide identified as active in section 4.1.3.1 in a reactor. The PbO reacts with the thiols to form lead thiolates

according to equation (4.10). The lead thiolates formed are yellow solids and insoluble in water, acetone, cyclohexane, or toluene at temperatures below about 50°C. The temperature at which the thiolates become miscible increases with increasing molecular weight of the alkyl thiolates.¹⁰²



This reaction occurs readily at room temperature. While the reaction can also be performed at an elevated temperature, heating to above 60-80°C causes the thiolates to melt and become miscible in hydrocarbons, preventing their separation. If heated, the reacted stream must first be cooled to near room temperature prior to separation to ensure that the thiolates have completely recrystallized. The solid thiolates can either be filtered or settled to achieve the desired separation.

Once the thiolates are separated from the hydrocarbon mixture, they can be converted back to the original thiols and a Pb salt by reactive extraction with a dilute oxidizing acid, such as nitric, as shown in reaction (4.11). The $\text{Pb}(\text{NO}_3)_2$ remains in the aqueous solution while the thiols separate into an organic phase. The reaction can be carried out at room temperature with solid lead thiolates, but the interfacial contacting can be improved by melting the thiolates and forming a miscible solution with an organic solvent.



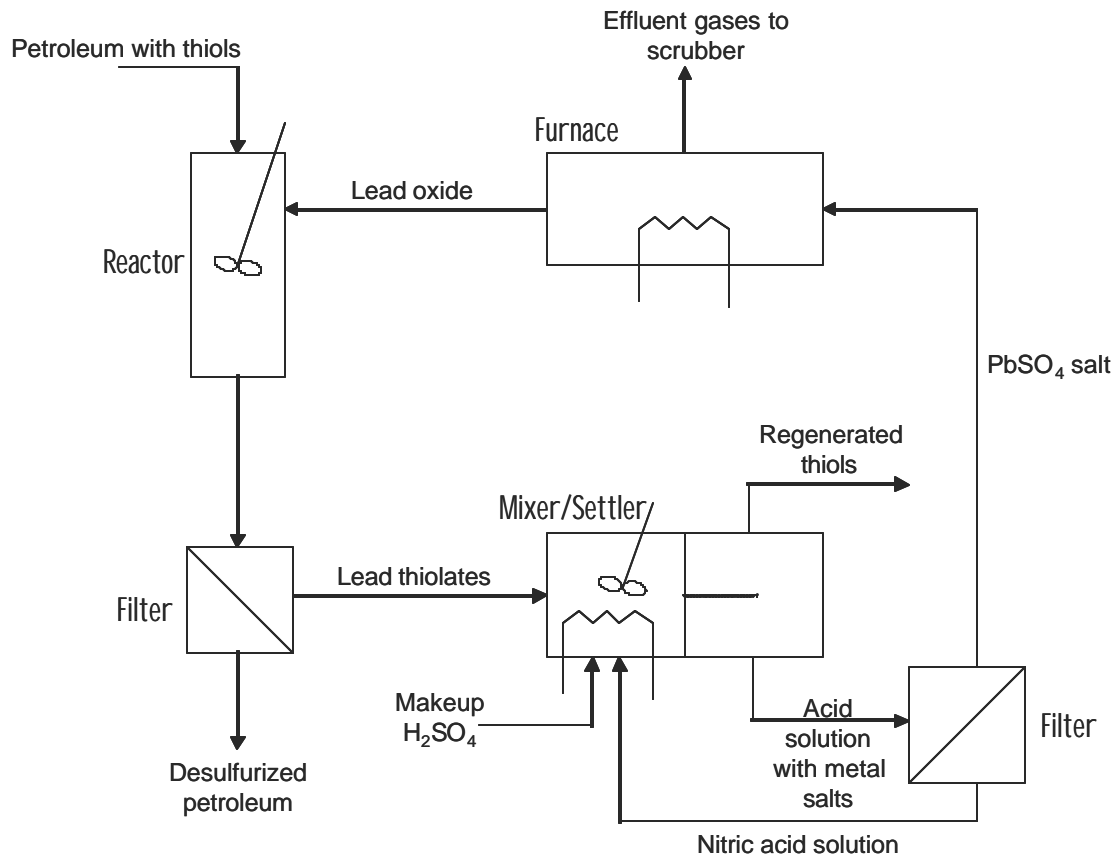


Figure 4.7: Diagram of the thiol removal process using lead oxides, showing the key operations including reaction, separation, and extraction.

The compound $\text{Pb}(\text{SC}_8\text{H}_{17})_2$ was found to form a miscible solution with the residual cyclohexane at 54-55°C,¹⁰² so the required operating temperature of the extractor is approximately 60-80°C, depending on the composition of the feed stream. The temperature at which the thiolates become miscible with hydrocarbon solvents is below the melting point of the purified thiolates,⁷⁷ reducing the heat load required in the extractor.

The two liquid phases, now consisting of an aqueous lead salt solution (or an acid and a precipitated lead salt such as PbSO_4) and a hydrophobic thiol layer, are allowed to settle and are separated. These two stages could be combined in a single unit operation such as a Karr column.⁴⁰ The aqueous layer is separated and filtered, leaving solid PbSO_4 . The acid can be recycled to the extractor. Active PbO can be regenerated by roasting PbSO_4 in air, liberating nitrogen and oxygen. The roasting of PbS , also called galena, is the source of most PbO .⁴¹

An alternative method for desulfurizing stocks of petroleum fuels is to use this reaction with metallic Pb as the PbO source. Metallic Pb oxidizes rapidly when exposed to humid air. The natural oxide coating on a piece of metallic Pb is also active for this reaction, provided that a supply of oxygen, such as air, is available to regenerate the surface oxide layer.¹⁰² The reactor and separator in Figure 4.7 could be replaced by rods of Pb placed into storage tanks of thiol-containing petroleum fractions.

4.2.3. Experimental

The heterogeneous reaction and the reactive extraction portions of this process were studied. The reaction was carried out in batch mode with powdered PbO (massicot form, Aldrich) and *n*-octanethiol (Aldrich) in a glass vial. The thiol was diluted with cyclohexane (Aldrich) to a concentration of 0.5-1.7 M thiol prior to the addition of the PbO. The reaction proceeds identically with toluene as the solvent. All reactions were performed at room temperature.

The reaction was also studied using metallic Pb wire (99.9% Pb, Alfa-Aesar) as the oxide source. Some of the oxide coating on the wire was removed by wiping with a paper towel, revealing fresh Pb. The wire was coiled and placed into a glass vial containing the same diluted thiol solution as was used in the PbO trials. The jar was not sealed airtight, providing an oxygen-containing atmosphere.

The reactive extraction was performed using 0.21 M HNO₃ and thiolates produced from the reaction of *n*-octanethiol and PbO. The thiolates were filtered from the original thiol-cyclohexane mixture, rinsed with water, cyclohexane, and pentane, and then dried before use. Cyclohexane was added to the hydrophobic phase to allow for easier measurement of the thiol recovery. The extraction was performed in a glass jar, heated to about 70°C. Agitation was provided by rapid stirring with a magnetic stir bar.

4.2.4. Results

The reaction of PbO with excess *n*-octanethiol produced thiolates at room temperature with or without mild agitation. The yield of thiolates, as determined by the change in mass of the solids divided by the theoretical change in mass to convert all PbO into Pb(SR)₂, corrected for water loss, is shown in Figure 4.8. The yield is above 80% on most runs, even at low thiol to PbO molar ratios. The low yield for the 179.5 molar ratio is most likely due to transfer and filtering losses, since this trial used the smallest mass of PbO. This result suggests that the conversion of PbO to thiolate proceeds to completion, although not all Pb atoms have two thiolate groups. A single thiolate and a hydroxide group is also possible on a small percentage of the metal atoms.

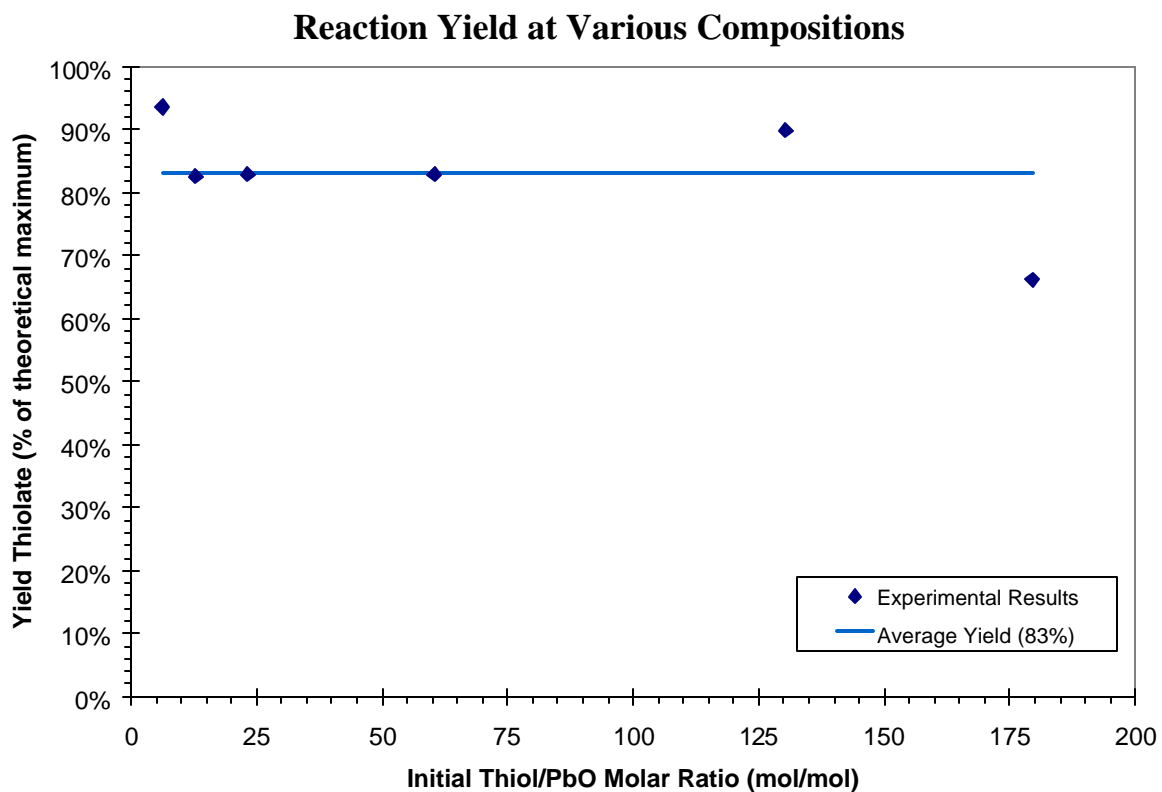


Figure 4.8: The yield of thiolates, indicating the degree to which PbO was converted into $\text{Pb}(\text{SR})_2$ in excess thiol.

The thermodynamic limit for the removal of thiols by this reaction can be determined from the heat of reaction. The equilibrium constant K is given by

$$-\Delta G_{rxn} = RT \ln K \quad (4.12)$$

where, from equation (4.10),

$$K = \frac{a_{Pb(SR)_2} a_{H_2O}}{a_{HSR}^2 a_{PbO}} \quad (4.13)$$

The solids PbO and $Pb(SR)_2$ both have unit activity. Assuming an ideal solution, the activity of the water and thiol are equal to their mole fraction in the hydrocarbon solvent. The value of ΔG_{rxn} estimated in section 4.1.3.3 is -121 kJ/mol. The equilibrium constant for this reaction, assuming unit water activity (saturated), is approximately 1.9×10^{21} , permitting the removal of thiols to 23 parts per trillion. The thermodynamic limit of this reaction permits desulfurization to extremely low levels, although kinetic and mass transfer limitations prevent this limit from being practically achieved.

Figure 4.8 presents a series of photographs demonstrating the reaction of 3 mL *n*-octanethiol diluted with 4 mL cyclohexane with 0.75g PbO_2 at room temperature, without agitation. PbO_2 was used in the photographs for color contrast purposes, since the massicot form of PbO and the thiolate product are both yellow. PbO_2 is black but reacts to form the same yellow thiolate product. Both compounds react in the same way. The reaction is marked by a rapid growth in apparent solids volume as the liquid thiol is converted into solid thiolate. The color change from the black PbO_2 to the yellow

$\text{PbO}(\text{SR})_2$ is also evident. The reaction front is also visible as the thiol, which was injected from the top of the jar, mixes with the oxide. The reaction shown occurred over an elapsed time of 23 min.

The reaction of *n*-octanethiol with metallic Pb wire was also successful. An example of this reaction is shown in Figure 4.8 in which a piece of Pb wire is placed into a liquid consisting of 2 mL cyclohexane and 4 mL of *n*-octanethiol. The reaction is much slower than the reaction with powdered PbO due to the time required diffusing oxygen to the Pb surface and the lower surface area of the wire compared to the powdered oxides. The reaction shown in the photographs occurred over a period of about 62 hours. The thiolates that were formed on the Pb wire grew in the form of plates which were pushed outwards as new thiolates were produced at the Pb surface. Figure 4.8 shows the product of similar reaction conditions after 14 days. The growing thiolate plates uncoiled the wire, pushing it upwards. The structure was able to fill the vial because the thiolates are wetted by the organic mixture in bottom of the jar, acting like a sponge and drawing the liquid upward, allowing the structure above the liquid to continue growing.

In the extraction studies, the Pb thiolates were successfully decomposed back to the original thiols and $\text{Pb}(\text{NO}_3)_2$ under the experimental conditions. The thiol recovery in the organic phase, as determined by GC, was 78.4%, assuming $\text{Pb}(\text{SR})_2$ as the starting stoichiometry. The recovery of Pb as $\text{Pb}(\text{NO}_3)_2$, as determined by weighing the crystals produced after evaporation of the aqueous phase, was 102%. The slight excess mass is

considered experimental error. A second trial using thiolates produced from PbO_2 and using 0.3 M nitric acid yielded a thiol recovery of 90.1% and a Pb recovery of 94.6%.

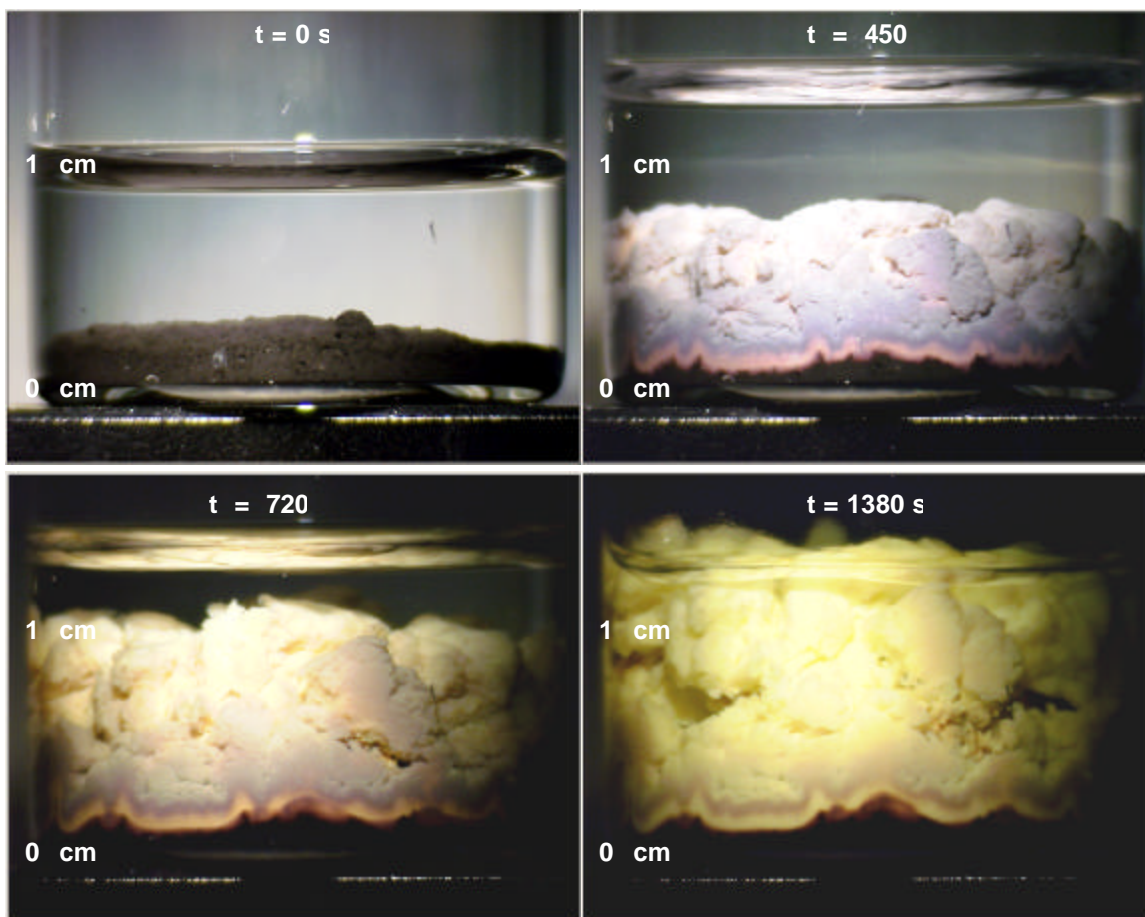


Figure 4.8: Photographs of the reaction of PbO_2 with *n*-octanethiol. Photographs are chronological, starting from top left, occurring at elapsed times shown. The initial mixture was 0.75 g PbO_2 , 4 mL cyclohexane, and 3 mL *n*-octanethiol (added after first picture).

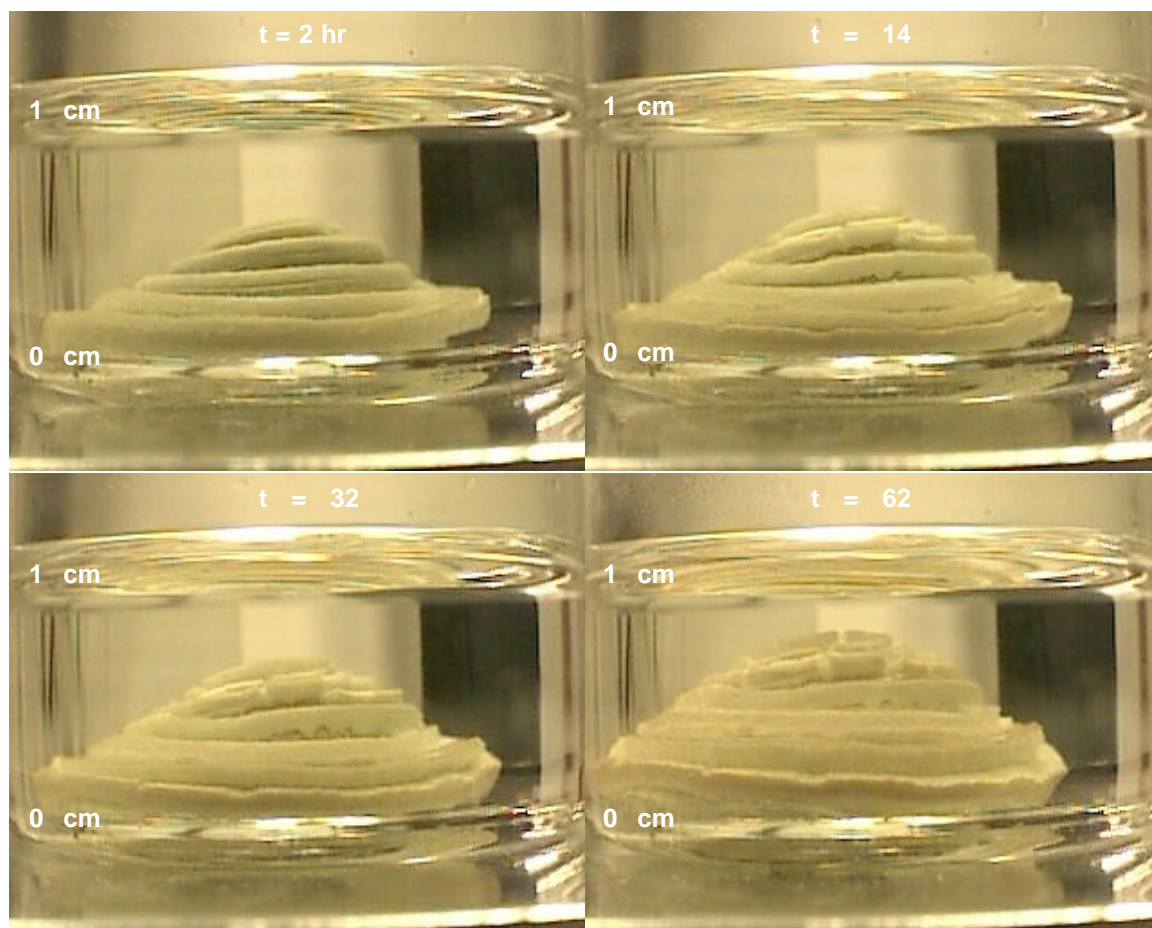


Figure 4.8: Photographs of the reaction of *n*-octanethiol and metallic Pb wire. Initial conditions are a coil of Pb wire (approx. 8 cm long) in a mixture of 2 mL cyclohexane and 4 mL *n*-octanethiol.

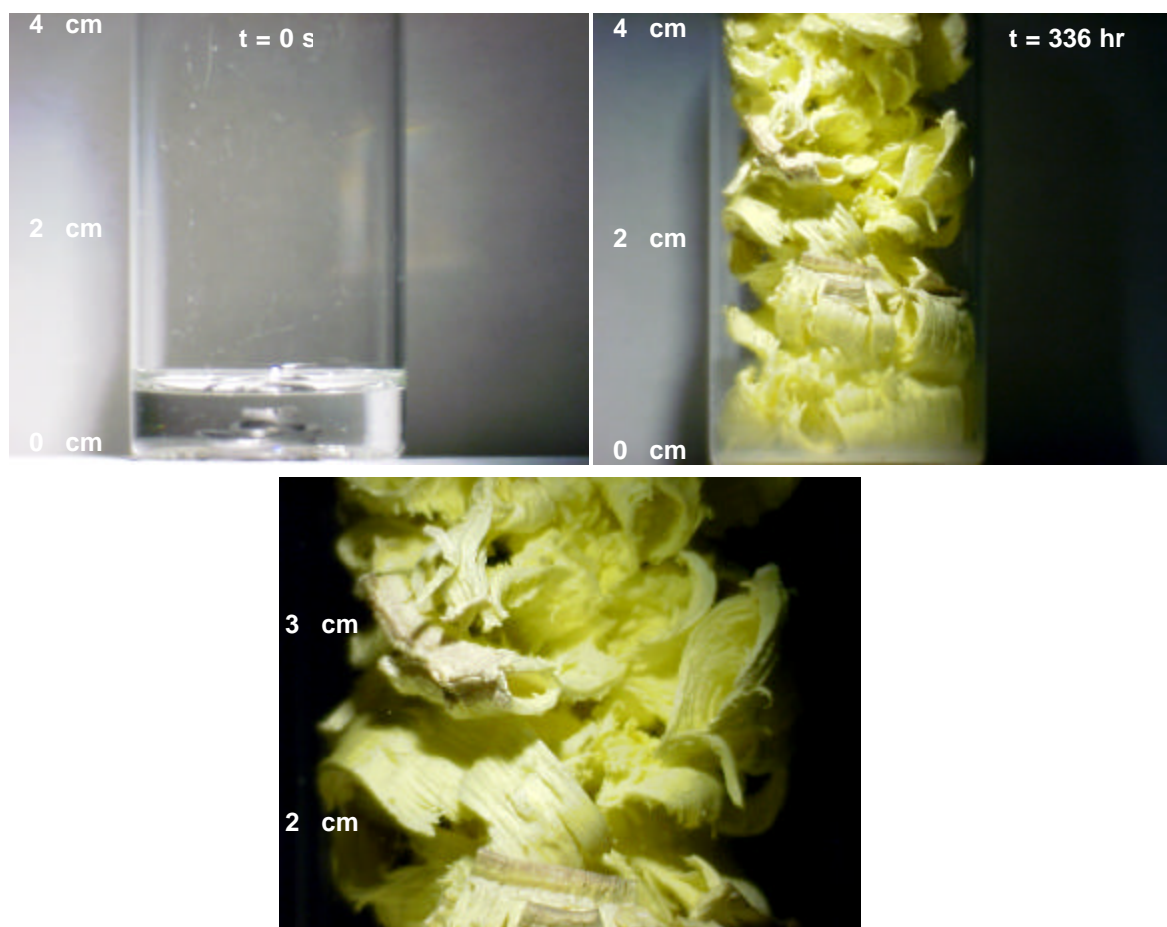


Figure 4.8: Photographs of the reaction of Pb wire with *n*-octanethiol. Top left: Pb wire in cyclohexane before reaction. Top right: After reaction with *n*-octanethiol for 14 days. Bottom: Detail view of same reaction product structure shown above right. Initial mixture was 2 mL cyclohexane and 4 mL *n*-octanethiol (added after first picture).

Water was found to catalyze the reaction between PbO and thiols. The rate of reaction was measured for both a reactor containing excess water in the form of a second liquid phase and for a reactor containing a desiccant to remove water formed by the reaction. Toluene was the solvent, excess PbO was used, and other reaction conditions were identical to those previously described.

The reaction proceeded much faster in the presence of water. The reaction rate was constant at 1.07 ppm S/sec in the reactor with excess water, and 0.0172 ppm S/sec when the water was removed, as shown in Figure 4.9. In the presence of water, the reaction reached completion in less than 30 minutes with a final sulfur concentration of approximately 12 ppm S. Additionally, the reaction rate appeared to be zero order with respect to thiol even to very low thiol concentrations, perhaps owing to the strong adsorption of thiols onto the metal oxide surface.

The reaction order was confirmed with batch reaction rate data, shown in Figure 4.10. The batch data are fit well by a rate law that is zero order in thiol and proportional to water concentration. The line shown in Figure 4.10 is the rate law fit to the data using the kinetic rate constant and the initial water concentration as fitting parameters. The initial and final water concentration determined from this fit are both within the solubility of water in toluene. The catalytic effect of water is likely due to the water acting as a proton transfer agent, aiding the movement of the proton from the thiol to the metal oxide. In this reaction, the thiols are slightly acidic and the oxygen in the metal oxide acts as a base (proton acceptor). The water will solvate the proton, facilitating the transfer.

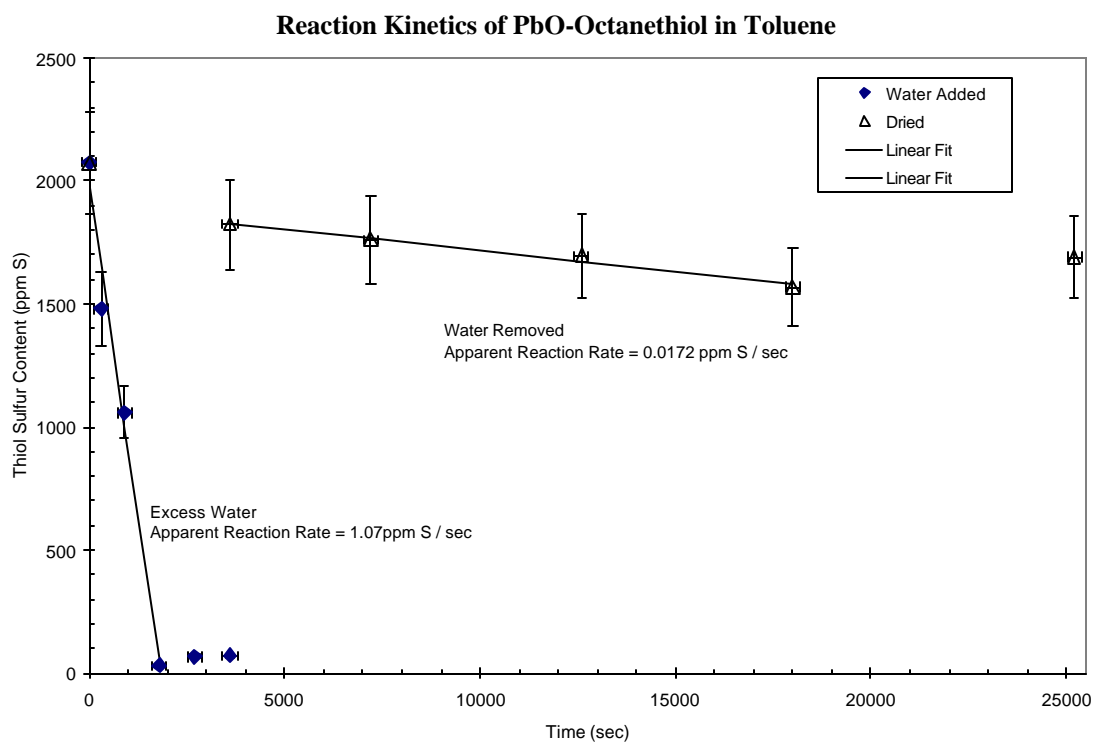


Figure 4.9: Reaction rate of PbO and octanethiol with water added and water removed from the reactor.

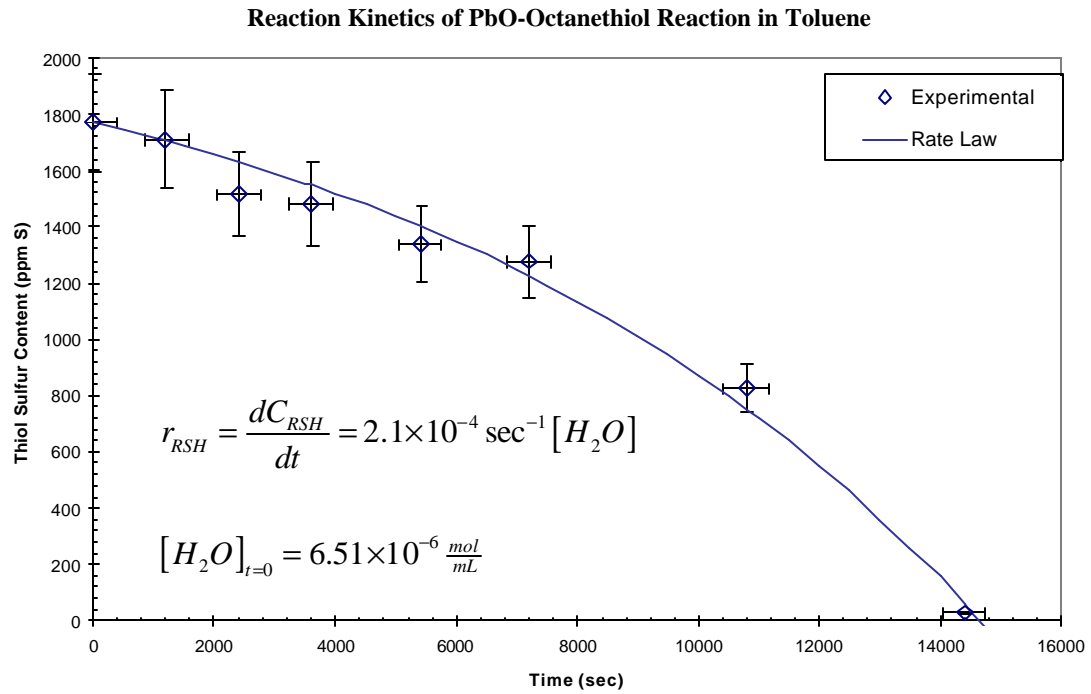


Figure 4.10: Batch reaction rate of PbO and octanethiol. Solid line is fit of the rate law shown to the data using a two parameter fit, with parameter values given in the figure.

4.2.5. Conclusions

The heterogeneous reaction of thiols with lead oxide can be used to remove and recover thiols from a petroleum stream. Experimental results suggest that a simple process consisting of reaction, filtration, and extraction is all that is required to separate and recover the thiols. The PbO can be recovered by additional evaporation and roasting steps. Most of the required unit operations have low energy requirements and low reagent material costs.

The use of metallic Pb rods placed into storage tanks also shows promise for the reduction of the sulfur content of certain fuels without significant capital requirements. Pb rods placed into storage tanks could be removed periodically for cleaning, and the thiolates could be collected for regeneration at another facility.

The reaction is autocatalytic; water produced by the reaction of a metal oxide and a thiol species accelerates the reaction between the two. The catalytic effect of water is assumed to result from water acting as a proton transfer agent during the reaction, facilitating the transfer of the thiol proton to the oxide oxygen. The reaction rate follows a rate law that is zero order in thiol concentration and proportional to water concentration. The observed reaction rate is ideal for removal of thiols to very low levels since the reaction does not slow down appreciably until thiol concentrations reach levels on the order of 20 ppm S. Thiol removal down to 12 ppm S have been observed.

This relatively simple process was not previously recognized, most likely, due to the requirement of keeping the operating temperatures sufficiently low. At temperatures above about 50°C, the thiolates become miscible in hydrocarbons and a simple physical separation is no longer possible. Additionally, previous processes, such as Doctor Sweetening, relied on the thermal decomposition of lead thiolates to remove Pb as PbS while converting thiols into disulfides.¹⁰⁴ During the development of the Doctor Sweetening process, the removal of sulfur compounds was less important than the elimination of the odor and acidity caused by thiols. By the time sulfur removal became relevant, HDS technology was available to remove thiols as well as other organo-sulfur compounds.

This process can reduce the sulfur content of fuels for environmental benefits. It could also reduce the load on a conventional HDS unit when sour feedstocks are used by removing the thiols before the feed is introduced to the HDS unit, saving costs in hydrogen and catalyst life. This process can also be used to remove recombinant mercaptans from hydrotreated streams. Operation of the HDS reactor under mild conditions will reduce the operating costs and this process will ensure that product sulfur levels meet regulatory criteria.

5. Oxidation of Aliphatic and Aromatic Sulfides Using Sulfuric Acid

5.1. Introduction to Oxidative Desulfurization

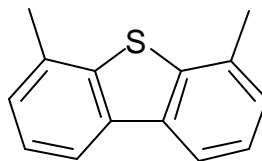
Advances in refining technology ultimately lead to large-scale desulfurization of petroleum fuels in the 1960s. Platinum catalysts used during reforming of gasoline, which converts low octane linear hydrocarbons into high octane branched paraffins, are poisoned by sulfur compounds.⁷¹ Desulfurization of naphtha streams became necessary in order to produce high quality gasoline.

Desulfurization has only been performed for environmental reasons recently. The advent of “three-way” catalytic converters in automobiles required the elimination of tetraethyl lead from gasoline in the early 1970s due to lead poisoning of the Pt-Rh catalyst. Sulfur was already being removed from gasoline, so no other changes were made to refining practices at that time. Diesel fuel, along with other heavier fuels such as gas oil and fuel oil, continued not to be treated and thus catalytic converters were not useable on diesel powered vehicles.

Environmental pressures have only recently forced the legislation of low-sulfur diesel to permit the use of emission control technologies on diesel engines. A new US law limits the level of sulfur permitted in diesel fuel to 15 ppm by 2006.¹⁰⁵ Sulfur levels as low as 5 ppm in diesel are also suggested as a future regulatory limit in the same law.

Existing hydrodesulfurization (HDS) technology, based on the catalytic hydrogenation of sulfur compounds over cobalt promoted molybdenum sulfide catalysts,¹⁴ is highly effective for reactive compounds having accessible sulfur atoms, such as thiols, disulfides, and some sulfides. Lower boiling streams, such as straight-run gasoline, contain mostly thiols and some small sulfides which are successfully removed by HDS.¹⁴

Diesel fuel, gas oil, and other heavier streams, however, contain primarily heavy polynuclear aromatics that include a thiophene structure. These larger compounds, particularly those with sterically hindered sulfur atoms, are not easily hydrogenated.^{106,107} The usual example of this class of compounds is 4,6-dimethyldibenzothiophene, shown below. The sulfur is relatively inaccessible when adsorbed onto a heterogeneous catalyst, limiting the reactivity.

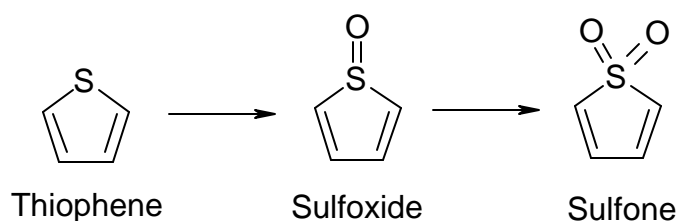


4,6-dimethyldibenzothiophene

While operating an HDS reactor at high pressure and temperature can remove some sulfur in this form, the harsh conditions required (800-2500 psig, up to 370°C)¹⁰⁶ typically result in high hydrogen consumption and lowered octane rating due to hydrogenation of olefins.¹⁰⁸

Other techniques are required to efficiently remove these types of sulfur compounds from diesel and other heavy streams. Oxidative desulfurization (ODS) is one such

process. ODS is based on the facile oxidation of organic sulfur. The concept is not new, spawning patents as early as 1967.¹⁰⁹ ODS relies on the ability of bivalent sulfur in organic compounds to expand its valence shell and add oxygen without needing to break carbon-sulfur bonds. The oxidation of thiophene is shown below.



The oxidized sulfur atom becomes highly polar and enhances the subsequent extraction or adsorption^{37,110} of the sulfoxide or sulfone to effect the removal of the sulfur from the feed stream.

The oxidizer used in ODS must be very selective for sulfur to prevent the oxidation of olefins or aromatic compounds present in the feed. Oxidation of these compounds reduces the octane rating (if performed on olefin-containing gasoline) and also increases the loss of feed material by extracting oxidized hydrocarbon compounds in addition to sulfur compounds.

The oxidant system of choice is hydrogen peroxide combined with acetic or formic acid.^{37,106,110} When combined, a peroxyacid, having a C-O-O-H peroxide bond, is formed. The peroxyacid oxidizes the sulfur compounds and is reduced back to the original carboxylic acid. The exact mechanism of this reaction is not known. Other oxidizing systems including oxygen and aldehydes¹¹¹, nitrogen dioxide,¹¹² and ultrasound and

water¹¹⁰ have also been explored. Reaction conditions are typically atmospheric pressure and less than 120°C.

The oxidized sulfur compounds are subsequently extracted, adsorbed, or both.³⁷ Methanol,³⁷ acetonitrile,¹¹³ butyrolactone,¹¹² and other solvents are used for solvent extraction and alumina is the primary adsorbent.

Three commercial versions of ODS have been reported.^{37,110} The first is from Petro Star, Inc. which uses peroxyacetic acid followed by solvent extraction. Peroxyacetic acid is an oxidizing acid formed by mixing hydrogen peroxide and acetic acid. This or similar reaction and extraction steps form the core of all three commercial ODS processes.

The ASR-2 process³⁷, developed by UniPure Corp. and ChevronTexaco, is based on a two liquid phase reactive extraction using a hydrogen peroxide – organic acid mixture. The organic acid is unspecified, although formic and acetic acids are typical. The resulting sulfones are extracted by methanol and separated by flash distillation of the methanol-sulfone mixture. The treated diesel stream is neutralized and any remaining sulfones are adsorbed over alumina. The simplified process flowsheet is shown as Figure 5.1.

UniPure ASR-2 Simplified Flow Plan

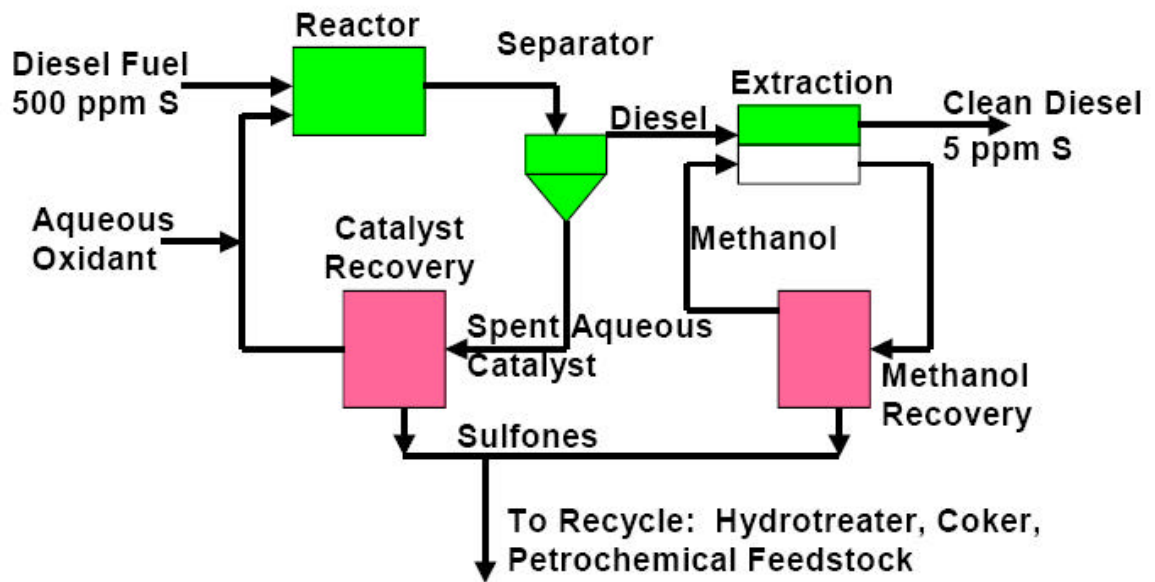


Figure 5.1: ASR-2 oxidative desulfurization process developed by UniPure. Adapted from ³⁷.

SulphCo, Inc. licenses a technology based on in situ generation of hydroxyl radicals by ultrasonication of a water-oil emulsion in the presence of proprietary hydrogen peroxide generating catalyst.^{110,114} The hydroxyl and atomic hydrogen radicals react with hydrocarbons in the high temperature and pressure center of imploding cavitations caused by the ultrasonication. Control over the reactions that occur in these cavitations is suspect, and the selectivity is likely to be low.

ODS has one significant advantage over HDS that makes it the ideal complement to existing HDS units. The least reactive compounds in HDS, such as substituted dibenzothiophenes, are highly reactive in ODS due to the high electron density on the sulfur atom. Although the order of reactivity seems to vary with the oxidant and catalyst,¹¹⁵ no major category of sulfur compound found in petroleum is unreactive towards ODS. This process has been shown to effectively remove virtually all of the sulfur from a diesel fuel stream³⁷ and is effective on the polynuclear aromatic family of sulfur compounds including substituted dibenzothiophene.^{113,116}

Limitations of ODS are primarily economic. UniPure has acknowledged that the cost of the hydrogen peroxide oxidant is the limiting economic factor for their process.³⁷ Difficulties inherent in manufacturing, concentrating, transporting, and storing oxidizers should also be considered, particularly as more refineries are built in the Middle East and in developing countries where safe and reliable access to a broad range of chemicals may be limited.

5.2. *The Use of Sulfuric Acid in ODS*

The traditional method of removing sulfur, hydrodesulfurization (HDS), has limited effectiveness at removing thiophene derivatives, such as dibenzothiophene, from heavier diesel fuel.¹⁰⁷ Given the economic limitations of peroxide-based ODS and the need for an alternate technology for refineries where a supply of hydrogen peroxide is not readily available, oxidation methods besides H_2O_2 are needed.¹¹¹

We report here the oxidation and extraction of organo-sulfur compounds, including thiophene and alkyl sulfides with concentrated sulfuric acid. Sulfuric acid is not typically regarded as an oxidizing acid due to the stability of the sulfate ion. However, in the presence of sulfur atoms with a lower oxidation state, such as those in sulfides, sulfate can be reduced.¹¹⁷ The reaction between H_2S and concentrated sulfuric acid is known to be fast and yield elemental sulfur, water, and SO_2 as reaction products.¹¹⁸ Here we describe the oxidation of thiophene and alkyl sulfides with sulfuric acid. The oxidized organosulfur compounds separated into the aqueous phase, demonstrating that these sulfide compounds can be reduced to low levels in hydrocarbon solutions. This new approach employing sulfuric acid to oxidize organosulfur compounds and extract the oxidized products offers an alternative or supplement to peroxide-based ODS.

5.3. *Experimental*

Solutions of several sulfides in hydrocarbon solvents were desulfurized in a glass reaction vessel. Four test solutions were prepared: (1) 2000 ppmw sulfur (~0.047 M) as

tetrahydrothiophene (Aldrich, 99%) in cyclohexane (Alfa Aesar, 99+%), (2) 2000 ppmw sulfur (~0.047 M) as tetrahydrothiophene in tetrahydrofuran (Alfa Aesar, 99+%), (3) 2050 ppmw sulfur (0.056 M) as thiophene (Aldrich, 99+%) in toluene (Sigma-Aldrich, 99.5%) and (4) dibutyl sulfide (Aldrich, 96%) in toluene. A small amount of decane (Aldrich, 99+%) was added to each stock solution as an internal standard for GC analysis.

Ten mL of the organic solution and 10 mL of sulfuric acid (dilutions of 96% H₂SO₄, Fisher) were added to the reaction vessel, forming two liquid phases. The reaction temperature was 22°C. The two phase mixture was vigorously stirred for 1 hour (unless otherwise indicated). After reaction, the phases were allowed to separate and the organic layer was removed by syringe to prevent further reaction.

The concentration of the sulfide species in the organic layer was measured by gas chromatography (30m methyl silicone capillary column, flame ionization detector). The concentration of unreacted sulfide species was determined by normalizing all results using the internal standard (decane). We were unable to accurately analyze the composition of the aqueous layer by GC due to the high acid content. Compositions of organic species in the aqueous phases are only semiquantitative. To analyze the aqueous phase by GC the solutions were diluted to reduce the acid concentration. However, the acid either adsorbed or reacted with the GC column packing and results were only semiquantitative. Quantitative analysis was limited to the organic phase.

Tetrahydrothiophene also was reacted in a homogeneous solution of tetrahydrofuran and sulfuric acid. The reaction products obtained by this technique were analyzed by mass spectrometry.

5.4. Results

All three sulfide compounds were successfully removed from the hydrocarbon solvent by oxidation and extraction into the aqueous (acid) phase. No oxidized reaction products remained in the organic phase, and only trace amounts (<50 ppm) of the sulfide compounds were detected in the aqueous phase. Colloidal elemental sulfur was formed in the aqueous phase, evidenced by the classic Tyndall “sunset” effect, shown in Figure 5.2. The aqueous phase became yellow upon mixing with the organic phase. As the reaction proceeds, the aqueous phase color changed first to orange, then brownish-red. If high concentrations of sulfide were used, the colloid concentration became large enough to eventually turn dark red and finally black, as no light was transmitted. The aqueous phase containing the colloidal sulfur was recovered by gravity separation. This colloidal solution became milky white if the acid was diluted sufficiently with water, forming “milk of sulfur”. The colloidal sulfur could be slowly dissolved with CS₂, yielding an optically clear aqueous phase.

Gas chromatography analysis of the aqueous phases revealed three primary oxidized sulfide products for the tetrahydrothiophene reaction. All three oxidized products were extracted completely into the aqueous phase, there was no evidence for any of these

products in the organic phase. The same three products were detected by GC for the reaction of tetrahydrothiophene in THF as in the diluted aqueous phase. The products were analyzed by mass spectrometry, shown in Figure 5.3. The mass fragmentation patterns were compared to those in the NIST database (<http://webbook.nist.gov>). The spectrum of product B matches tetrahydrothiophene sulfoxide. Product A was not able to be positively identified, but based on the parent peak and fragmentation the compound is likely a ketosulfoxide species or the dehydrogenated sulfone. Product C yielded a highly fragmented spectrum with mass fragments going up to $m/z=189$. The mass spectrum appears best described as an adduct of tetrahydrothiophene and sulfuric acid, shown in figure 2.

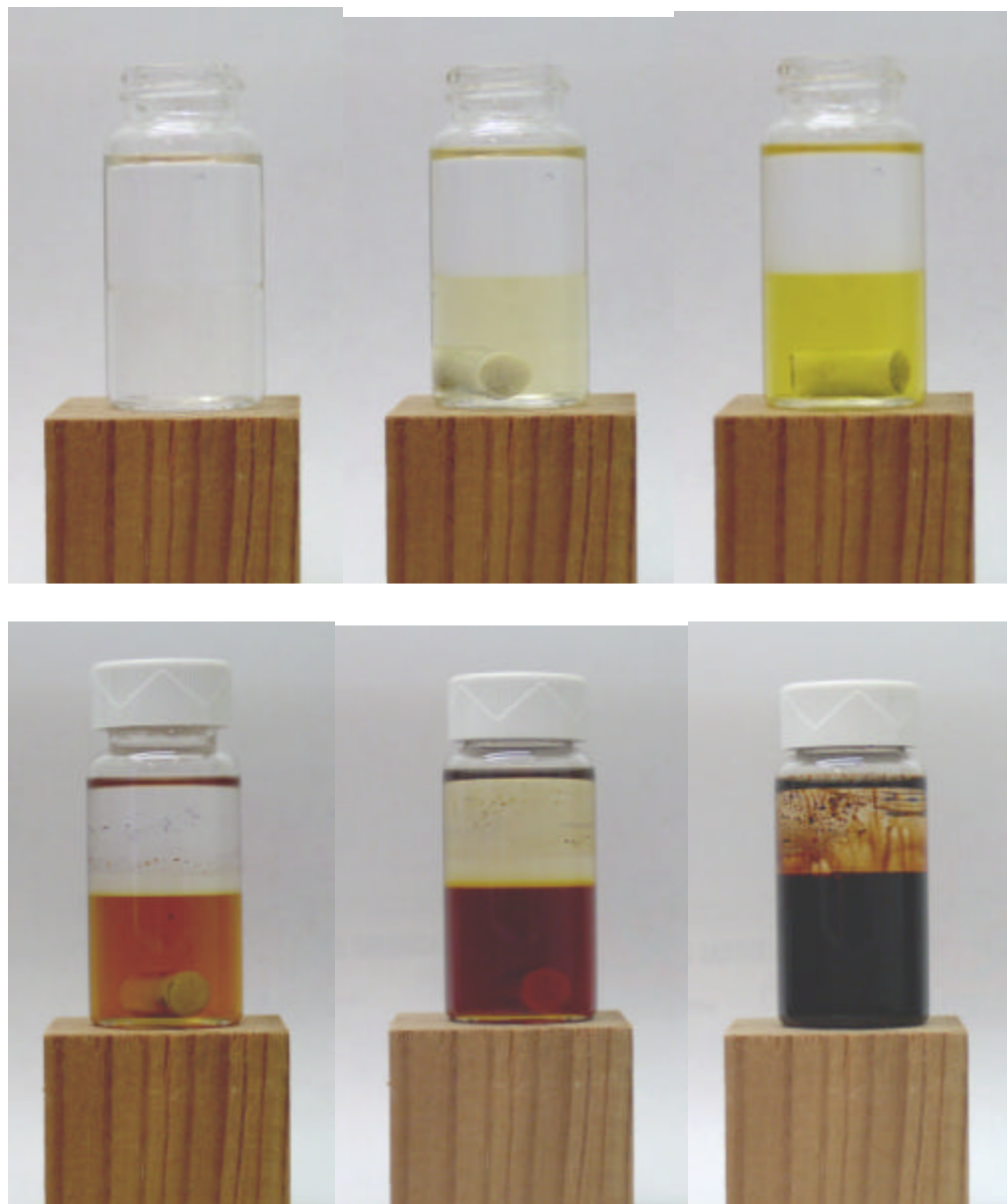


Figure 5.2: Photographs of the Tyndall sunset effect in a solution of toluene, tetrahydrothiophene, and thiophene.

The reaction rate was measured for each of the three sulfides when reacting with 16M H_2SO_4 (18 M sulfuric acid is fully concentrated (96 wt% H_2SO_4)). The stirring was stopped for several seconds after various time intervals and the phases allowed to separate. Samples were drawn from the organic phase and the concentration of unreacted sulfide was determined by GC. The results are shown in Figure 5.4; the observed reaction rates are well fit by a first order rate law. Dibutyl sulfide was removed to about 27 ppm S within 5 minutes and was undetectable (<10 ppm S) at 20 minutes. Tetrahydrothiophene was reduced to 120 ppm in 5 minutes, and reached 66 ppm S after 65 minutes. Thiophene reacted more slowly, being reduced to 283 ppm S at 20 minutes and 113 ppm S after 65 minutes. Values below about 150 ppm S are near the limit of reliable quantification for the analysis method used.

The reaction rate appears to be first order with respect to sulfuric acid concentration at lower acid concentrations. Figure 5.5 shows the integrated reaction rate of the tetrahydrothiophene solution over 1 hour for various acid concentrations. Figure 5.6 shows the extent of reaction over time for the same system using 9M acid. The reaction rate shown in Figure 5.6 is constant over time, suggesting that the reaction is now zero order in sulfide concentration. Considering Figure 5.5 and Figure 5.6, the lower acid concentration appears to shift the reaction from being first order in sulfide concentration to first order in sulfuric acid concentration. A reaction scheme consistent with these results is presented in the following section.

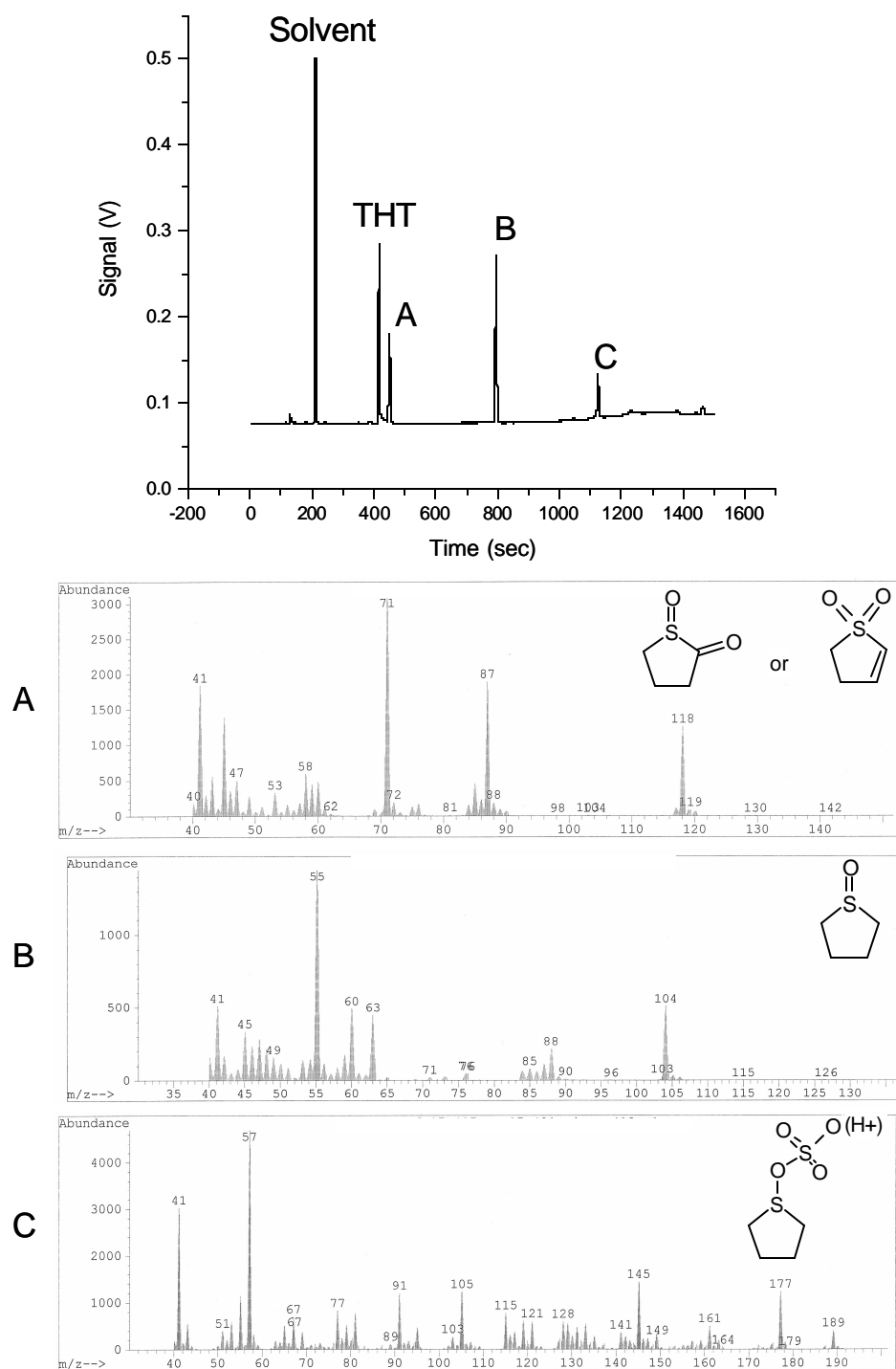


Figure 5.3: GC/MS spectra for the reaction products of tetrahydrothiophene and sulfuric acid. The mass spectrum for product B matches that of tetrahydrothiophene 1-oxide. The spectrum of product A suggests a species with two oxygen atoms, such as the sulfone or ketosulfone. Mass spectrum C could be the adduct of sulfuric acid and tetrahydrothiophene.

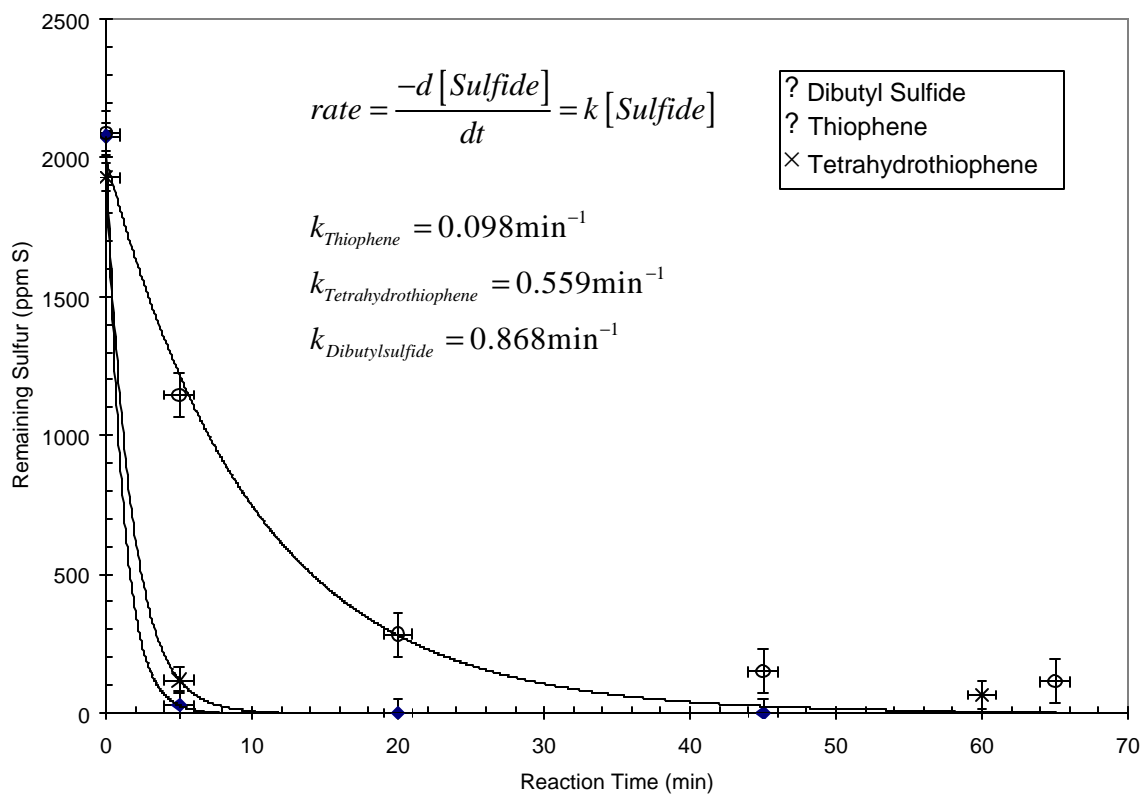


Figure 5.4: Reaction rate of 2000 ppm solutions of thiophene, tetrahydrothiophene, and dibutyl sulfide with 16M H₂SO₄. Data are fit by a rate law that is first order in sulfide concentration, shown above. For the given rate constants, sulfide concentration is given in units of ppm S.

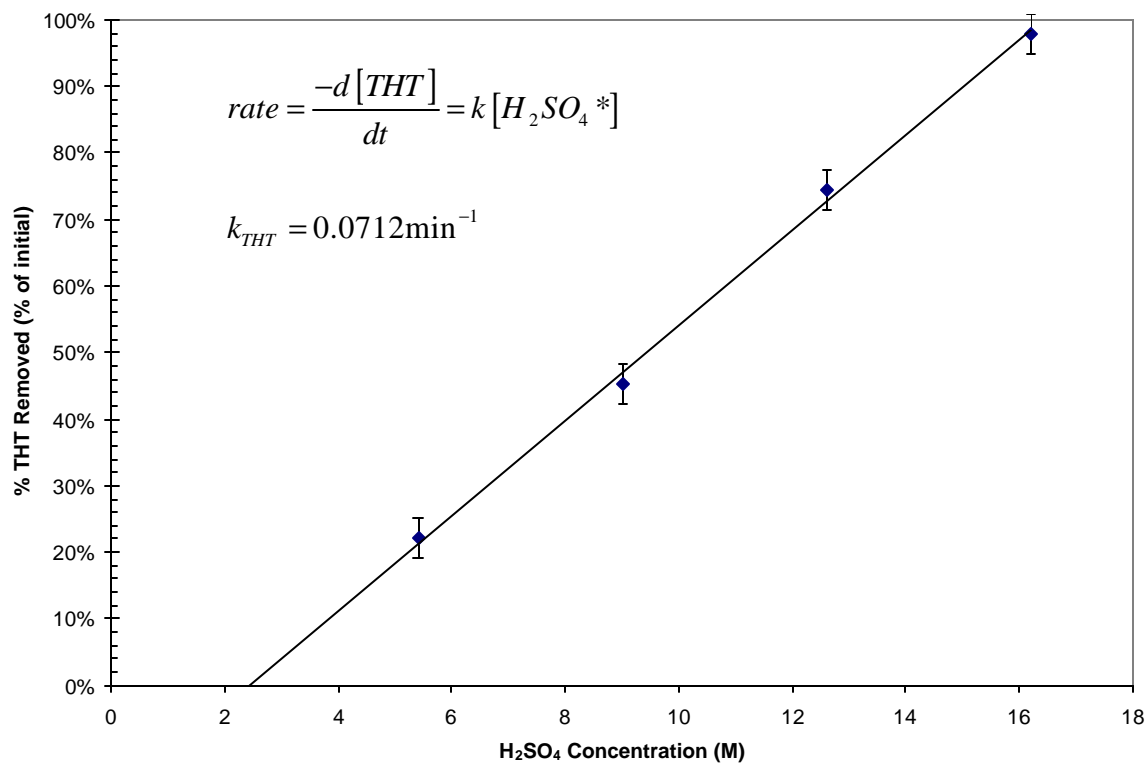


Figure 5.5: Consumption of tetrahydrothiophene from a 2000 ppm S solution after 1 hour reaction with various concentrations of sulfuric acid. Data is fit by a rate law first order in acid concentration shown. $[\text{H}_2\text{SO}_4^*]$ is acid concentration above the threshold value shown by the intercept (2.4 M).

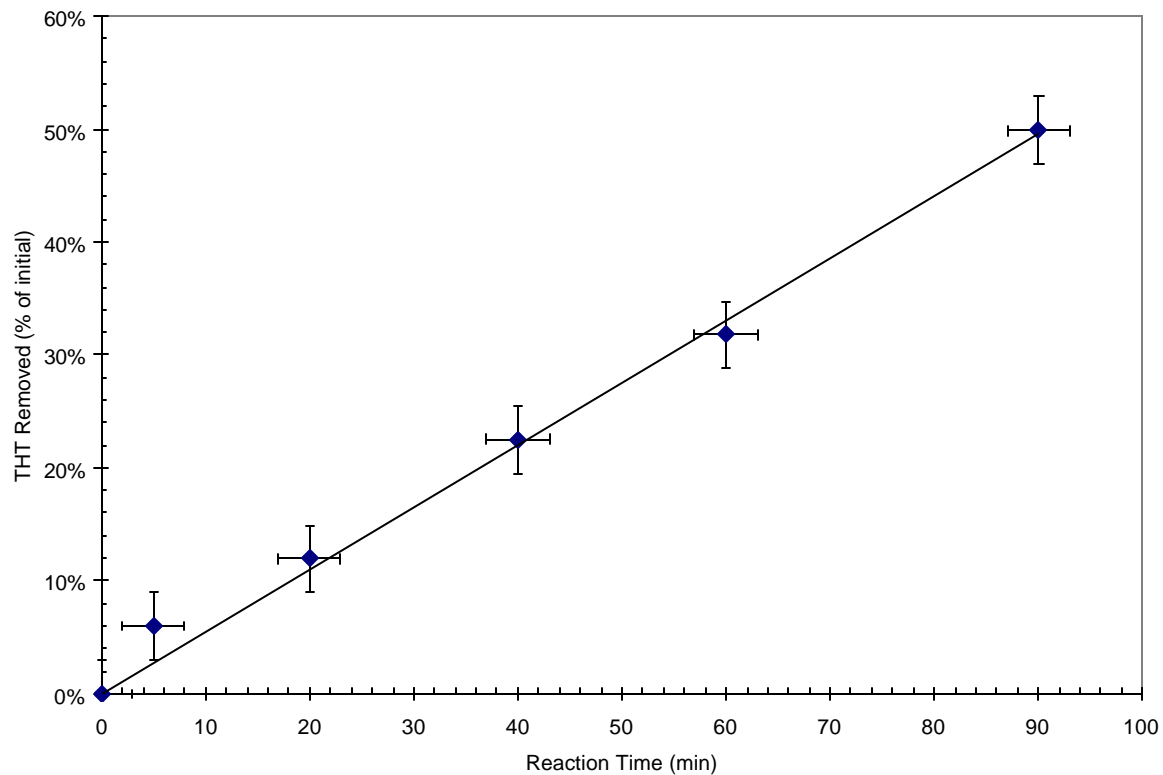
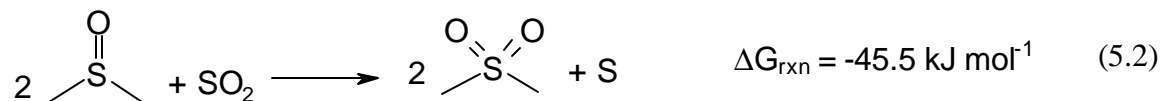
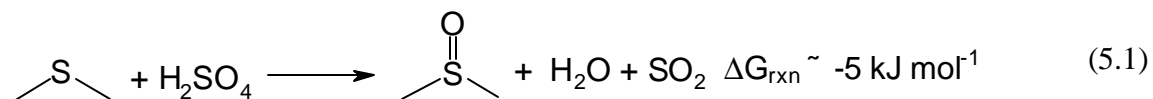


Figure 5.6: Reaction rate of tetrahydrothiophene from a 2000 ppm S solution reacting with 9M H_2SO_4 . Rate is constant at 0.0055 min^{-1} .

5.5. Discussion

A reaction scheme developed for the reaction of H₂S with sulfuric acid can be easily adapted to explain the observed results. Chuang, et al^{118,119} have shown that a two step reaction, consisting first of reaction between H₂S and H₂SO₄, produces SO₂, which is then consumed by further reduction to elemental sulfur. If a similar scheme is assumed for sulfides, the resulting reactions are:

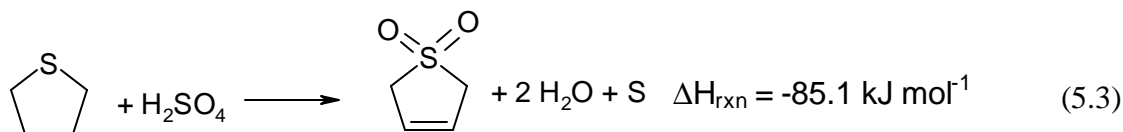


where the dimethyl sulfide compounds shown can be replaced by any sulfide.

Using dimethyl sulfide as an example in the above reactions, the Gibbs energy of reaction (5.1) is +25.5 kJ mol⁻¹, using each material in its standard state.¹²⁰ However, in concentrated acid solutions, the heat of mixing of water and sulfuric acid is considerable. The partial molar enthalpy of formation of water in a 96 wt% solution of sulfuric acid is higher by about 30 kJ/mol than the standard state¹²¹, making the overall $\Delta G_{\text{rxn}} \sim -5$ kJ/mol. Other sulfide compounds have approximately the same free energy change for the formation of the sulfoxide from the sulfide. The large excess of sulfuric acid and the consumption of SO₂ by reaction (5.2) favor formation of the product sulfoxide. No gas was ever observed being evolved from the reaction, probably due to the very high solubility of SO₂ in the concentrated acid. The solubility of SO₂ in sulfuric acid ranges

from 10-100+ g SO₂/kg H₂SO₄, depending on concentration and temperature. At the experimental conditions, the solubility is about 30 g SO₂/kg H₂SO₄. SO₂ is also soluble in most organic liquids.¹²²

Several other reactions are also possible, though most are not thermodynamically favorable. One reaction that might occur with tetrahydrothiophene is a modification of reaction (5.1), shown below. This reaction explains the presence of product A from Figure 5.3. Note that the double bond can be formed at either of the two possible positions with about the same energy. The formation of the ketosulfoxide would occur from electrophilic attack on the ring, with the second oxygen adding at the alpha carbon, rather than the sulfur.



These proposed reactions are thermodynamically favorable, account for the observed products and also agree with the observed reaction rate laws. Figure 5.4 shows that at high acid concentrations, the rate of oxidation is first order in sulfide concentration, in agreement with reactions (5.1) and (5.3). The initial reaction between the sulfide and H₂SO₄ appears to be rate limiting. This result agrees with the rate law determined for H₂S reacting with sulfuric acid.¹¹⁹

The active acid species has been proposed to be H₂SO₄, rather than HSO₄⁻.¹¹⁹ At high acid concentrations, the H₂SO₄ species is abundant and reaction 1 is the rate limiting step.

At lower acid concentrations, however, the dissociated species is more prevalent. The reaction rate may then become limited by the rate of association of H_2SO_4 from the ions, $\text{H}^+ + \text{HSO}_4^- \rightarrow \text{H}_2\text{SO}_4$, which must occur before the oxidation step can proceed. Under these conditions, the rate would appear first order in acid concentration and zero order in sulfide concentration, despite the acid being far in excess of the sulfide. The data in Figure 5.6 supports this hypothesis, showing that the reaction rate in 9M H_2SO_4 is constant (since the concentration of H_2SO_4 is not appreciably changed by the reaction with small amounts of sulfide), and Figure 5.5 confirms the reaction is first order in acid concentration. Below the threshold acid concentration shown in Figure 5.5, the rate of association is likely too small to permit the oxidation reaction and the thermodynamics of the reaction become unfavorable.

The reaction of sulfide species with concentrated sulfuric acid was previously reported by Meadow, et al^{123,124}, who attributed the desulfurization effect to NO_2 additives in small quantities of H_2SO_4 . However, their analysis method could not distinguish between sulfoxides and other oxidized sulfur species present in the hydrocarbon phase and unreacted sulfide, nor did they report the reduction of sulfuric acid.

Early work of Wood et al suggested that sulfides were removed by dissolution into sulfuric acid.¹²⁵ In the present work, all of the oxidized sulfur compounds were extracted into the aqueous phase, while the unreacted sulfides remained in the organic phase. The octanol-water partition coefficients¹²⁶ for the three sulfides studied here are summarized in Table 5.1. All three sulfides show a strong preference for the organic phase.

Furthermore, very little of the original sulfide was detected in the acid phase after the reaction. The absence of the sulfide species and the presence of the sulfoxides and other oxidized species reveal that the observed “solubility” only occurs after the sulfides are converted to the more polar oxidized species.

Table 5.1: Partition coefficients for the sulfides studied. Data from Yaws.¹²⁶

Species	Log of Octanol-Water Partition Coefficient (25°C)
Thiophene	1.81
Tetrahydrothiophene	1.79
Dibutyl sulfide	3.87

This simple extraction method reported here may not work with higher molecular weight sulfides. The higher molecular weight sulfoxides and sulfones may not be sufficiently polar to be fully extracted into the aqueous phase. These higher molecular weight species may require the sulfoxides and sulfones to be extracted with methanol or adsorbed onto alumina to effect their removal, as is done in conventional peroxide-based ODS.³⁷

The ability of sulfuric acid to quickly remove sulfide species by converting them into sulfoxides and other oxidized species provides a possible addition to or replacement for ODS performed by hydrogen peroxide. Since peroxide-based ODS is limited by the cost of the oxidant, a pre-treatment with sulfuric acid could remove much of the original sulfur content before the stream is sent to the ODS reactor. A sulfuric acid wash could also reduce the load on hydrodesulfurization (HDS) reactors when processing high-sulfur

crude. The reactor design for such a sulfuric acid system is essentially the same as for sulfuric acid-based alkylation reactors. Only low olefin feeds could be used since the acid will catalyze polymerization reactions.

5.6. Conclusions

Oxidative extraction of thiophene, tetrahydrothiophene, and dibutyl sulfide was demonstrated in a two phase reactor using concentrated sulfuric acid. The oxidized products are likely the sulfoxides and other oxidized sulfur species, which are effectively extracted into the acid phase. Sulfuric acid is reduced to elemental sulfur, which remains in a colloidal state in the aqueous phase. The reaction rates are first order in sulfide concentration when performed in concentrated (16M+) sulfuric acid, and first order in sulfuric acid when performed in less concentrated acids. This reaction could be used to greatly reduce the sulfur concentration in petroleum fractions prior to HDS or ODS processes.

6. Conclusions

Despite extensive research into desulfurization by the petrochemical industry over the last thirty years, few viable alternatives to hydrodesulfurization have been developed. The lack of progress is likely due to a combination of factors including the effectiveness of HDS, the cost associated with installing new processes, and resistance to change in the established community of refineries.

Regulatory limitations on sulfur levels in automotive fuels, particularly diesel, have led to a renewed interest in alternative desulfurization technologies, as demonstrated by the commercial development of several oxidative desulfurization technologies. The scope of new technologies under development is still limited, however. For example, virtually all ODS research is based on hydrogen peroxide-organic acid systems.

The need exists for a wider variety of desulfurization techniques; particularly as refineries are built in many parts of the world and a wider variety of crude sources are used. The increasing variety of crude compositions, including the use of high-sulfur “sour” crude from Russia and Canada, poses a particular challenge to refiners. The existence of multiple desulfurization techniques would allow the efficient removal of sulfur from these petroleum sources.

Despite the effectiveness of other catalytic processes such as HDS in sulfur removal, PEMHRs were not successful. The reactions occurring in PEMHRs are catalytic and follow the same rate laws as those occurring in conventional hydrogenation reactors.

Except perhaps at very low current densities, the reaction step (addition of first hydrogen) becomes rate limiting. Despite the similarities to HDS, the temperature, pressure, and choice of catalysts available in PEMHRs are insufficient to effectively remove sulfur from petroleum.

The removal of thiols from petroleum using metal oxides is very promising. PbO is able to scavenge alkanethiols from a hydrocarbon solution to very low (~10 ppm S) levels. The reaction is catalyzed by water, which likely functions as a proton transfer agent during the reaction. The reaction is zero order in thiol concentration and proportional to water concentration, permitting the fast removal of small amounts of thiols. This process could complement HDS by performing a post-treating function to remove recombinant thiols formed in the HDS reactor, minimizing the amount of metal oxide used and thiolate formed. The product thiolates can also be easily decomposed to regenerate the original thiols and metal oxide.

The primary limitations of this process are its specificity to thiols and the use of heavy metals. The specificity of the reaction prevents this process from being applied independently from an HDS unit unless the feed stream contains almost exclusively thiol sulfur. The use of heavy metals, such as Pb, is also undesirable due to the risk of contamination of the refinery site or the environment. The use of Bi instead of Pb can mitigate this problem somewhat, although containment will remain an issue.

The effectiveness of this process on actual crude or gasoline streams needs to be investigated. These streams contain a wide variety of thiols and other organic compounds that may complicate the removal of the thiols. Retail gasoline is not suited for this type of analysis because it has already been hydrotreated to remove all of the thiols.

The use of sulfuric acid as a selective oxidizing agent for desulfurization of sulfides and thiophene derivatives is also promising. This process relies on the thermodynamic equilibrium between sulfur in the +6 oxidation state (sulfate) and sulfur in the -2 oxidation state (organic sulfide). Despite the stability of the sulfate ion, a mixture of these two oxidation states will try to move towards equilibrium, generating the 0 (elemental) and +4 (dioxide) oxidation states of sulfur. At sufficiently high concentrations of sulfuric acid, sulfides and thiophene are oxidized to sulfoxides and other oxidized species in a reaction that is first order in sulfide concentration until an equilibrium concentration is reached.

The oxidation of the sulfides permits selective extraction or adsorption of the sulfur compounds, identical to ODS. The effectiveness of this extraction is demonstrated by the removal of the product species to undetectable levels in the hydrocarbon phase after reactive extraction with concentrated sulfuric acid. This process replaces oxidation by the expensive hydrogen peroxide with inexpensive sulfuric acid, without significant changes to the remaining ODS flowsheet.

The oxidation of sulfur compounds with sulfuric acid has two limitations. First, the reaction reaches equilibrium for some compounds at sulfur levels that are above the legal limits, requiring removal of the products and long reaction times. This limitation can be overcome by combining the most desirable features of sulfuric acid-based ODS and hydrogen peroxide-based ODS. A pretreatment with sulfuric acid can cheaply remove most of the sulfur from petroleum streams. A peroxide unit can then oxidize the remaining traces of sulfur to meet regulatory limits. The two units can share many of the extraction, adsorption, and neutralization process steps.

The second limitation is the use of a liquid sulfuric acid. Extensive efforts are being made to eliminate the use of sulfuric acid as a catalyst for alkylation due, in part, to the need to dispose of large quantities of petroleum-contaminated acid. The introduction of the same material into a new process is somewhat counterproductive, although the technology for safely using and disposing of such acid already exists. Also, this process could only be used on streams that do not contain significant amounts of olefins, since sulfuric acid will catalyze alkylation and oligomerization reactions.

The effect of this treatment technique on actual diesel streams should be evaluated. Specifically, the sulfur levels obtained and any side reactions occurring are of particular importance. Methods to regenerate the sulfuric acid and remove the colloidal sulfur are also needed before commercialization.

Two new desulfurization techniques have been demonstrated here, each applicable to different aspects of refining. Each permits the more efficient use of other desulfurization technologies by the pre- or post-treatment of streams desulfurized by ODS or HDS. Application of these technologies could permit the efficient production of ultra-low sulfur fuels from lower quality, high-sulfur crude.

7. References

1. Office of Energy Markets and End Use, *World Energy Use and Carbon Dioxide Emissions, 1980-2001*. 2004, US Energy Information Administration.
2. Clean Air Markets Division, *EPA Acid Rain Program 2003 Progress Report*. 2004, US EPA Office of Air and Radiation. p. 20 pages.
3. Office of Air Quality Planning & Standards, *SO₂ - How Sulfur Dioxide Affects the Way We Live & Breathe*. 2000, US EPA.
4. Rao, T., *Effects of Sulfur on Exhaust Emissions*. 1997, US EPA - Office of Mobile Sources: Ann Arbor, MI.
5. Fowler, R. and L. Boock. *AdVanta FCC Catalyst*. in *Grace 2002 Latin American and Caribbean Refining Seminar*. 2002. Lima, Peru.
6. Beck, J. *EMICT, A Regenerable Paraffin Isomerization Catalyst*. in *MCCJ 15th Anniversary Symposium*. 2000. Japan.
7. Ackerman, S., G.K. Chitnis, and D.S. McCaffery, Jr., Advances in Sulfuric Acid Alkylation Process Improve Gasoline Blending Economics in *World Refining*, 7, 2002,
8. Irion, W.W. and O.S. Neuwirth, *Oil Refining*, in *Ullmann's Encyclopedia of Industrial Chemistry*. 2003, Wiley-VCH: Weinheim. p. 205-256.
9. Firor, R. and B. Quimby, Determine low-level sulfur in hydrocarbon gases in *Hydrocarbon Processing*, February, 2003, pp.79-81.
10. Pafko, W., *Case Study: Petroleum, Modern Refining*, 2000, http://www.pafko.com/history/h_refine.html.
11. Shiflett, W.K. and L.D. Krenzke, Consider improved catalyst technologies to remove sulfur in *Hydrocarbon Processing*, February, 2002, pp.41-43.
12. Knudsen, K.G., B.H. Cooper, and H. Topsøe, *Catalyst and process technologies for ultra low sulfur diesel*. *Applied Catalysis A: General*, 1999. **189**: p. 205-215.
13. Anonymous, Refining Processes 2002 in *Hydrocarbon Processing*, 11, 2002, pp.85-148.
14. Gates, B.C., J.R. Katzer, and G.C.A. Schuit, *Chemistry of Catalytic Processes*. McGraw-Hill Chemical Engineering Series. 1979, New York: McGraw-Hill. 464.

15. Sweed, N.H. *SCANfining for Low Sulfur Gasoline*. in *Latin American and Caribbean Refining Seminar*. 2002. Lima, Peru: ExxonMobil Research and Engineering Co.
16. Lauritsen, J.V., et al., *Atomic-Scale Structure of Co-Mo-S Nanoclusters in Hydrotreating Catalysts*. *Journal of Catalysis*, 2001. **197**(1): p. 1-5.
17. Kishan, G., J.A.R. van Veen, and J.W. Niemantsverdriet, *Realistic Surface Science Models of Hydrodesulfurization Catalysts on Planar Thin-Film Supports: The Role of Chelating Agents in the Preparation of CoW/SiO₂ catalysts*. *Topics in Catalysis*, 2004. **29**(3 - 4): p. 103-110.
18. Kim, T.S., H.Y. Kim, and B.H. Kim, *Petroleum Desulfurization by Desulfovibrio-Desulfuricans M6 Using Electrochemically Supplied Reducing Equivalent*. *Biotechnology Letters*, 1990. **12**(10): p. 757-760.
19. Borole, A.P., et al., *Comparison of the emulsion characteristics of Rhodococcus erythropolis and Ecsherichia coli SOXC-5 cells expressing biodesulfurization genes*. *Biotechnology Progress*, 2002. **18**(1): p. 88-93.
20. Gray, K.A., G.T. Mrachko, and C.H. Squires, *Biodesulfurization of fossil fuels*. *Current Opinion in Microbiology*, 2003. **6**(3): p. 229-235.
21. Philip, L. and M.A. Deshusses, *Sulfur dioxide treatment from flue gases using a biotrickling filter - bioreactor system*. *Environmental Science & Technology*, 2003. **37**(9): p. 1978-1982.
22. Gupta, N., P.K. Roychoudhury, and J.K. Deb, *Biotechnology of desulfurization of diesel: prospects and challenges*. *Applied Microbiology and Biotechnology*, 2005. **66**(4): p. 356-366.
23. Li, F.L., et al., *Deep desulfurization of hydrodesulfurization-treated diesel oil by a facultative thermophilic bacterium Mycobacterium sp. X7B*. *FEMS Microbiology Letters*, 2003. **223**(2): p. 301-307.
24. Marcelis, C.L.M., et al., *Model description of dibenzothiophene mass transfer in oil/water dispersions with respect to biodesulfurization*. *Biochemical Engineering Journal*, 2003. **16**(3): p. 253-264.
25. Olmo, C.H.d., et al., *Production of a Rhodococcus erythropolis IGTS8 biocatalyst for DBT biodesulfurization: influence of operational conditions*. *Biochemical Engineering Journal*, 2005. **22**(3): p. 229-237.
26. Konishi, M., et al., *The separation of oil from an oil-water-bacteria mixture using a hydrophobic tubular membrane*. *Biochemical Engineering Journal*, 2005. **24**(1): p. 49-54.

27. Velu, S., X.L. Ma, and C.S. Song, *Selective adsorption for removing sulfur from jet fuel over zeolite-based adsorbents*. Industrial & Engineering Chemistry Research, 2003. **42**(21): p. 5293-5304.
28. Hernandez-Maldonado, A.J., et al., *New sorbents for desulfurization of diesel fuels via pi complexation: Layered beds and regeneration*. Industrial & Engineering Chemistry Research, 2004. **43**(3): p. 769-776.
29. Shiraishi, Y., A. Yamada, and T. Hirai, *Desulfurization and denitrogenation of light oils by methyl viologen-modified aluminosilicate adsorbent*. Energy & Fuels, 2004. **18**(5): p. 1400-1404.
30. Haji, S. and C. Erkey, *Removal of dibenzothiophene from model diesel by adsorption on carbon aerogels for fuel cell applications*. Industrial & Engineering Chemistry Research, 2003. **42**(26): p. 6933-6937.
31. Rosso, I., et al., *Zinc oxide sorbents for the removal of hydrogen sulfide from Syngas*. Industrial & Engineering Chemistry Research, 2003. **42**(8): p. 1688-1697.
32. Ma, X., L. Sun, and C. Song, *A new approach to deep desulfurization of gasoline, diesel fuel and jet fuel by selective adsorption for ultra-clean fuels and for fuel cell applications*. Catalysis Today, 2002. **77**(1-2): p. 107-116.
33. Fukunaga, T., et al., *Development of kerosene fuel processing system for PEFC*. Catalysis Today, 2003. **84**(3-4): p. 197-200.
34. Mikhail, S., T. Zaki, and L. Khalil, *Desulfurization by an economical adsorption technique*. Applied Catalysis A: General, 2002. **227**(1-2): p. 265-278.
35. Zainudin, N.F., et al., *Study of adsorbent prepared from oil palm ash (OPA) for flue gas desulfurization*. Separation and Purification Technology, 2005. In Press, Corrected Proof.
36. Jeevanandam, P., K.J. Klabunde, and S.H. Tetzler, *Adsorption of thiophenes out of hydrocarbons using metal impregnated nanocrystalline aluminum oxide*. Microporous and Mesoporous Materials, 2005. **79**(1-3): p. 101-110.
37. Levy, R.E., et al. *Unipure's Oxidative Desulfurization Process Creates New Market Opportunities For Supply Of Ultra-low Sulfur Fuels*. in *AICHE Spring Meeting*. 2002. New Orleans.
38. An, W.D., et al., *The electrochemical hydrogenation of edible oils in a solid polymer electrolyte reactor. I. Reactor design and operation*. Journal of the American Oil Chemists Society, 1998. **75**(8): p. 917-925.
39. An, W.D., et al., *The electrochemical hydrogenation of edible oils in a solid polymer electrolyte reactor. II. Hydrogenation selectivity studies*. Journal of the American Oil Chemists Society, 1999. **76**(2): p. 215-222.

40. Perry, R.H. and D.W. Green, eds. *Perry's Chemical Engineer's Handbook*. 7th ed. ed. 1997, McGraw-Hill: New York.
41. Kroschwitz, J. and M. Howe-Grant, eds. *Kirk-Othmer Encyclopedia of Chemical Technology*. 4th ed. ed. Vol. Vols. 1, 2, 9, 10. 1991, John Wiley and Son: New York.
42. Gerhartz, W. and Y.S. Yamamoto, eds. *Ullman's Encyclopedia of Industrial Chemistry*. 5th ed. ed. Vol. Vol. A13. 1996, VCH: Weinheim.
43. Engelhard Corporation, *Engelhard Catalysts*. 1977, Iselin: Engelhard Corporation. 60 pages.
44. Haussinger, P., R. Lohmuller, and A. Watson, *Hydrogen*, in *Ullmann's Encyclopedia of Industrial Chemistry*. 2003, Wiley-VCH: Weinheim. p. 85-240.
45. Yi, H.M., *Dense palladium and perovskite membranes and membrane reactors*. Mrs Bulletin, 1999. **24**(3): p. 46-49.
46. Itoh, N., W.C. Xu, and K. Haraya, *Basic Experimental-Study on Palladium Membrane Reactors*. Journal of Membrane Science, 1992. **66**(2-3): p. 149-155.
47. Young, S.K. and K.A. Mauritz, *Dynamic mechanical analyses of Nafion (R)/organically modified silicate nanocomposites*. Journal of Polymer Science Part B-Polymer Physics, 2001. **39**(12): p. 1282-1295.
48. Ogumi, Z., K. Nishio, and S. Yoshizawa, *Application of the SPE Method to Organic Electrochemistry. 2. Electrochemical Hydrogenation of Olefinic Double-Bonds*. Electrochimica Acta, 1981. **26**(12): p. 1779-1782.
49. Ogumi, Z., S. Ohashi, and Z. Takehara, *Application of the SPE Method to Organic Electrochemistry. 6. Oxidation of Cyclohexanol to Cyclohexanone on Pt-SPE in the Presence of Iodine and Iodide*. Electrochimica Acta, 1985. **30**(1): p. 121-124.
50. Ogumi, Z., et al., *Application of the Solid Polymer Electrolyte (SPE) Method to Organic Electrochemistry. 3. Kolbe Type Reactions on Pt-SPE*. Electrochimica Acta, 1983. **28**(11): p. 1687-1693.
51. Inaba, M., Z. Ogumi, and Z. Takehara, *Application of the Solid Polymer Electrolyte Method to Organic Electrochemistry .14. Effects of Solvents on the Electroreduction of Nitrobenzene on Cu, Pt-Nafion*. Journal of the Electrochemical Society, 1993. **140**(1): p. 19-22.
52. Kunugi, A., et al., *Electroreduction of 2-cyclohexen-1-one on metal-solid polymer electrolyte composite electrodes*. Electrochimica Acta, 1998. **44**(4): p. 653-657.

53. Sarrazin, J. and A. Tallec, *Use of Ion-Exchange Membranes in Preparative Organic Electrochemistry - New Processes for Electrolysis*. Journal of Electroanalytical Chemistry, 1982. **137**(1): p. 183-188.
54. An, W., J.K. Hong, and P.N. Pintauro, *Current efficiency for soybean oil hydrogenation in a solid polymer electrolyte reactor*. Journal of Applied Electrochemistry, 1998. **28**(9): p. 947-954.
55. Cook, R., R.C. MacDuff, and A.F. Sammells, *Ambient Temperature Gas Phase CO₂ Reduction to Hydrocarbons at Solid Polymer Electrolyte Cells*. Journal of the Electrochemical Society, 1988. **135**(6): p. 1470-1471.
56. Komatsu, S., et al., *Preparation of Cu-Solid Polymer Electrolyte Composite Electrodes and Application to Gas-Phase Electrochemical Reduction of Co₂*. Electrochimica Acta, 1995. **40**(6): p. 745-753.
57. Lamy-Pitara, E., I. Belegri, and J. Barbier, *Liquid-Phase Catalytic-Hydrogenation under Potential Control of the Catalyst*. Catalysis Today, 1995. **24**(1-2): p. 151-156.
58. Cleghorn, S.J.C. and D. Pletcher, *The Mechanism of Electrocatalytic Hydrogenation of Organic-Molecules at Palladium Black Cathodes*. Electrochimica Acta, 1993. **38**(2-3): p. 425-430.
59. Horanyi, G., *In Horiuti's footsteps: links between catalysis and electrocatalysis*. Journal of Molecular Catalysis A - Chemical, 2003. **199**(1-2): p. 7-17.
60. Adamson, A.W. and A.P. Gast, *Physical Chemistry of Surfaces*. 6 ed. 1997, New York: John Wiley & Sons, Inc. 784.
61. Lasia, A. and A. Rami, *Kinetics of hydrogen evolution on nickel electrodes*. Journal of Electroanalytical Chemistry, 1990(294): p. 123-141.
62. Pardillos-Guindet, J., et al., *Electrode Potential of a Dispersed Raney-Nickel Electrode During Acetone Hydrogenation - Influence of the Solution and Reaction-Kinetics*. Journal of Catalysis, 1995. **155**(1): p. 12-20.
63. Lasser, R. and K.H. Klatt, *Solubility of Hydrogen Isotopes in Palladium*. Physical Review B, 1983. **28**(2): p. 748-758.
64. Langmuir, I., *The Adsorption of Gases on Plane Surfaces of Glass, Mica, and Platinum*. Journal of the American Chemical Society, 1918. **40**: p. 1361-1403.
65. Rositani, F., et al., *Kinetics of Acetone Hydrogenation over Pt/Al₂O₃ Catalysts*. Journal of Chemical Technology and Biotechnology A - Chemical Technology, 1985. **35**(5): p. 234-240.

66. Sun, Y., et al., *Asymmetric Hydrogenation of Ethyl Pyruvate: Diffusion Effects on Enantioselectivity*. Journal of Catalysis, 1996. **161**(2): p. 759-765.
67. Singh, U.K. and M.A. Vannice, *Kinetics of liquid-phase hydrogenation reactions over supported metal catalysts -- a review*. Applied Catalysis A: General, 2001. **213**(1): p. 1-24.
68. Hernandez-Maldonado, A.J. and R.T. Yang, *Desulfurization of liquid fuels by adsorption via pi complexation with Cu(I)-Y and Ag-Y zeolites*. Industrial & Engineering Chemistry Research, 2003. **42**(1): p. 123-129.
69. Popp, F.D. and H.P. Schultz, *Electrolytic Reduction of Organic Compounds*. Chemical Reviews, 1962. **62**(1): p. 19-&.
70. Sharipov, A.K., *Mercaptans from Gas Condensate and Crude Oils*. Chemistry and Technology of Fuels and Oils, 2002. **38**(4): p. 280-285.
71. Satterfield, C.N., *Heterogeneous Catalysis in Industrial Practice*. 2nd ed. ed. 1991, New York: McGraw-Hill. 554 pages.
72. *Control of Air Pollution From New Motor Vehicles: Tier 2 Motor Vehicle Emissions Standards and Gasoline Sulfur Control Requirements*, in *Federal Register*. 2000. p. p. 6697-6870.
73. Naim, M., et al., *Inhibition by Thiol Compounds of Off-Flavor Formation in Stored Orange Juice .2. Effect of L-Cysteine and N-Acetyl-L-Cysteine on P-Vinylguaiacol Formation*. Journal of Agricultural and Food Chemistry, 1993. **41**(9): p. 1359-1361.
74. Mottram, D.S., C. Szauman-Szumski, and A. Dodson, *Interaction of thiol and disulfide flavor compounds with food components*. Journal of Agricultural and Food Chemistry, 1996. **44**(8): p. 2349-2351.
75. Herradura, P.S., K.A. Pendola, and R.K. Guy, *Copper-mediated cross-coupling of aryl boronic acids and alkyl thiols*. Organic Letters, 2000. **2**(14): p. 2019-2022.
76. Reid, E.E., *Organic Chemistry of Bivalent Sulfur*. Vol. Vol. 1. 1958, New York: Chemical Publishing Co. 539 pages.
77. Tiers, G.V.D. and M.L. Brostrom, *Lead mercaptides: materials useful as powder secondary standards and internal references for calibration of X-ray diffractometers at small and medium angles*. Journal of Applied Crystallography, 2000. **33**(3, Pt. 2): p. 915-920.
78. Borgstrom, P., L.M. Ellis, and E.E. Reid, *Preparation, Properties, and Reactions of Lead Mercaptides*. Journal of the American Chemical Society, 1929. **51**: p. 3649-51.

79. Chen, S.W., L.A. Truax, and J.M. Sommers, *Alkanethiolate-protected PbS nanoclusters: Synthesis, spectroscopic and electrochemical studies*. Chemistry of Materials, 2000. **12**(12): p. 3864-3870.
80. Liu, G., et al., *Chemistry of sulfur-containing molecules on Au(111): thiophene, sulfur dioxide, and methanethiol adsorption*. Surface Science, 2002. **505**(1-3): p. 295-307.
81. Benziger, J.B. and R.E. Preston, *Organosulfur Chemistry on W(211) Surfaces. I. A Comparison of Methanethiol and Methanol*. Journal of Physical Chemistry, 1985. **89**(23): p. 5002-5010.
82. Kuhnle, A., et al., *Adsorption of dodecanethiol on Cu(110): Structural ordering upon thiolate formation*. Langmuir, 2002. **18**(14): p. 5558-5565.
83. Ma, F.Y. and R.B. Lennox, *Potential-assisted deposition of alkanethiols on Au: Controlled preparation of single- and mixed-component SAMs*. Langmuir, 2000. **16**(15): p. 6188-6190.
84. Widrig, C.A., C. Chung, and M.D. Porter, *The Electrochemical Desorption of N-Alkanethiol Monolayers from Polycrystalline Au and Ag Electrodes*. Journal of Electroanalytical Chemistry, 1991. **310**(1-2): p. 335-359.
85. Liu, G., et al., *Adsorption of methanethiol on stoichiometric and defective TiO₂(110) surfaces: A combined experimental and theoretical study*. Journal of Physical Chemistry B, 2002. **106**(38): p. 9883-9891.
86. Cheng, L.C., et al., *Coadsorption of ethanethiol with sulfur, oxygen, and water on the Fe(100) surface*. Langmuir, 1996. **12**(2): p. 392-401.
87. Meagher, K.K., et al., *Interaction of neopentyl thiol with clean and oxygen-modified Fe(100) surfaces*. Journal of Physical Chemistry B, 2000. **104**(14): p. 3320-3326.
88. Oae, S., ed. *Organic Chemistry of Sulfur*. 1st ed. ed. 1977, Plenum Press: New York. 713 pages.
89. Oae, S., *Organic Sulfur Chemistry: Structure and Mechanism*. 1991, Boca Raton: CRC Press. 433 pages.
90. Bensebaa, F., et al., *XPS studies of metal-sulfur bonds in metal-alkanethiolate materials*. Surface Science, 1998. **405**: p. L472-476.
91. Souza, A.G.d., et al., *Standard enthalpy of formation of diisobutyldithiocarbamate complexes of zinc-group elements and mean M-S bond-dissociation enthalpies*. Thermochemica Acta, 1994. **231**: p. 31-38.

92. Ribeiro da Silva, M.A.V., A.M.M.V. Reis, and M.M.R. Ferreira da Silva, *Enthalpies of formation of crystalline dimethyldithiocarbamate complexes of chromium(III) and iron(III): the estimation of the mean M-S bond-dissociation enthalpies*. Journal of Chemical Thermodynamics, 2000. **32**: p. 1319-1325.
93. Ribeiro da Silva, M.A.V., A.M.M.V. Reis, and R.I.M.C.P. Faria, *Standard enthalpies of formation of crystalline dimethyl ammoniumdimethyldithiocarbamate and dimethyldithiocarbamate complexes of copper(II) and nickel(II). The mean Cu-S and Ni-S bond-dissociation enthalpies*. Journal of Chemical Thermodynamics, 1995. **27**: p. 1365-1372.
94. Lide, D.R., ed. *CRC Handbook of Chemistry and Physics*. 81st Ed. ed. 2000, CRC Press: Boca Raton.
95. Barin, I., *Thermochemical Data of Pure Substances, Parts I and II*. 1993, Weinheim: VCH.
96. Ellis, E.S., et al., *Meeting the demands of low sulphur gasoline*. Petroleum Technology Quarterly, 2002. Spring.
97. Ondrey, G., *This process makes low-sulfur gasoline without additional hydrotreating*. Chemical Engineering, 2003. December.
98. Hernandez-Maldonado, A.J., S.D. Stamatis, and R.T. Yang, *New Sorbents for Desulfurization of Diesel Fuels via Pi-Complexation: Layered Beds and Regeneration*. Industrial and Engineering Chemistry Research, 2004. **43**: p. 769-776.
99. Shan, G., et al., *Separation of Polycyclic Aromatic Compounds from Model Gasoline by Magnetic Alumina Sorbent Based on Pi-Complexation*. Industrial and Engineering Chemistry Research, 2004. **43**: p. 758-761.
100. Yang, R.T., A. Takahashi, and F.H. Yang, *New sorbents for desulfurization of liquid fuels by, pi-complexation*. Industrial & Engineering Chemistry Research, 2001. **40**(26): p. 6236-6239.
101. Dvorak, J., T. Jirsak, and J.A. Rodriguez, *Fundamental studies of desulfurization processes: reaction of methanethiol on ZnO and Cs/ZnO*. Surface Science, 2001. **479**(1-3): p. 155-168.
102. Nehlsen, J.P., J.B. Benziger, and I.G. Kevrekidis, *Removal of Alkanethiols from a Hydrocarbon Mixture by Heterogeneous Reaction with Metal Oxides*. Industrial and Engineering Chemistry Research, 2003. **42**(26): p. 6919-6923.
103. Wizig, H. and R. Maple, *Removal of Sulfur from a Light FCC Gasoline Stream*, 1999, Merichem Chemicals & Refinery Services LLC.
<http://www.merichem.com/Process/TechnicalArticles/SulfurGas1to3.htm>.

104. McBryde, W.A.E., *Petroleum Deodorized: Early Canadian History of the 'Doctor Sweetening' Process*. *Annals of Science*, 1991. **48**: p. 103-111.
105. *Control of Air Pollution from New Motor Vehicles: Heavy-Duty Engine and Vehicle Standards and Highway Diesel Fuel Sulfur Control Requirements*, in *Federal Register*. 2001. p. 5001-5051.
106. Dishun, Z., et al., *A review of desulfurization of light oil based on selective oxidation*. *Chemistry Journal on the Internet*, 2004. **6**(3): p. 17.
107. Song, C., *An overview of new approaches to deep desulfurization for ultra-clean gasoline, diesel fuel and jet fuel*. *Catalysis Today*, 2003. **86**: p. 211-263.
108. Sweed, N.H. and E.S. Ellis, *Meeting the Low Sulfur Mogas Challenge*. *Petroleum Technology Quarterly*, 2001(Autumn).
109. Ford, J.F., T.A. Rayne, and D.G. Adlington, *Desulfurization of Hydrocarbons Using Oxidative and Hydro-treatments*, US Patent 3,341,448. British Petroleum, Inc., 1967.
110. Babich, I.V. and J.A. Moulijn, *Science and technology of novel processes for deep desulfurization of oil refinery streams: a review*. *Fuel*, 2003. **82**: p. 607-631.
111. Murata, S., et al., *A Novel Oxidative Desulfurization System for Diesel Fuels with Molecular Oxygen in the Presence of Cobalt Catalysts and Aldehydes*. *Energy & Fuels*, 2004. **18**: p. 116-121.
112. Tam, P.S., J.R. Kittrell, and J.W. Eldridge, *Desulfurization of Fuel-Oil by Oxidation and Extraction .I. Enhancement of Extraction Oil Yield*. *Industrial & Engineering Chemistry Research*, 1990. **29**(3): p. 321-324.
113. Shiraishi, Y. and T. Hirai, *Desulfurization of vacuum gas oil based on chemical oxidation followed by liquid-liquid extraction*. *Energy & Fuels*, 2004. **18**(1): p. 37-40.
114. SulphCo, *Technology*, 2004, <http://www.sulphco.com/technology.htm>.
115. Collins, F.M., A.R. Lucy, and C. Sharp, *Oxidative desulphurisation of oils via hydrogen peroxide and heteropolyanion catalysis*. *Journal of Molecular Catalysis A-Chemical*, 1997. **117**(1-3): p. 397-403.
116. Yazu, K., et al., *Oxidation of dibenzothiophenes in an organic biphasic system and its application to oxidative desulfurization of light oil*. *Energy & Fuels*, 2001. **15**(6): p. 1535-1536.
117. Greenwood, N.N. and A. Earnshaw, eds. *Chemistry of the Elements*. 2nd ed. 1997, Elsevier. 1341.

118. Zhang, Q.L., et al., *Reactions between hydrogen sulfide and sulfuric acid: A novel process for sulfur removal and recovery*. *Industrial & Engineering Chemistry Research*, 2000. **39**(7): p. 2505-2509.
119. Wang, H., I.G. Dalla Lana, and K.T. Chuang, *Kinetics and mechanism of oxidation of hydrogen sulfide by concentrated sulfuric acid*. *Industrial & Engineering Chemistry Research*, 2002. **41**(26): p. 6656-6662.
120. Dean, J.A., ed. *Lange's Handbook of Chemistry*. 15th ed. 1999, McGraw-Hill: New York. 1521.
121. Washburn, E.W., ed. *International Critical Tables of Numerical Data, Physics, Chemistry and Technology*. 1st Electronic ed. 2003, Knovel. 3414.
122. Muller, H., *Sulfur Dioxide*, in *Ullmann's Encyclopedia of Industrial Chemistry*. 2003, Wiley-VCH: Weinheim. p. 659-704.
123. Meadow, J.R. and R.H. Graves, *Desulfurization of Heptane Solutions Using Nitrogen Dioxide-Sulfuric Acid Mixtures*. *Industrial & Engineering Chemistry*, 1953. **45**(9): p. 2113-2117.
124. Meadow, J.R. and T.A. White, *Desulfurization of Heptane Solutions of Organic Sulfur Compounds*. *Industrial and Engineering Chemistry*, 1950. **42**(5): p. 925-929.
125. Wood, A.E., A. Lowy, and W.F. Faragher, *Action of Petroleum-Refining Agents on Pure Organic Sulfur Compounds Dissolved in Naphtha*. *Industrial & Engineering Chemistry*, 1924. **16**(11): p. 1116-1120.
126. Yaws, C.L., ed. *Yaws' Handbook of Thermodynamic and Physical Properties of Chemical Compounds*. 2003, Knovel.

Acknowledgements

The work described here represents both a success and a failure. It was a failure because the original intent, to use membrane reactors to perform some interesting reactions, didn't work at all. In fact, few of the ideas that I thought would certainly work did. Fortunately, careful observation and some curiosity led me to find two unique and interesting processes that wouldn't have been discovered were it not for all of the other failures. I guess the adage is true: we do learn more from our mistakes than our successes. So goes academic research.

Research, I have come to find, is like a mule. When it moves along, it is capable of reshaping the world. But most of the time it just sits there, no matter how hard you pull at the reins. Persistence is the key. The researcher must be more stubborn than the mule, constantly coaxing it down the path. It is not always easy to remain so determined. And so I want to thank all of those who encouraged me and helped me pull this mule.

I want to first thank my advisors, Professors Benziger and Kevrekidis, for allowing this research to veer off course from time to time. It was largely due to their flexibility that these processes were discovered. You both have provided excellent guidance and taught me much about how to think, evaluate, and communicate.

I also want to thank all of my labmates and fellow students. You know perhaps better than anyone else how difficult it can be to make things work. I want to thank Sonia, Dom, and Carlos for their friendship and advice during the "early years." Thank you Barclay,

Warren, and Joanne for keeping me sane and listening to my unsolicited advice. Thank you to all of the many REUs and seniors who worked in our lab, especially Joel, for providing a change of pace and teaching all of us a few things. I thank the “chemistry people,” Kev, Chris, Jonathan, Paul, Brent, Tao, Lakshmi, and of course Prof. Bocarsly, for answering my many questions. And thank you to my fellow graduate students for making my time here an experience I will always cherish.

Of course, none of this would have been possible without the love and support from my family. To my wife, Amy, thank you for always being there, and being patient with me. You always believed, even when I didn't. I also owe the Di Stasio family a great deal of thanks, and probably a lot more, for their unending support and encouragement. I also want to thank my family, Mom, Dad, Karen, Hollis, and Katie for convincing me that this is all worthwhile.

Many people have shaped my time here at Princeton, and I am grateful for them all. After all, there is no point to learning if we can't first enjoy life. With those thanks said, now let's get on with the science, for that is why we are all here.